EG&G Idaho, Inc.

FORM EG&G-398
(Rev. 11-79)

INTERIM REPORT

Accession No. _____

Report No. _____

Contract Program or Project Title: Code Assessment and Applications Program

Subject of this Document: An Analysis of Semiscale MOD-1 LOCE S-04-6 Using the TRAC-P1A Computer Program

Type of Document: Preliminary Assessment Report

Author(s): P. N. Demmie

Date of Document: June 1980

Responsible NRC Individual and NRC Office or Division: F. Odar, NRC-RSR

This document was prepared primarily for preliminary or internal use. It has not received full review and approval. Since there may be substantive changes, this document should not be considered final.

EG&G Idaho, Inc.
Idaho Falls, Idaho 83415

Prepared for the
U.S. Nuclear Regulatory Commission
Washington, D.C.
Under DOE Contract No. DE-AC07-76ID01570
NRC FIN No. A6047

INTERIM REPORT

ABSTRACT

An analysis of Semiscale Mod-1 LOCE (Loss-of-Coolant Experiment) S-04-6 was performed using the TRAC-P1A computer program. The main purpose of this analysis was to contribute data for the assessment of the capability of TRAC-P1A to simulate blowdown, refill, and reflood phenomena during a postulated LOCA (Loss-of-Coolant Accident). A TRAC-P1A Semiscale Mod-1 system model was created and TRAC-P1A was used to obtain initial conditions for LOCE S-04-6. After this initialization, TRAC-P1A was used to simulate the first 60 s of this experiment. The results of this simulation are presented and discussed.

CONTENTS

FIGURES

TABLES

SUMMARY

An analysis of Semiscale Mod-1 LOCE (Loss-of-Coolant Experiment) S-04-6 was performed using the TRAC-P1A computer program. The main purpose of this analysis was to contribute data for the assessment of the capability of TRAC-P1A to simulate blowdown, refill, and reflood phenomena during a postulated LOCA (Loss-of-Coolant Accident). A second purpose of this analysis was to formulate a set of modeling techniques for application of TRAC-P1A to further analyses of Semiscale Mod-1 experiments.

The Transient Reactor Analysis Code (TRAC) is an advanced best estimate systems computer program designed for the analysis of postulated accidents in light water reactors. TRAC-P1A is the latest publicly released version of TRAC and is designed primarily for the analysis of large break LOCAs in pressurized water reactors (PWRs). Its main features are a three-dimensional representation of the reactor pressure vessel with two-fluid nonequilibrium fluid dynamics models and a one-dimensional representation of piping and other components with two-phase nonequilibrium fluid dynamics models.

The simulation of the first 60 s of Semiscale Mod-1 LOCE S-04-6 was used to evaluate the capability of TRAC-P1A to simulate blowdown, refill, and reflood phenomena during Semiscale Mod-1 experiments. The Semiscale Mod-1 system is a small scale model of a four-loop PWR. It consists of a pressure vessel with a core region containing 40 electrically-heated rods, an intact loop, broken loop, pressure suppression system, and coolant injection system. LOCE S-04-6 was the sixth experiment in the baseline ECC (Emergency Core Cooling) test series which was designed to study the integral blowdown-reflood response of the Semiscale Mod-1 system with an electrically-heated core. This experiment simulated a complete double-ended offset shear break in a cold leg of a PWR with ECC injection into the intact and broken loop cold legs.

A TRAC-P1A Semiscale Mod-1 system model was created. The choices made in selecting components and options for this model were based on accurately representing the Semiscale Mod-1 system with TRAC-P1A's capabilities and user experience at the Idaho National Engineering Laboratory.

The initial conditions for the simulation of LOCE S-04-6 were obtained by executing an appropriately modified version of this system model in the steady-state mode for 60 s and maintaining a volumetric flow through the core and intact loop of 9.11×10^{-3} m^3/s at a system pressure of 1.5528×10^7 N/m^2 and core power of 1.44 MW.

After initial conditions were obtained, the simulation of LOCE S-04-6 commenced.

The results of this simulation showed that an adequate calculation of rod cladding temperatures during the blowdown and refill phases of LOCE S-04-6 was provided by TRAC-P1A when it correctly calculated the occurrence of CHF (critical heat flux). During this simulation, the calculated rod cladding temperatures agreed well with the experimental data in the lower part of the heated core and fell within the data range in the high-powered middle part of the heated core. However, except for the low-powered top of the heated core, these calculated temperatures were considerably higher than the experimental data in the upper part of the heated core. At all these parts , TRAC-P1A's capability to calculate rod cladding temperatures correlated well with its ability to calculate the occurrence of CHF.

In general the mass flows, pressures, densities, and fluid temperatures calculated by TRAC-P1A during this simulation do not agree well with these quantities obtained from the experimental data. The poor calculation of mass flow in the broken loop hot and cold legs during the

blowdown phase has significance for the poor calculation of rod cladding temperatures in the upper part of the heated core, since this poor calculation yielded incorrect fluid conditions early in the blowdown which resulted in the failure to delay the initiation of CHF.

Refill of the lower plenum did not occur during this 60 s simulation of LOCE S-04-6 although refill did occur in LOCE S-04-6 at approximately 57 s. A significant factor in causing this refill delay is the use of one-sided, lumped-parameter heat slabs in the TRAC-P1A vessel component. Although sufficient ECC liquid was injected into the vessel to refill the lower plenum, the enhanced energy transfer rate of such heat slabs representing the downcomer and lower plenum walls inhibited this liquid's reaching and remaining in the lower plenum.

Since refill did not occur during the first 60 s of the simulation and the intact loop accumulator was nearly empty at 60 s, the simulation was terminated at 60 s.

This analysis shows that the capability of TRAC-P1A to simulate blowdown, refill, and reflood phenomena during Semiscale Mod-1 experiments would be enhanced by (a) improving the capability of TRAC-P1A to calculate break mass flow to simulate blowdown phenomena better, and (b) implementing two-sided, distributed-parameter heat slabs in the TRAC-P1A vessel component to simulate refill phenomena better.

AN ANALYSIS OF SEMISCALE MOD-1 LOCE S-04-6 USING THE TRAC-P1A COMPUTER PROGRAM

1. INTRODUCTION

An analysis of Semiscale Mod-1 LOCE (Loss-of-Coolant Experiment) S-04-6 was performed using the TRAC-P1A computer program.[1] The main purpose of this analysis was to contribute data for the assessment of the capability of TRAC-P1A to simulate blowdown, refill, and reflood phenomena during a postulated LOCA (Loss-of-Coolant Accident). A second purpose of this analysis was to formulate a set of modeling techniques for application of TRAC-P1A to further analyses of Semiscale Mod-1 experiments.

The Transient Reactor Analysis Code (TRAC) is an advanced best estimate systems computer program designed for the analysis of postulated accidents in light water reactors. TRAC-P1A is an improved version of TRAC-P1, the first publicly released version of TRAC, and is designed primarily for the analysis of large break LOCAs in pressurized water reactors. The main features of TRAC are a three-dimensional representation of the reactor pressure vessel with two-fluid nonequilibrium fluid dynamics models and a one-dimensional representation of piping and other components with two-phase nonequilibrium fluid dynamics models. Other features include a flow-regime dependent constitutive equation package, comprehensive heat transfer capability, a consistent analysis of entire accident sequences, and component and functional modularity. A more detailed description of TRAC-P1A is found in Reference 1.

An essential prelude to the application of a best estimate systems computer program to the analysis of LWR (light water reactor) safety issues is the independent assessment of the computer program, since the independent assessment of such a computer program is a prime ingredient in any procedure leading to its acceptance. The goals of independent assessment are:

1. To ascertain that the best estimate systems computer program adequately simulates all thermal-hydraulic phenomena that play an important role in determining the fuel rod cladding temperatures and peak cladding temperature (PCT) in a LWR during a postulated accident.

2. To determine which input parameters containing uncertainties play important roles in determining cladding temperatures and then to determine their uncertainty ranges and probability distributions.

3. To determine the code error in computing cladding temperatures in integral test facilities, where code error reflects discrepancies between calculated and measured cladding temperatures that cannot be attributed to input parameter uncertainties and measurement errors, and then to extrapolate this code error to full scale LWRs.

The present analysis is a contribution towards reaching the first of these goals for the TRAC-P1A computer program.

The simulation of the first 60 s of LOCE S-04-6 was used to evaluate the capability of TRAC-P1A to simulate blowdown, refill, and reflood phenomena during Semiscale Mod-1 experiments. This simulation is discussed in Section 2. In this section short descriptions of the Semiscale Mod-1 experimental apparatus and LOCE S-04-6 are given. A description of the TRAC-P1A Semiscale Mod-1 system model used in this simulation is found in Section 2.1. In Section 2.2 some operational information about this simulation is found.

A presentation and discussion of the results of this simulation are given in Section 3. Included in this presentation are plots showing rod cladding temperatures, pressures, mass and volumetric flows, and densities as calculated by TRAC-P1A and as measured during LOCE S-04-6.

The conclusions obtained from this analysis of LOCE S-04-6 and some recommendations based on these conclusions are given in Section 4.

2. THE SIMULATION OF SEMISCALE MOD-1 LOCE S-04-6

The simulation of the first 60 s of Semiscale Mod-1 LOCE S-04-6 was used to evaluate the capability of TRAC-P1A to simulate blowdown, refill, and reflood phenomena during Semiscale Mod-1 experiments. A description of the TRAC-P1A Semiscale Mod-1 system model used in this simulation is found in Section 2.1. In Section 2.2 some operational information about this simulation is given.

The Semiscale Mod-1 system[2] and instrumentation for the cold leg break configuration is depicted in Figure 1. This system is a small scale model of a four-loop pressurized water reactor (PWR). It consists of a pressure vessel with simulated reactor internals (downcomer, lower plenum, core region, and upper plenum); an intact loop with a pressurizer, steam generator, active pump, and associated piping; a broken loop with a simulated steam generator, simulated pump, associated piping, and break assemblies; a pressure suppression system with a header and suppression tank; and a coolant injection system with high and low pressure injector pumps and accumulators. The core region contains 40 electrically-heated rods. The heated length of each of these rods is 1.68 m with ten power steps providing a slightly bottom-skewed axial power profile. This axial power profile is shown in Figure 2.

The locations of various instruments throughout the Semiscale Mod-1 system are shown in Figure 1. Those instruments shown in this figure and those instruments in the vessel whose measurements are used to make comparisons with TRAC-P1A calculated quantities are listed in Table 1. This table gives for each listed instrument (a) the quantity it measures, (b) its location, and (c) an estimate of its measurement uncertainty. The measurement uncertainty estimates are calculated from expected errors in the single-phase calibration curves, calibration standards, and data acquisition and processing.[3,4] No uncertainties associated with transient, two-phase, and nonhomogeneous phenomena are included.

Semiscale Mod-1 LOCE S-04-6 was the sixth experiment in the baseline emergency core cooling (ECC) test series which was designed to study the integral blowdown-reflood response of the Semiscale Mod-1 system with an electrically-heated core.[5] It simulated a complete double-ended offset shear break in a cold leg of a PWR with ECC injection into the intact and broken loop cold legs. Three of the four center rods and 33 of the remaining 36 rods were powered. The remaining, unpowered rods represented control rods within the reactor core. A top view of a cross section of the heated core for LOCE S-04-6 is shown in Figure 3. The fluid conditions prior to blowdown initiation were those conditions obtained by maintaining a volumetric flow through the core and intact loop of 8.895×10^{-3} m^3/s at a system pressure of 1.5528×10^7 N/m^2 with a core power of 1.44 MW. After blowdown initiation the electrical power in the powered rods was programmed so that the thermal response of each rod simulated the thermal response of a nuclear rod. The core power as a function of time is given in Figure 4 for the baseline ECC test series.

2.1 TRAC-P1A Semiscale Mod-1 System Model

The TRAC-P1A Semiscale Mod-1 system model used for this simulation of LOCE S-04-6 was formulated after an extensive study of the Semiscale Mod-1 system. The nodalization used for this system model is given in Figures 5 and 6. Figure 5 shows all the nodalization except the nodalization of the vessel and break nozzles and also shows assessment measurement locations. Figure 6 gives the nodalization of the vessel and break nozzles. These figures show that this Semiscale Mod-1 system model consists of 25 components with 212 computational cells and 25 junctions.

The choices made in selecting components and options for this model were based on accurately representing the Semiscale Mod-1 system with TRAC-P1A's capabilities as ascertained from Reference 1 and user experience at the Idaho National Engineering Laboratory. The main features of this model are:

1. The vessel contains 18 axial levels with each axial level containing two radial segments and two azimuthal segments. This nodalization has 72 cells in the vessel. The lower plenum is represented by two of these axial levels, and the upper plenum is represented by one of these axial levels.

2. The active heated rods are represented axially with 10 of the 18 vessel axial levels. Each rod level corresponds to a power step in the slightly bottom-skewed axial power profile. Each heated rod has 10 radial heat transfer nodes.

3. Each cell in the vessel has a lumped-parameter heat slab whose area and mass are determined from the actual area and volume of vessel material thermally interacting with it.

4. The intact loop is represented by two tee components, a steam generator component, a pipe component, and a pump component. A pressurizer is connected to the secondary of one tee component, and intact loop ECC piping is connected to the secondary of the other tee component. Feedwater flow in the steam generator secondary is maintained for the required one second using a fill component with the velocity versus time option. A break component with the constant pressure option is connected to the other end of the steam generator secondary.

5. The pump speed versus time option is used in the pump component since the pump coastdown option was found to produce a considerably retarded coastdown rate.

6. The broken loop is represented by a pipe and a tee component. The piping represented by these components includes the simulated steam generator and pump, the break nozzles, and piping from the break nozzles to the presure suppression system. The broken loop ECC piping is connected to the secondary of the tee component.

7. The pressure suppression system is represented by break components with the constant pressure option. These components are connected to the broken loop pipe and tee components.

8. The break nozzles are finely nodalized to attempt to calculate break flow correctly.

9. The intact and broken loop ECC systems each are represented by an accumulator component, a valve component with the check valve option, two fill components representing the high pressure injection system (HPIS) and the low pressure injection system (LPIS) pumps, and two tee components. The fill components employ the velocity versus pressure option to simulate actual pump performance.

10. The fully-implicit hydrodynamics option is employed exclusively in the components connected to the vessel. This option is particularly important in the broken loop where the cell lengths are quite varied.

11. In all one-dimensional components representing piping or pumps, wall heat transfer with one heat transfer node is calculated. The thermal coupling between the steam generator's primary and secondary is accomplished using three heat transfer nodes. Critical heat flux (CHF) calculations are performed only in the vessel and the steam generator secondary.

12. The homogeneous flow friction factor is used in all components where a choice is required. Added friction was included as calculated for area change losses, bends, tees, and instrumentation. Added friction was also included as experimentally determined for the pressurizer surge line, the accumulator lines, the steam generator, the simulated steam generator and pump, and the core to upper plenum region.

This Semiscale Mod-1 system model was modified slightly to obtain the initial conditions for the simulation of LOCE S-04-6. The break components representing the pressure suppression system were replaced with fill components having a zero fill velocity specified for the initialization.

2.2 Discussion of the Simulation

Initial conditions were obtained for the simulation of LOCE S-04-6 by executing TRAC-P1A in the steady-state mode for 60 s. These initial conditions are given in Table 2. The simulation of the first 60 s of LOCE S-04-6 then commenced. This simulation was terminated at 60 s since refill had not occurred and the intact loop accumulator was nearly empty at 60 s. It required a total of 5.75 hr central processing unit (CPU) time on the CDC 176 computer. All iteration numbers and convergence criteria were input as recommended in Reference 1. An outer iteration convergence problem occurring at approximately 35 s when the broken loop accumulator was nearly empty was solved by setting the flow area in its check valve to zero.

3. PRESENTATION AND DISCUSSION OF THE RESULTS OF THE SIMULATION OF SEMISCALE MOD-1 LOCE S-04-6

In this section the results of this simulation of Semiscale Mod-1 LOCE S-04-6 are presented and discussed.

Comparisons of quantities calculated by TRAC-P1A and obtained from the experimental data are given in Section 3.1. These comparisons include rod cladding temperatures, mass and volumetric flows, pressures, differential pressures, fluid densities, and fluid temperatures. These comparisons and other pertinent information found in this section are results contributing to the qualitative assessment of TRAC-P1A. The purpose of this qualitative assessment is to ascertain whether certain results calculated by TRAC-P1A are physically reasonable.

Results contributing to the quantitative assessment of TRAC-P1A are presented and discussed in Section 3.2. These results are presented in the form of key indicators whose values characterize important blowdown, refill, and reflood phenomena that occurred during the simulation of LOCE S-04-6. The purpose of quantitative assessment is, by use of scatter plots of the calculated versus the measured values of these key indicators, to give information that reflects TRAC-P1A's capability to describe a single parameter in a normalized manner. This parameter is then described in a manner that is invariant under changes in test geometry, scale, break size, etc., and thus permits the extrapolation of its calculated error to full scale systems.

3.1 Results Contributing to the Qualitative Assessment of TRAC-P1A

Comparisons of quantities calculated by TRAC-P1A during this simulation of Semiscale Mod-1 LOCE S-04-6 and obtained from the experimental data for this experiment are given in this section. In these figures, time after rupture is measured along the horizontal axis, and the quantities compared are measured along the vertical axis. In all figures the unmarked curves are TRAC-P1A calculated quantities, and the curves marked with solid circles are the corresponding quantities obtained from the experimental data.

Since the performance of the heated rods during a postulated LOCA is the primary concern in the analysis of this accident, Figures 7 through 11 show rod cladding temperatures. Figures 7 and 8 show these temperatures in Cells 1 and 2 for each of the 10 power steps of the heated core. In these figures the unmarked curves are the calculated rod cladding temperatures, and curves marked with the 1's and the 2's are the low and high extrema, respectively, of the measured temperature range for the cell and power step depicted. Figures 9, 10, and 11 show rod cladding temperature histories at Power Steps 2, 5, and 8, respectively. These power steps are three of the 10 power steps in the heated core and are located at the lower, middle, and upper parts, respectively. In these figures the unmarked curves are the average calculated temperatures at a given power step. The curves marked with the 1's and the 2's are the low and high extrema, respectively, of the measured temperature data range for the power step depicted, and the curves marked with the stars are the average measured cladding temperatures at the corresponding power step. The data ranges are large, since critical heat flux (CHF), indicated in these figures by a large rate of change of temperature with respect to time, occurred at different times at various thermocouples in a given power step.

Figures 9 and 10 show that the calculated and average measured cladding temperatures agree well at Power Steps 2 and 5. Figure 10 also shows that the peak cladding temperature was calculated within 100 K, although the time at which this peak temperature occurred differs from the time it occurred during the experiment.

Although adequate cladding temperature calculations were made at the lower and middle parts of the heated core, the calculated cladding temperatures at Power Step 8 are considerably higher than the data, as shown in Figure 11. The reason for this disagreement is that during LOCE S-04-6 CHF occurred at between 0.5 and 1 s at the lower and middle parts of the heated core and after 2 s at the upper part; whereas TRAC-P1A calculated CHF to occur at approximately 1 s at all these parts. Thus, TRAC-P1A's capability to calculate rod cladding temperatures correlated well with its capability to calculate the occurrence of CHF.

TRAC-P1A calculated simultaneous CHF without rewet at the lower and upper parts of the heated core. This calculation is seen in Figure 12, which shows the calculated temperatures at Power Steps 2 and 8 for the first 2 s of the simulation. This calculation was consistent with the identical rod power at these power steps and the nearly identical fluid conditions calculated at these levels at the time CHF occurred.

Calculated and experimental mass flow histories at the core inlet are shown in Figure 13. This figure shows particularly poor agreement between calculated and experimental mass flows at approximately 1 s and 56 s. The disagreement early in the simulation is more clearly seen in Figure 14, which shows these mass flow histories during the first 2 s of the simulation.

Figures 15, 16, 17, and 18 show calculated and experimental mass flow histories in the broken loop hot leg, broken loop cold leg, intact loop hot leg, and intact loop cold leg, respectively. In general, the calculated and experimental mass flows shown in these figures do not agree well. For example, the calculated and experimental mass flows shown in Figure 15 for the broken loop hot leg do not agree well until after 28 s. The negative flow that occurred in LOCE S-04-6 between 23 and 28 s was not calculated by TRAC-PIA during the simulation.

The effect of these mass flows in depleting the upper plenum of mass is shown in Figure 19, which gives the calculated upper plenum mass.

The incorrect calculation of mass flows in the broken loop early in the blowdown contributed to the poor calculation of rod cladding temperatures at the upper part of the heated core. Figures 15 and 16 show that early in the blowdown the calculated mass flow was too high in the broken loop hot leg and too low in the broken loop cold leg, and Figure 14 shows that the calculated mass flow was incorrect at the core inlet. A better calculation of break mass flow would result in a better calculation of mass flow at the core inlet and more liquid from the upper plenum reaching the upper part of the heated core. More liquid in the upper part of the heated core would delay the initiation of CHF and thus result in a better calculation of cladding temperatures. The additional liquid should improve slightly the calculation of cladding temperatures at the middle part of the heated core, but hardly affect the calculation of cladding temperatures at the lower part of the heated core, since this liquid would be vaporized in passing from the upper plenum to the lower part of the heated core.

Although correct fluid conditions are important for correct CHF and rewetting calculations, these phenomena will not be calculated correctly unless the correct boiling curves are simulated. The capability of TRAC-PIA to correctly simulate these boiling curves, given correct fluid conditions, cannot be ascertained from the present analysis.

Figures 20, 21, 22, and 23 show calculated and measured pressure histories in the upper plenum, pressurizer, intact loop accumulator, and broken loop accumulator, respectively. During the blowdown phase (0 to 23 s), the calculated system (upper plenum) pressure did not agree well with the measured system pressure. This disagreement resulted primarily from the poor break mass flow calculation. Although this calculation contributed to the disagreement between calculated and measured pressures in the pressurizer and accumulators, the use of added friction, obtained from experimentally-determined hydraulic resistances in the pressurizer and accumulator lines, resulted in excessive friction in these lines. The exclusion of this added friction and an improvement in the break flow calculation would result in a significant improvement in calculated pressures.

Differential pressures across the steam generator, pump, simulated pump, and vessel are shown in Figures 24, 25, 26, and 27, respectively. While the calculated and measured differential pressure across the steam generator and pump generally agree well after about 7 s, the differential pressures across the simulated pump and vessel do not agree well. An improved break flow calculation would result in an improvement in these calculated differential pressures during the blowdown phase.

Figures 28, 29, 30, 31, and 32 show calculated and experimental densities at the core inlet, in the broken loop hot leg, broken loop cold leg, intact loop hot leg, and intact loop cold leg, respectively. These figures show that often good agreement exists between trends in calculated and experimental densities, and, over some time intervals, between the actual densities. For example, the calculated core inlet densities shown in Figure 28 decrease rapidly after rupture and agree with the experimental densities to within 100 kg/m^3 from approximately 2 to 7 s. From 7 to approximately 54 s the agreement between these core inlet densities is good. After 54 s the agreement is poor. Similar good agreement between trends in calculated and experimental densities, and, over some time intervals, between the actual densities can be found upon examining the remaining density figures.

In Figure 28 a significant disagreement between calculated and measured densities at the core inlet is seen after 54 s. Since refill occurred in LOCE S-04-6 at approximately 57 s, this disagreement indicates that refill did not occur during this simulation of LOCE S-04-6. Figure 33, which gives the calculated fluid mass in the lower plenum, shows that the lower plenum did not refill during this simulation. This figure also shows that the refill phase of this simulation began at about 23 s.

Poor intact loop ECC performance during the simulation could have been responsible for the failure of the lower plenum to refill. Figures 34 through 39 show the performance of the ECC system during this simulation. These figures give the respective calculated and measured volumetric flows in the intact loop accumulator, intact loop HPIS pump, intact loop LPIS pump, broken loop accumulator, broken loop HPIS pump, and broken loop LPIS pump. Outstanding features of these figures are that during the simulation, intact loop accumulator flow was initiated about 3 s early, broken loop accumulator flow was initiated about 2 s late, and the intact loop LPIS flow was zero for most of the simulation. The agreement between the calculated and measured volumetric flows shown in these figures would be better if the agreement between calculated and measured pressures were better. The rapid drop in broken loop accumulator volumetric flow shown in Figure 37 at 35 s results from setting the flow area in its check valve to zero at this time to solve an outer iteration convergence problem.

The low intact loop LPIS flow suggests that an explanation for the failure of the lower plenum to refill is that not enough intact loop ECC liquid was injected into the vessel. However, Figure 40 shows that sufficient intact loop ECC liquid was injected into the vessel. Figure 40 gives the total calculated and measured intact loop accumulator, HPIS, and LPIS flows. This figure shows that the amount of ECC liquid injected during this simulation of LOCE S-04-6 is larger than the amount of ECC liquid injected during LOCE S-04-6. Although generally the HPIS volumetric flow calculated during the refill phase is lower than the measured HPIS

volumetric flow and the calculated LPIS volumetric flow is nearly always zero, the total calculated ECC volumetric flow is larger than the measured ECC volumetric flow since the calculated accumulator volumetric flow is sufficiently large to overcome these deficiencies.

The downcomer penetration of this ECC liquid as well as the voiding of the downcomer during the blowdown phase of this simulation can be traced in Figures 41 through 43. These figures show the calculated void fractions in all the cells of the downcomer.

One reason that refill failed to occur during this simulation is not that insufficient liquid was injected by the ECC system, but that only one-sided, lumped-parameter heat slabs are available in TRAC-P1A to model heat transfer between the fluid in the downcomer and lower plenum and the downcomer and lower plenum walls. Since the heat slabs are one-sided, the only mechanisms available for cooling the heat slabs representing the downcomer and lower plenum walls were the vaporization of ECC liquid and the superheating of the resulting steam. Refill was delayed because these heat slabs could not also be cooled by energy transfer to the atmosphere or core region. Furthermore, the uniform temperature heat slab assumption implicit in the lumped-parameter heat transfer solution technique is not valid for heat slabs of the masses used in this Semiscale Mod-1 system model. Its use resulted in overestimating the rate at which energy was transferred to the fluid and in inhibiting the delivery of ECC liquid to the lower plenum.

That the one-sided, lumped parameter heat slabs used to model the downcomer walls inhibited the delivery of ECC liquid to the lower plenum longer during the simulation of LOCE S-04-6 than the actual downcomer walls did during LOCE S-04-6 can be seen as follows. During LOCE S-04-6, the delivery of ECC liquid to the lower plenum was inhibited by (a) countercurrent steam flow during the period when the system pressure was

higher than the suppression system pressure and (b) the flow of additional steam generated by the vaporization of ECC liquid once this liquid began to penetrate the downcomer. Since the system pressure equals the suppression system pressure during LOCE S-04-6 at approximately 43 s,[6] downcomer countercurrent steam flow inhibited ECC liquid delivery until approximately 43 s. Since Figure 20 shows excellent agreement between calculated and measured system pressures near 43 s, ECC liquid delivery was also inhibited by this mechanism during the simulation until approximately 43 s. Figure 28 shows that the fluid density at the core inlet increases rapidly at approximately 54 s during LOCE S-04-6. Therefore, the generation of steam by the hot downcomer walls inhibited ECC liquid delivery during LOCE S-04-6 until approximately 54 s. Since refill did not occur during the simulation by 54 s and since the printout shows that the temperatures of the heat slabs representing the downcomer walls remained above the saturation temperature during refill, the generation of steam by the hot heat slabs also inhibited ECC liquid delivery during the simulation until at least 54 s. However, Figure 16 shows that from 54 to 60 s the calculated broken loop cold leg mass flows are generally higher than the measured broken loop cold leg mass flows; whereas Figure 18 shows that the total mass injected from the intact loop cold leg into the vessel during the simulation and LOCE S-04-6 from 54 to 60 s is about the same. Therefore, since (a) more mass was removed from the vessel from 54 to 60 s during the simulation than during LOCE S-04-6, (b) about the same fluid mass was injected into the vessel from 54 to 60 s during both the simulation and LOCE S-04-6, (c) the printout shows that the temperatures of the heat slabs representing the lower plenum walls were below the saturation temperatures from 54 to 60 s during the simulation, and (d) since the temperatures of the heat slabs representing the downcomer walls remained above the saturation temperature during refill, it must be concluded that much of the ECC liquid injected into the vessel after 54 s during the simulation continued to be vaporized by the heat slabs representing the downcomer walls and did not reach the lower plenum. Thus the one-sided, lumped parameter heat slabs used to model the downcomer walls inhibited the delivery of ECC liquid to the lower plenum longer during the simulation of LOCE S-04-6 than the actual downcomer walls did during LOCE S-04-6.

Fluid temperatures are shown in Figures 44 through 50 in various parts of the broken and intact loops, pressurizer and steam generator secondary. The calculated and measured fluid temperatures shown in Figures 44 and 45 for the broken loop hot and cold legs, respectively, agree within 70 K during the simulation. The calculated and measured temperatures shown in Figures 46 and 47 for the intact loop hot leg and the cold leg near the pump, respectively, agree well only during most of the blowdown phase. However, Figure 48 shows that the calculated and measured fluid temperatures for the intact loop cold leg near the vessel agree well until nearly 35 s. Since this location is near the point of the intact loop ECC injection, this agreement would persist longer if the intact loop LPIS pump were operating. Finally, the calculated and measured fluid temperatures for the pressurizer do not agree well, as shown in Figure 49, but these temperatures for the steam generator secondary agree within 8 K, as shown in Figure 50. No explanation is available for the spike in calculated fluid temperature in the pressurizer at approximately 51 s. However, the divergence between the calculated and measured fluid temperatures in the pressurizer and intact loop piping when the void fraction is high can be attributed to the heating of the thermocouples measuring fluid temperatures by radiation from the hot metal walls.

Figures 51, 52, and 53 show fluid temperatures in the lower plenum, core inlet, and upper plenum, respectively. The calculated and measured fluid temperatures in the lower plenum agree well; while the calculated and measured fluid temperatures in the core inlet and upper plenum do not agree as well as these temperatures in the lower plenum. The divergence between calculated and measured fluid temperatures in the upper plenum begins at nearly the same time as the calculated liquid mass in the upper plenum is zero. Therefore, this divergence can be attributed to the heating of the thermocouples measuring upper plenum fluid temperatures by radiation from the hot vessel walls.

3.2 Results Contributing to the Quantitative Assessment of TRAC-P1A

Results contributing to the quantitative assessment of TRAC-P1A are presented in this section. These results are presented in the form of key indicators whose values characterize important blowdown, refill, and reflood phenomena that occurred during the simulation of LOCE S-04-6. These key indicators are displayed in Figures 54 through 57 and summarized in Table 3. Table 3 also gives the values of these quantities for LOCE S-04-6.

Figure 54 shows the calculated upper plenum pressure and displays the values of three key indicators that characterize the upper plenum pressure-time history. These key indicators are the time to reach HPIS activation (0 s), the time of start of intact loop accumulator discharge (14 s), and the time when upper plenum pressure equaled 1 MPa (28 s). Table 3 shows that the intact loop accumulator discharge began 3 s earlier during the simulation than during LOCE S-04-6 and the upper plenum pressure's reaching 1 MPa occurred at 28 s during the simulation and at 26 s during LOCE S-04-6; whereas HPIS activation occurred at the same time during the simulation and LOCE S-04-6.

Figure 55 shows the calculated fraction of initial mass in the lower plenum and displays the value of one of two key indicators that characterize the lower plenum mass inventory and the beginning of sustained core reflood. These key indicators are the time when the mass in the lower plenum reached 1.1 times the minimum mass (M_{min}) after this minimum occurred and the time when sustained core reflood began. Figure 55 shows that the lower plenum mass was 1.1 M_{min} at approximately 24 s and that core reflood did not begin during the 60 s of this simulation.

Figure 56 shows the core inlet mass flow and displays the value of the key indicator that characterizes core inlet flow. This key indicator is the time when core inlet flow was zero after the first negative flow cycle. Figure 14 shows that this event was calculated at approximately 0.95 s. Table 3 indicates that this event did not occur in LOCE S-04-6 until approximately 3 s.

Figure 57 shows the average calculated rod cladding temperature for Power Step 5 and displays the values of three key indicators that characterize flow near the core hot spot, peak cladding temperature, and quenching of the hot spot. These key indicators are the time of the quenches of the hot spot during the simulation and the peak cladding temperature. Table 3 indicates that the rods were neither quenched during the simulation nor during the first 60 s or LOCE S-04-6. Although the calculated peak cladding temperature of approximately 975 K is within 100 K of the value observed in LOCE S-04-6, it occurred approximately 47 s later than in LOCE S-04-6.

4. CONCLUSIONS AND RECOMMENDATIONS

Since the performance of the heated rods during a postulated LOCA is the primary concern in the analysis of this accident, the main conclusion of this analysis is:

1. An adequate calculation of rod cladding temperatures during the blowdown and refill phases of LOCE S-04-6 was provided by TRAC-P1A when the occurrence of CHF was calculated correctly.

During this simulation of LOCE S-04-6 the calculated rod cladding temperatures agreed well with experimental data in the lower and middle parts of the heated core. At these locations CHF occurred in LOCE S-04-6 between 0.5 and 1 s. However, in the upper part of the heated core, where CHF occurred in LOCE S-04-6 after 2 s, the calculated rod cladding temperatures were considerably higher than the experimental data. At all these core levels TRAC-P1A calculated CHF to occur at approximately 1 s. Thus TRAC-P1A's capability to calculate rod cladding temperatures correlated well with its capability to calculate the occurrence of CHF.

From the comparisons in Section 3 of quantities calculated by TRAC-P1A during this simulation of LOCE S-04-6 and quantities obtained from the experimental data it is concluded that:

2. The mass flows, pressures, densities, and fluid temperatures calculated by TRAC-P1A during this simulation of LOCE S-04-6 do not in general agree well with these quantities obtained from the experimental data.

This conclusion has significance for the poor calculation of rod cladding temperatures at the upper part of the heated core, since the simultaneous calculation of the occurrence of CHF without rewet at the lower and upper parts of the heated core is consistent with the identical heated rod power and nearly identical fluid conditions at these levels at the time CHF occurred. Based on this conclusion as it applies to the broken loop mass flows during the blowdown phase of this simulation and the importance of calculating the correct break mass flow for calculating correct system behavior during a blowdown, it is recommended that:

3. An effort should be made to improve the capability of TRAC-P1A to calculate break mass flow and thus improve its capability to simulate blowdown phenomena during a LOCE or postulated LOCA.

The results of this simulation indicate that break flow was poorly calculated although the break nozzles were finely nodalized. Critical flow modeling could be implemented in TRAC-P1A to better calculate break mass flow. This modeling would lead to a better prediction of system behavior during the blowdown phase of a LOCE or postulated LOCA.

From the results and discussion presented in Section 3 pertaining to the refill phase of this simulation of LOCE S-04-6, it is concluded that:

4. Refill of the lower plenum did not occur during this 60 s simulation of LOCE S-04-6, although refill did occur in LOCE S-04-6 at approximately 57 s. A significant factor in causing this refill delay is the use of one-sided, lumped-parameter heat slabs in the TRAC-P1A vessel component.

Although sufficient ECC liquid was injected into the vessel to refill the lower plenum, the only mechanisms available for cooling the heat slabs representing the downcomer and lower plenum walls were the vaporization of this ECC liquid and the superheating of the resulting steam, since the heat slabs were one-sided and hence thermally interacted only with the fluid in the downcomer and lower plenum. Refill of the lower plenum would have occurred sooner if the heat slabs were two-sided and thus would also have permitted cooling the heat slabs by energy transfer to the atmosphere or core region. Furthermore, the uniform temperature heat slab assumption implicit in the lumped-parameter heat transfer solution technique is not valid for heat slabs of the masses used in this Semiscale Mod-1 system model. Its use resulted in overestimating the rate at which energy was transferred to the fluid and in inhibiting the delivery of ECC liquid to the lower plenum. Therefore, it is recommended that:

5. *Although reducing the heat slab masses used in a Semiscale Mod-1 system model by assuming some "effective thickness" would lead to a better calculation of refill phenomena during a LOCE or postulated LOCA, two-sided heat slabs should be implemented in the TRAC-P1A vessel component and a distributed-parameter heat transfer solution technique should be employed in determining the temperature evolution of these heat slabs.*

Such two-sided, distributed-parameter heat slabs are employed in the TRAC-P1A one-dimensional piping components and should also be employed in the TRAC-P1A vessel component. If this recommendation and the recommendation given in Item 3 were followed, then the capability of TRAC-P1A to simulate blowdown, refill, and reflood phenomena during Semiscale Mod-1 experiments would be enhanced.

5. REFERENCES

1. D. R. Liles et al, TRAC-P1A An Advanced Best-Estimate Computer Program for PWR LOCA Analysis, Vol. 1, NUREG/CR-0665, LA-7777-MS, May 1979.

2. L. J. Ball et al, Semiscale Program Description, TREE-NUREG-1210, May 1978.

3. E. M. Feldman and S. A. Naff, Error Analysis for 1-1/2 Loop Semiscale Isothermal Test Data, ANCR-1188, May 1978.

4. M. S. Sahota, Recommended Parameters and Uncertainties for an Uncertainty Analysis of RELAP4/MOD6 as Applied to Semiscale Mod-1, PG-R-77-08, March 1977.

5. H. S. Crapo et al, Experimental Data Report for Semiscale Mod-1 Tests S-04-5 and S-04-6 (Baseline ECC Tests), TREE-NUREG-1045, January 1977.

6. J. M. Cozzuol, Thermal-Hydraulic Analyses of Semiscale Mod-1 Integral Blowdown - Reflood Tests (Baseline ECC Test Series), TREE-NUREG-1077, March 1977.

7. M. A. Langerman, Semiscale Mod-1 System Response During the ECC Baseline Test Series, TREE-NUREG-1058, June 1977.

APPENDIX A

EFFECTS OF AN ALTERNATE ACCUMULATOR NODALIZATION

In the Semiscale Mod-1 System Model and in the simulation of LOCE S-04-6 discussed in the main body of this report, the cells in both accumulators adjacent to the exit cells were 0.1 m long. A system model with the corresponding cells in the intact loop and broken loop accumulator 0.42 and 0.18 m long, respectively, was used for another 60 s simulation of LOCE S-04-6. In this appendix the effects of this alternate accumulator nodalization are discussed.

This alternate nodalization affects calculated quantities during the later stages of the simulation. The effects on some of the calculated quantities are shown in Figures A-1 through A-8. These figures show the calculated and measured fluid temperatures in the lower plenum, and cladding temperatures at Power Steps 2, 5, and 8, mass flows at the core inlet, and system pressures, and the calculated mass in the lower plenum and calculated void fractions in Cell 3 of Axial Level 17 in the downcomer, respectively. Figure A-1 shows that slightly after 56 s there is a rapid increase in the calculated fluid temperature of about 35 K. This calculated rapid temperature increase occurred closely with other phenomena calculated during the simulation. These phenomena include the rapid drop in rod cladding temperatures shown in Figures A-2 through A-4 the rapid increase in mass flow at the core inlet shown in Figure A-5, the increase in system pressure shown in Figure A-6, and rapid decrease in fluid mass in the lower plenum shown in Figure A-7. The rapid decrease in fluid mass in the lower plenum and the rapid increase in mass flow at the core inlet after 56 s imply that a plug of liquid was ejected from the lower plenum into the core. As this plug of liquid passed through the core it was heated, and this fluid heating caused a drop in rod cladding temperatures. The upper plenum pressure then increased from the rapid production of vapor as the liquid passed through the heated core.

This calculated water plug ejection at approximately 56 s and the lower plenum mass loss shown in Figure A-7 at this time imply that this ejection event is one reason that refill failed to occur during this simulation. Not only was approximately 4 kg of liquid expelled from the lower plenum, but also ECC liquid penetration into the lower plenum was inhibited by the increased system pressure.

The water plug ejected from the lower plenum was propelled by steam which entered the downcomer from the intact loop cold leg and steam which was generated by the vaporization of ECC liquid by the downcomer walls. That significant steam was injected into the vessel prior to 56 s is seen in Figure A-8. This figure shows the void fraction history for Cell 3 of Axial Level 17 which is connected to the intact loop cold leg. The source of the high void fraction fluid injected into this cell was not only the high void fraction fluid flowing through the intact loop, but also the high void fraction ECC fluid injected into the intact loop near the vessel. This ECC fluid had a high void fraction late in this simulation since (a) the water level in the intact loop accumulator was less than the length of the last computational cell in the accumulator module, and thus, with TRAC-P1A treating the gas component of this last cell as steam, the void fraction of the ejected fluid increased as the accumulator emptied, (b) the intact loop LPIS pump was not operating since the pressure in the accumulator line was greater than the LPIS initiation pressure, and (c) the intact loop HPIS volumetric flow was much lower than the accumulator flow. A way to avoid the accumulator emptying problem described in Item (a) is to make the length of the last computational cell in the accumulator extremely small. Making this cell much smaller would result in a longer time of pure liquid ECC injection.

TABLE 1. ASSESSMENT MEASUREMENTS AND THEIR UNCERTAINTIES

Instrument Designation	Approximate Location	Uncertainty
Quantity Measured		
Cladding Temperature		
TH-	Rod Cladding	$\pm$ 4 K
Volumetric Flow		
FTV-CORE-IN	Vessel Core Inlet	$\pm$ 0.0005 m^3/s at 0.03 m^3/s to $\pm$ 0.0001 m^3/s at flows near zero
FTU-1	Intact Loop Hot Leg	$\pm$ 0.0005 m^3/s at 0.03 m^3/s to $\pm$ 0.0001 m^3/s at flows near zero
FTU-15	Intact Loop Cold Leg	$\pm$ 0.0005 m^3/s at 0.03 m^3/s to $\pm$ 0.0001 m^3/s at flows near zero

TABLE 1. (continued)

Instrument Designation	Approximate Location	Uncertainty
FTB-30	Broken Loop Hot Leg	$\pm$ 0.0005 m^3/s at 0.03 m^3/s to $\pm$ 0.0001 m^3/s at flows near zero
FTB-21	Broken Loop Cold Leg	$\pm$ 0.0005 m^3/s at 0.03 m^3/s to $\pm$ 0.0001 m^3/s at flows near zero
FTU-ACC	Intact Loop Accumulator	$\pm$ 0.0005 m^3/s at 0.0025 m^3/s to $\pm$ 0.0004 m^3/s at flows near zero
FTU-HPIS	Intact Loop HPIS Pump	$\pm$ 0.0005 m^3/s at 0.0025 m^3/s to $\pm$ 0.0004 m^3/s at flows near zero
FTU-LPIS	Intact Loop LPIS Pump	$\pm$ 0.0005 m^3/s at 0.0025 m^3/s to $\pm$ 0.0004 m^3/s at flows near zero

TABLE 1. (continued)

Instrument Designation	Approximate Location	Uncertainty
FTB-ACC	Broken Loop Accumulator	0.0004 m^3/s for flows less than 0.0006 m^3/s
FTB-HPIS	Broken Loop HPIS Pump	0.0004 m^3/s for flows less than 0.0006 m^3/s
FTB-LPIS	Broken Loop LPIS Pump	0.0004 m^3/s for flows less than 0.0006 m^3/s
	Density	
GU-1R	Intact Loop Hot Leg	$\pm$ 8 kg/m^3 at 750 kg/m^3 to $\pm$ 5 kg/m^3 at densities near zero
GU-15R	Intact Loop Cold Leg	$\pm$ 8 kg/m^3 at 750 kg/m^3 to $\pm$ 5 kg/m^3 at densities near zero

TABLE 1. (continued)

Instrument Designation	Approximate Location	Uncertainty
GB-30VR	Broken Loop Hot Leg	$\pm$ 8 kg/m^3 at 750 kg/m^3 to $\pm$ 5 kg/m^3 at densities near zero
GB-21VR	Broken Loop Cold Leg	$\pm$ 8 kg/m^3 at 750 kg/m^3 to $\pm$ 5 kg/m^3 at densities near zero
GV-COR-150HZ	Vessel Core Inlet	$\pm$ 8 kg/m^3 at 750 kg/m^3 to $\pm$ 5 kg/m^3 at densities near zero
	Pressure	
PV-UP+10	Vessel Upper Plenum	$\pm$ 5 x 10^4 N/m^2
PV-LP-166	Vessel Lower Plenum	$\pm$ 4 x 10^4 N/m^2

TABLE 1. (continued)

Instrument Designation	Approximate Location	Uncertainty
PU-PRIZE	Pressurizer	$\pm$ 4 x 10^4 N/m^2
PU-ACC	Intact Loop Accumulator	$\pm$ 2 x 10^4 N/m^2
PB-ACC	Broken Loop Accumulator	$\pm$ 2 x 10^4 N/m^2
	Differential Pressure	
DPU-3-7	Intact Loop across Steam Generator	$\pm$ 2 x 10^3 N/m^2
DPU-12-10	Intact Loop across Pump	$\pm$ 2 x 10^3 N/m^2
DPB-38-40	Broken Loop across Simulated Pump	$\pm$ 1.2 x 10^5 N/m^2
	Fluid Temperature	
RBU-2	Intact Loop Hot Leg	$\pm$ 3 K
TFU-10	Intact Loop Cold Leg	$\pm$ 3 K
TFU-148	Intact Loop Cold Leg	$\pm$ 3 K
TFB-30	Broken Loop Hot Leg	$\pm$ 3 K
TFB-20	Broken Loop Cold Leg	$\pm$ 3 K

TABLE 2. INITIAL CONDITIONS FOR TRAC-P1A SIMULATION OF LOCE S-04-6

Quantity	TRAC-P1A	S-04-6
Intact Loop Volumetric Flow (m^3/s)	9.11×10^{-3}	8.89×10^{-3}
Pressurizer Pressure (MPa)	15.5	15.5
System Pressure (MPa)	15.5	15.5
Suppression Tank Pressure (MPa)	0.241	0.241
Intact Loop Fluid Temperature (K)		
Hot Leg Near Vessel	598.6	593.0
Cold Leg Near Pump	560.1	557.4
Cold Leg Near Vessel	560.1	554.7
Broken Loop Fluid Temperature (K)		
Hot Leg Near Vessel	589.7	589.7
Hot Leg Near Nozzle	588.3	587.4
Cold Leg Near Vessel	554.7	556.3
Cold Leg Near Nozzle	554.7	554.7
Lower Plenum Fluid Temperature (K)	560.2	557.4
Reactor Power (MW)	1.44	1.44

TABLE 3. SUMMARY OF KEY INDICATORS FOR TRAC-P1A SIMULATION OF LOCE S-04-6

Key Indicator	Simulation	Experiment
Time to reach HPIS activation	0 s *	0 s *
Time of start of accumulator discharge	14 s	17 s [7]
Time when upper plenum pressure equaled 1 MPa	28 s	26 s
Time when mass in lower plenum equaled 1.1 times minimum mass after this minimum occurred	24 s	not known
Time when sustained core reflood began	did not occur	57 s [7]
Time when core inlet flow was zero after first negative flow cycle.	0.95 s	3 s
Time of first quench of hot spot	did not occur	did not occur during first 60 s
Time of second quench of hot spot	did not occur	did not occur during first 60 s

TABLE 3. (continued)

Key Indicator	Simulation	Experiment
Time of final quench of hot spot	did not occur	did not occur during first 60 s
Peak cladding temperature	975 K	1075 K

*HPIS flow was present at the beginning of the experiment.

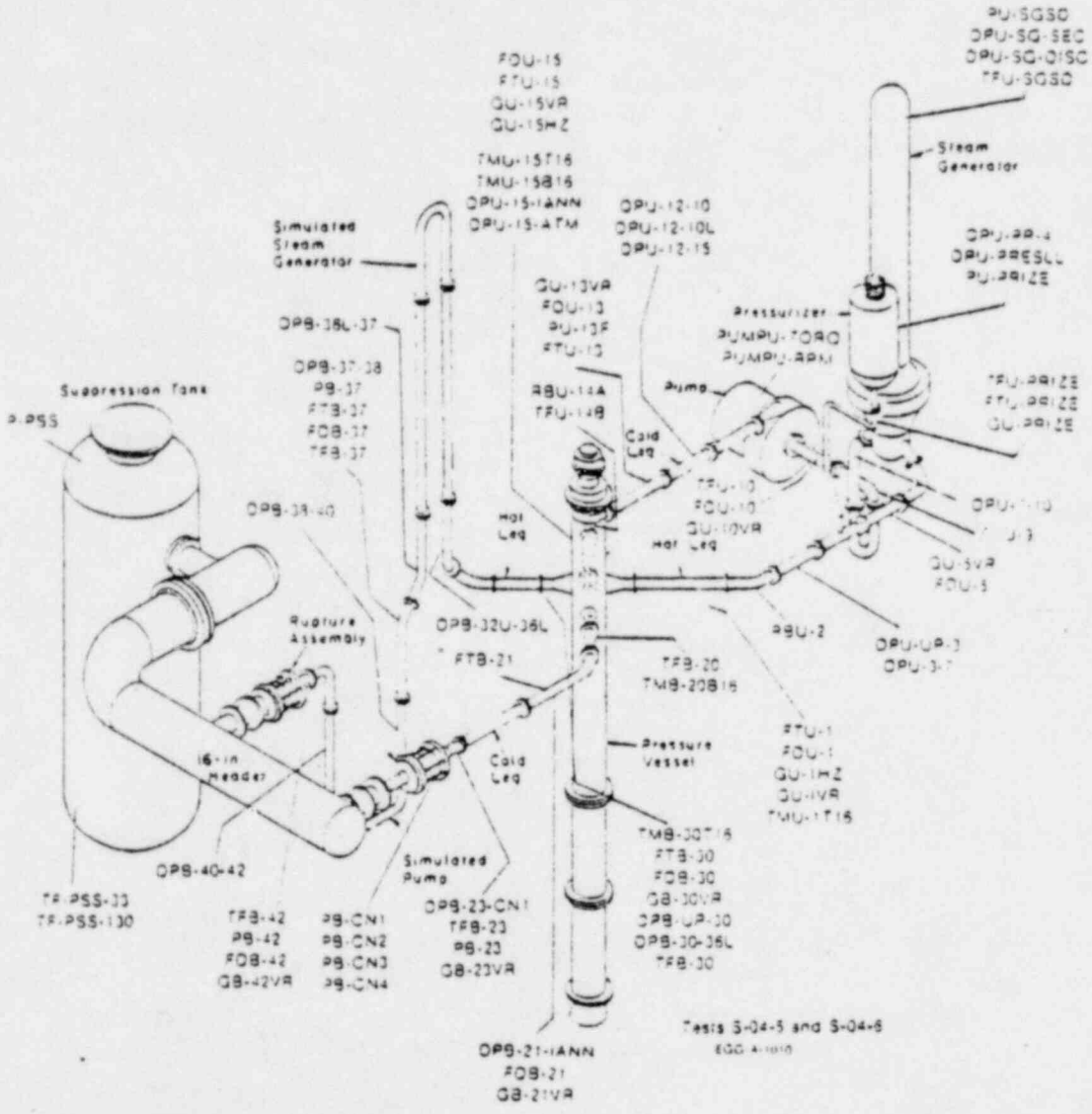

Figure 1. Semiscale Mod-1 system and instrumentation for cold leg break configuration.

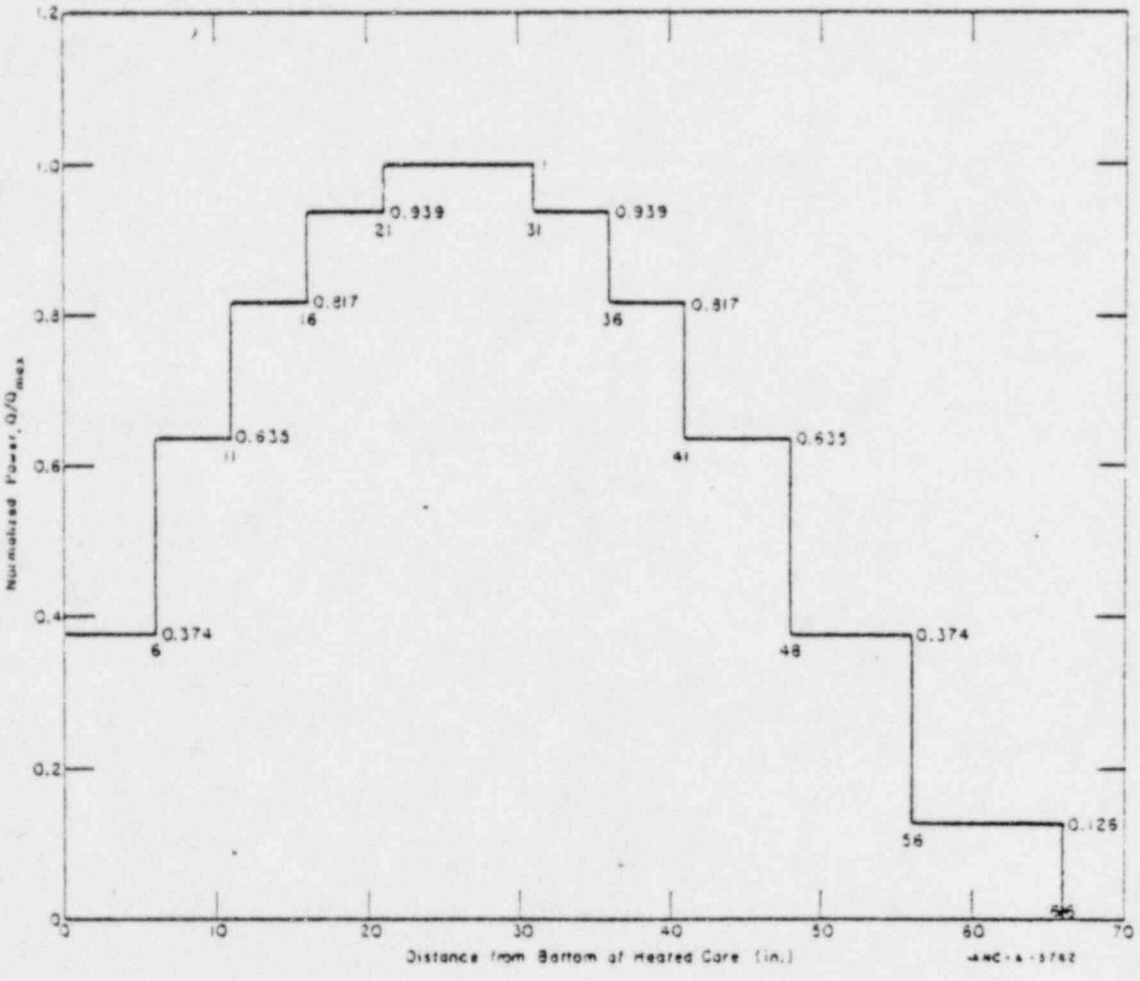

Figure 2. Semiscale Mod-1 heated rod axial power profile.

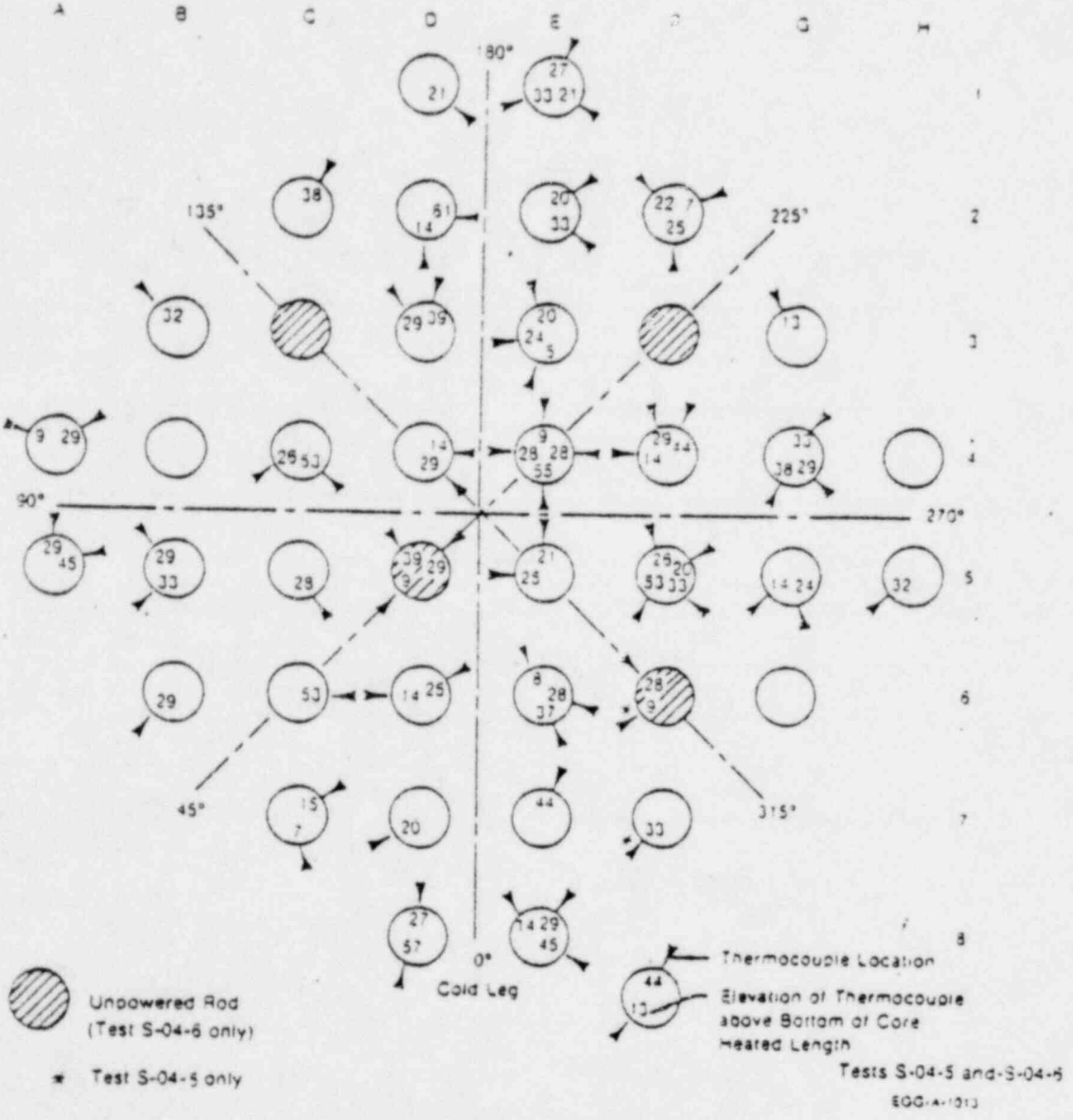

Figure 3. Semiscale Mod-1 heated core for LOCE S-04-6.

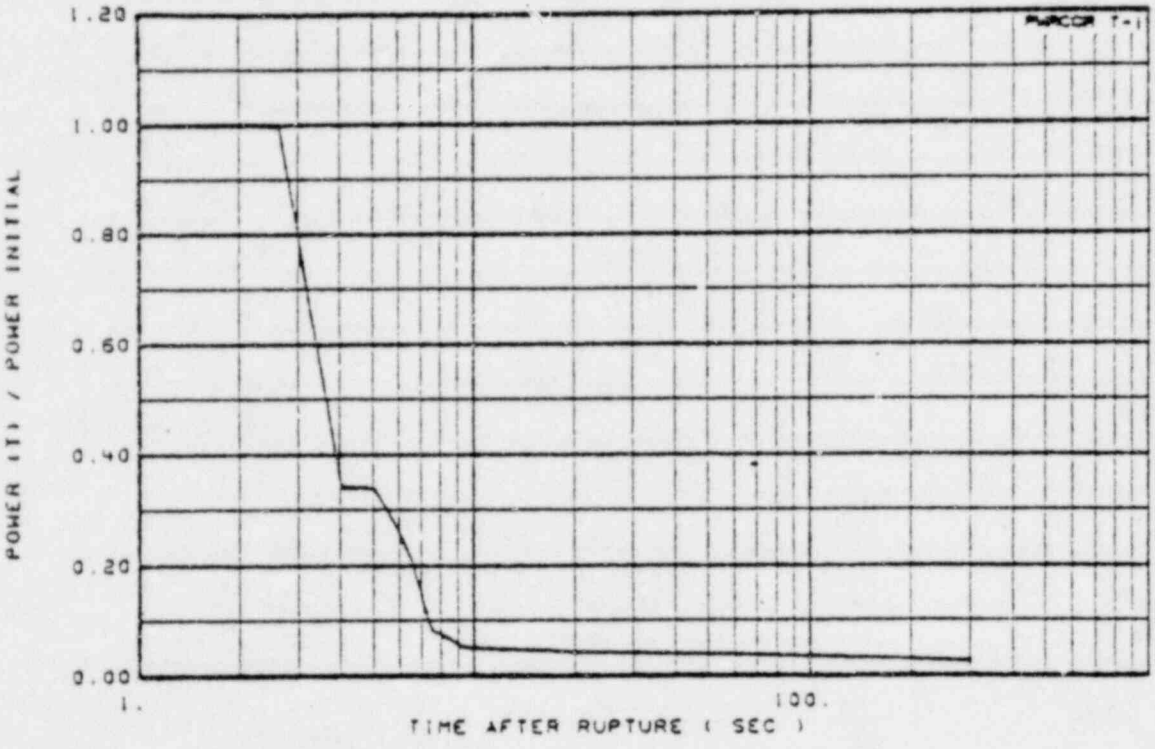

Figure 4. Core power control for baseline ECC tests.

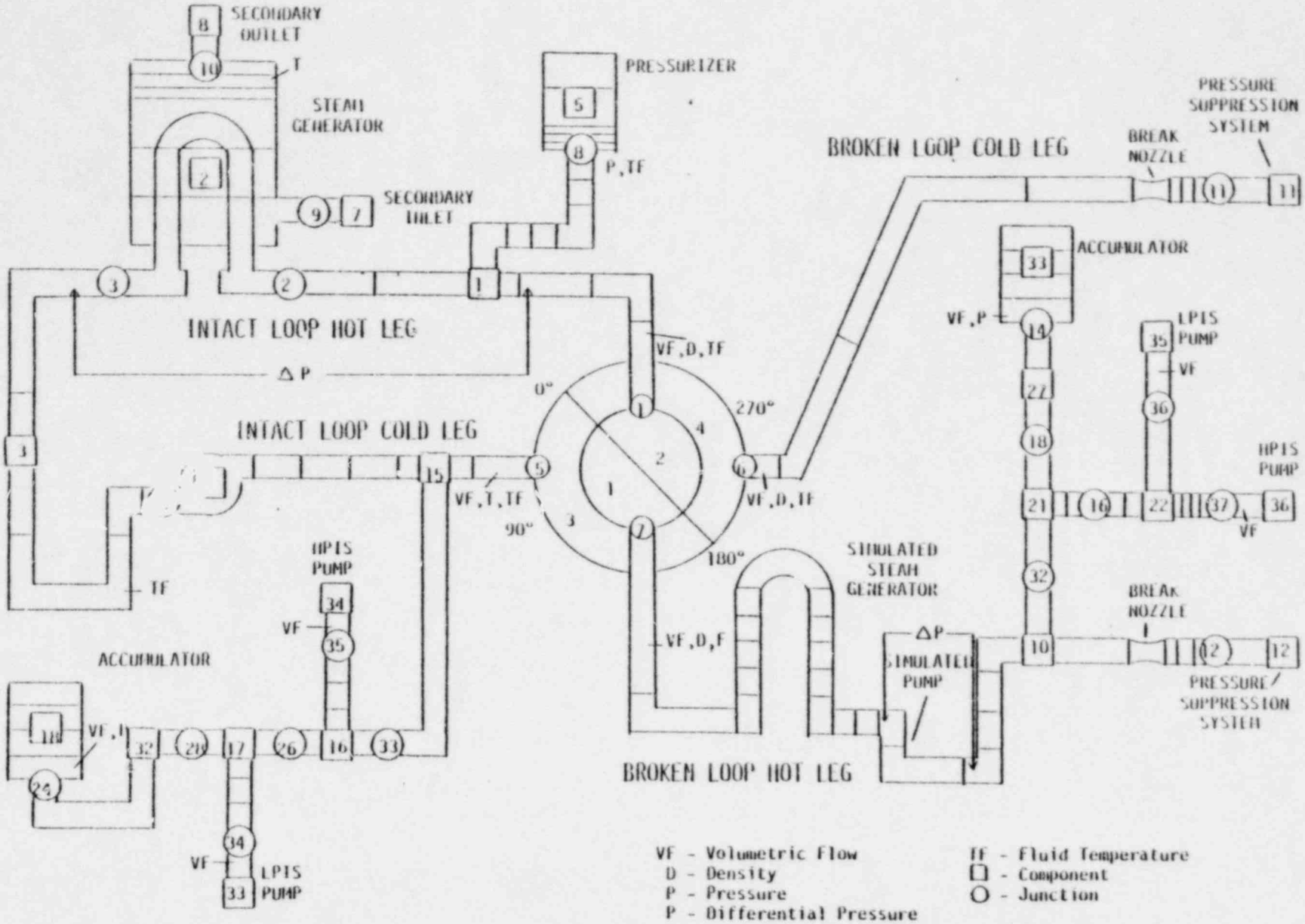

Figure 5. TRAC-P1A Semiscale Mod-1 system model nodalization and assessment measurement locations.

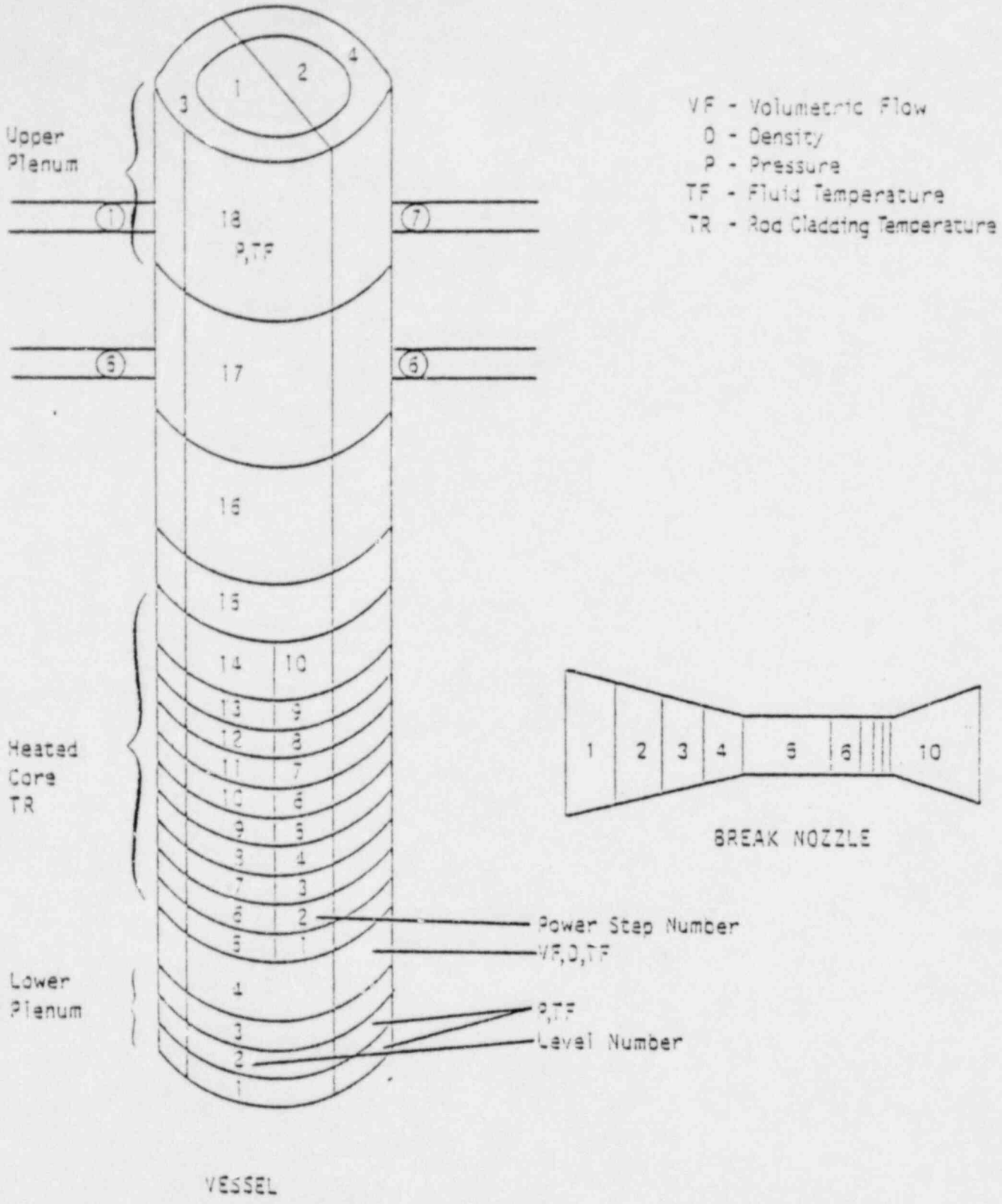

Figure 6. TRAC-P1A Semiscale Mod-1 model nodalization of the vessel and break nozzles.

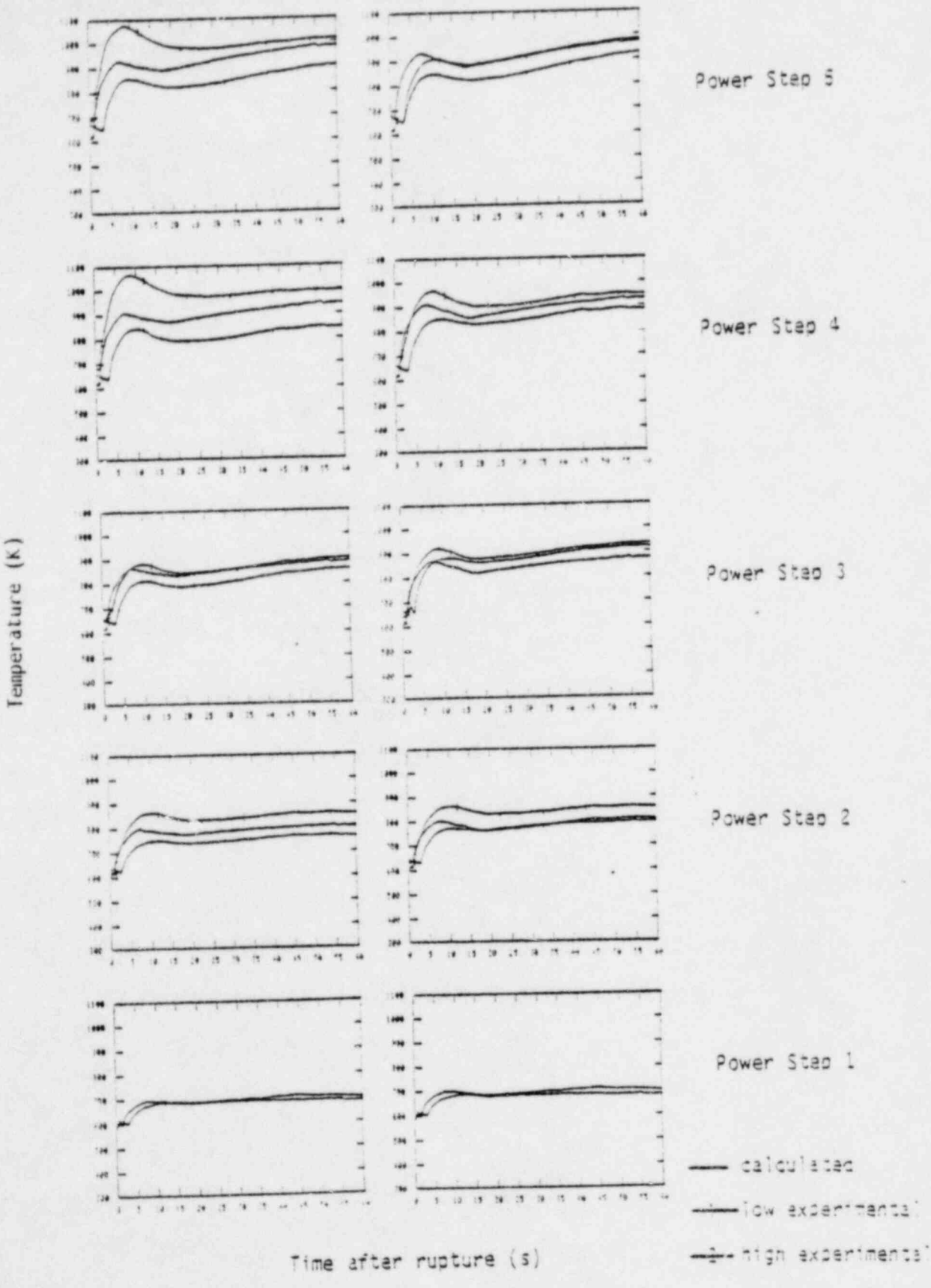

Figure 7. Rod cladding temperatures (Power Steps 1 through 5).

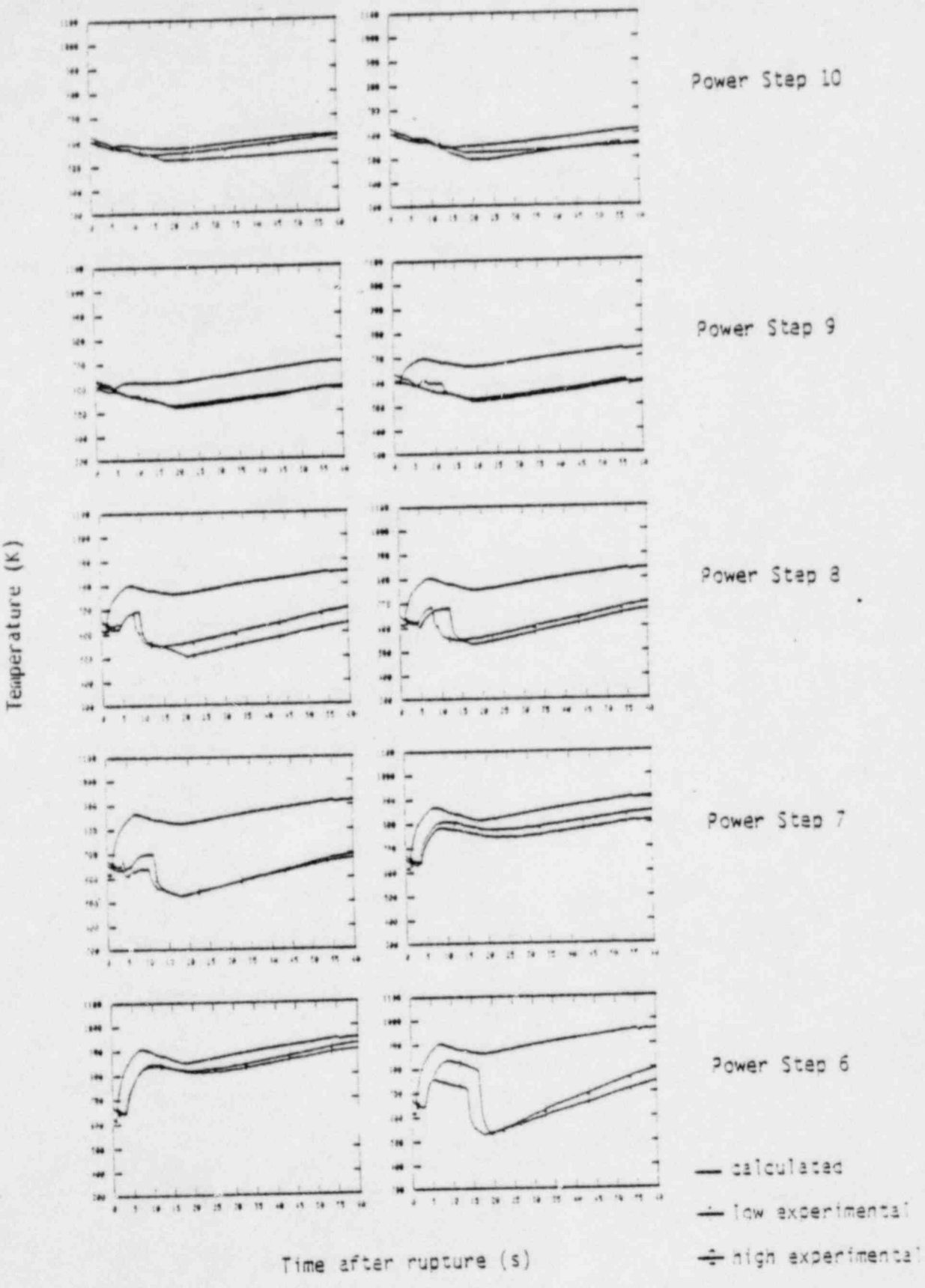

Figure 8. Rod cladding temperatures (Power Steps 6 through 10).

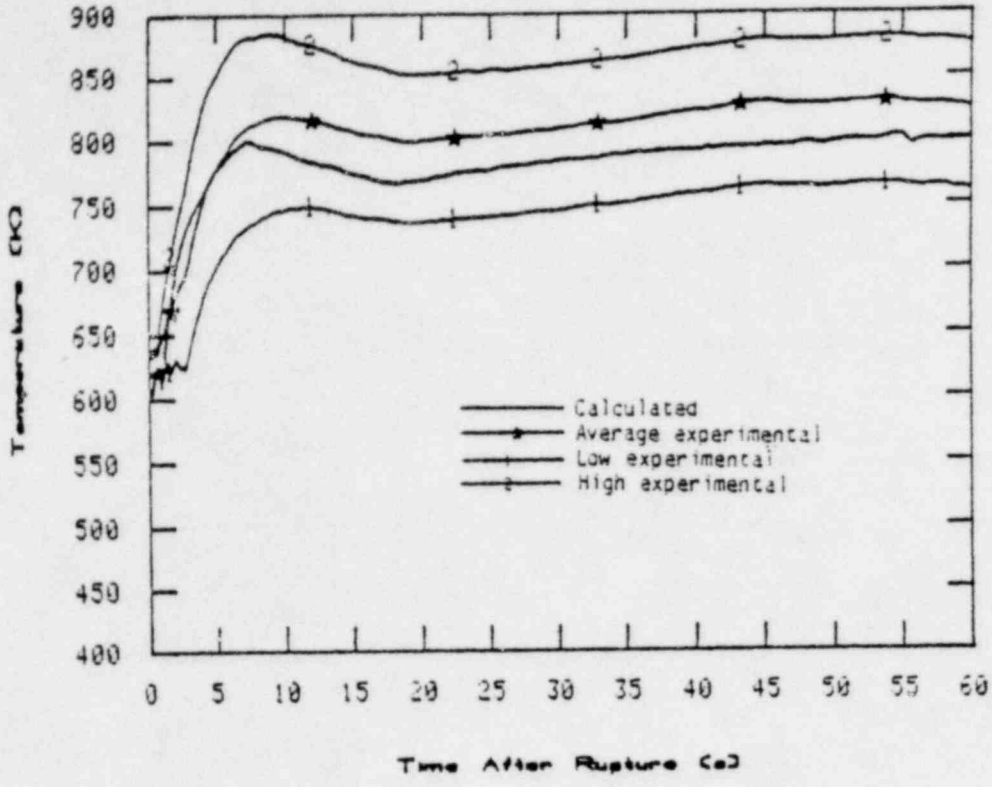

Figure 9. Rod cladding temperatures at power step 2.

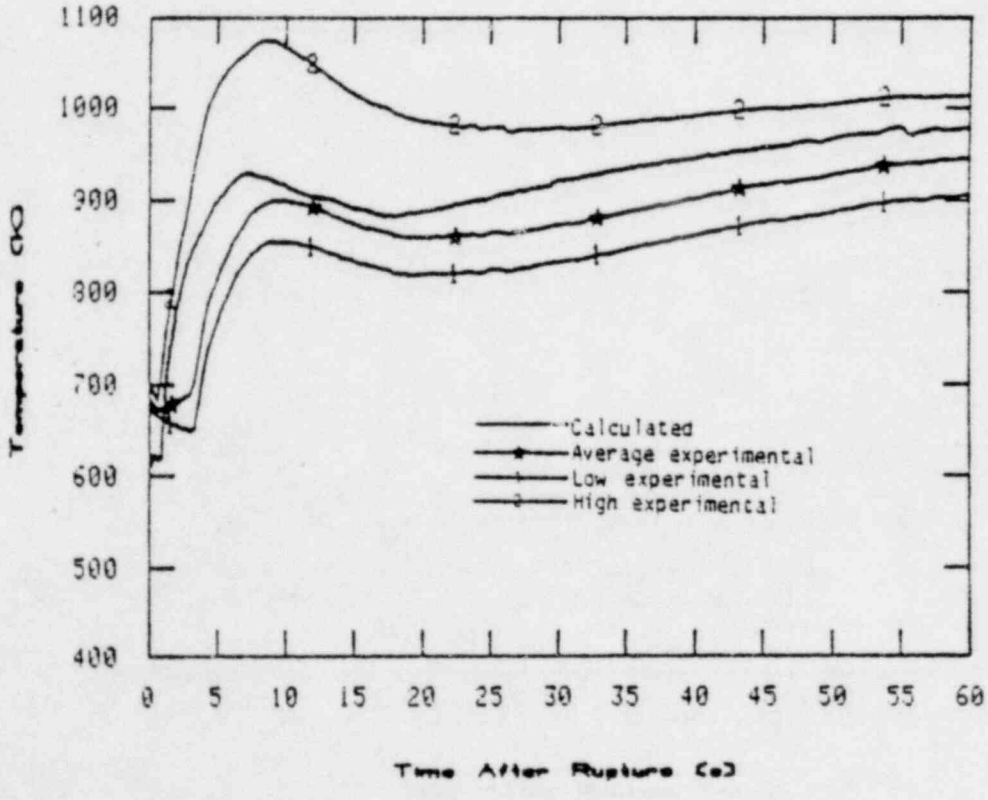

Figure 10. Rod cladding temperatures at power step 5.

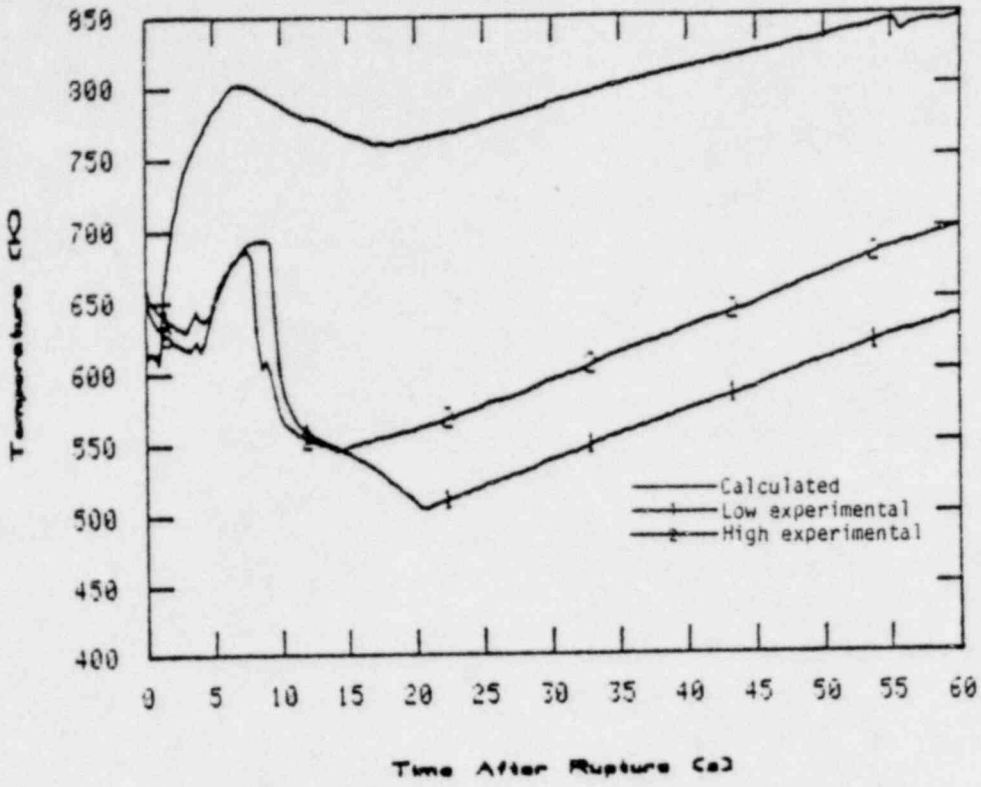

Figure 11. Rod cladding temperatures at power step 8.

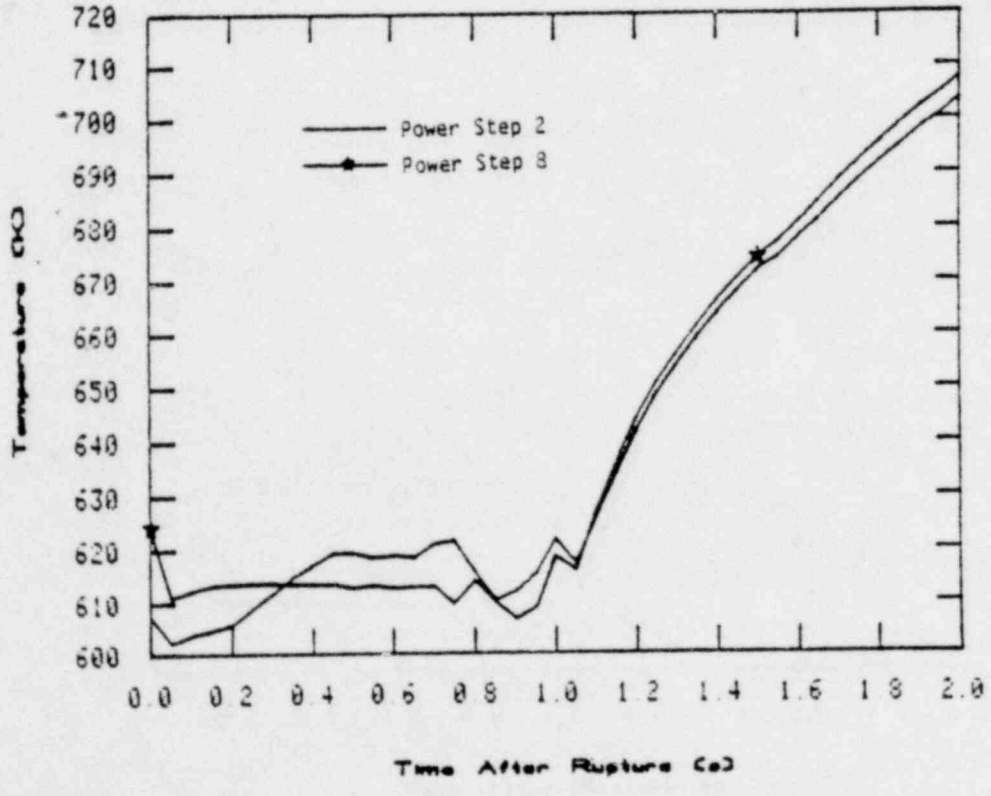

Figure 12. Calculated rod cladding temperatures at power steps 2 and 8.

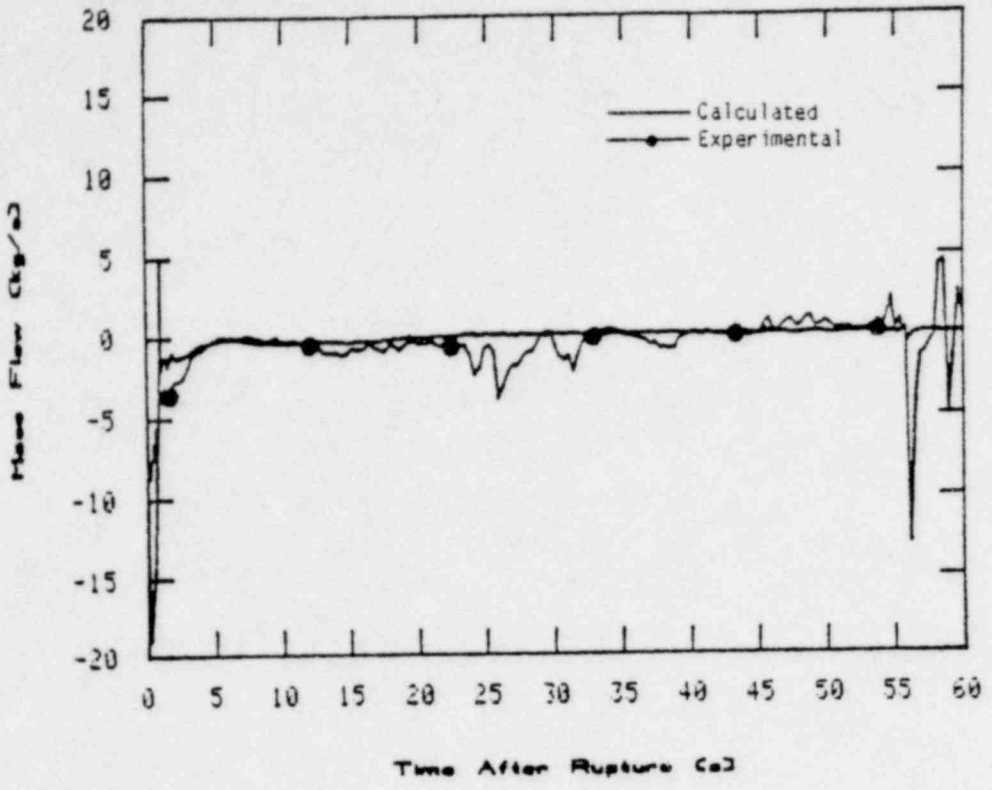

Figure 13. Mass flows at core inlet.

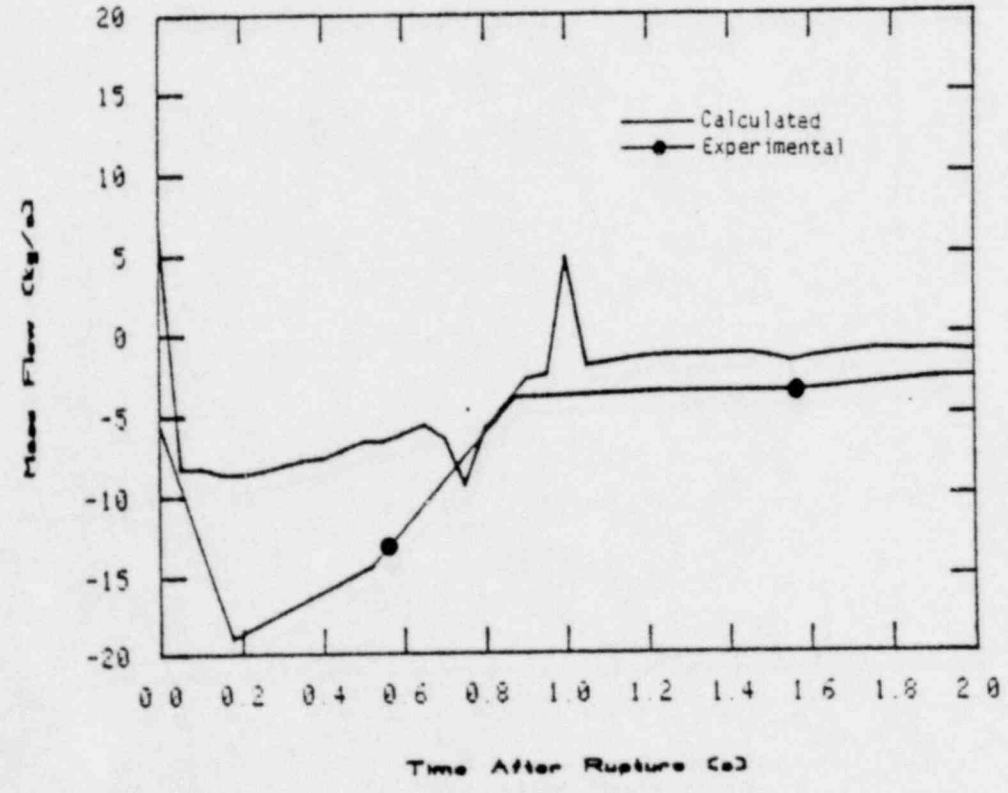

Figure 14. Mass flows at core inlet from 0 to 2 seconds.

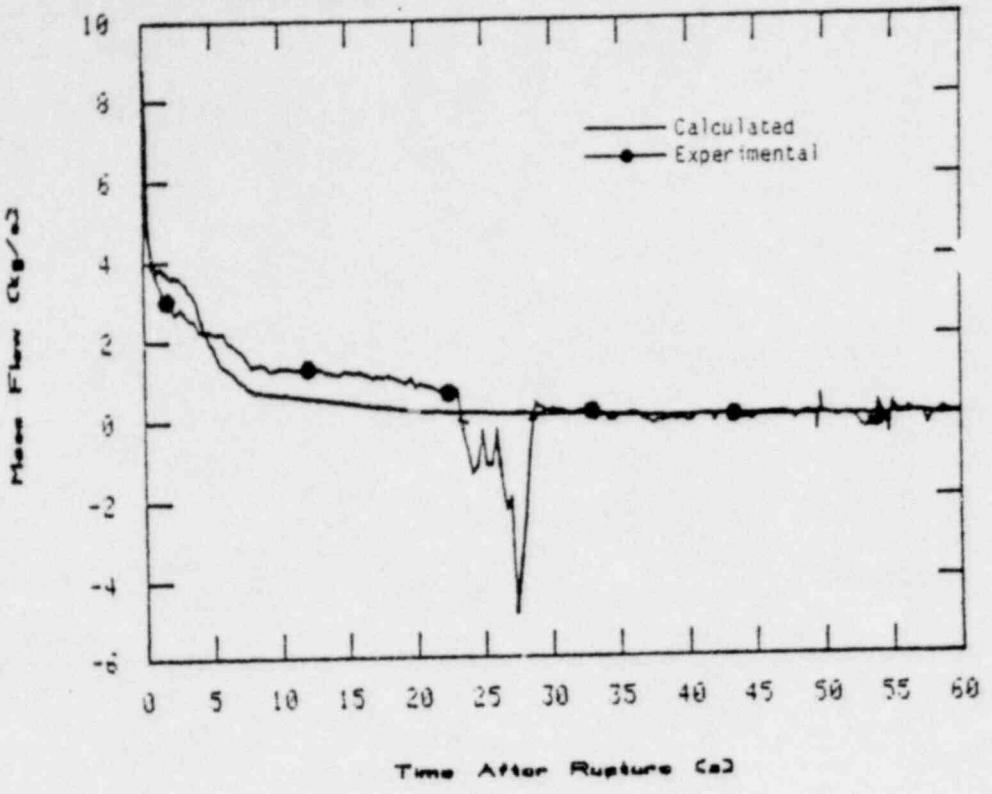

Figure 15. Mass flows in broken loop hot leg.

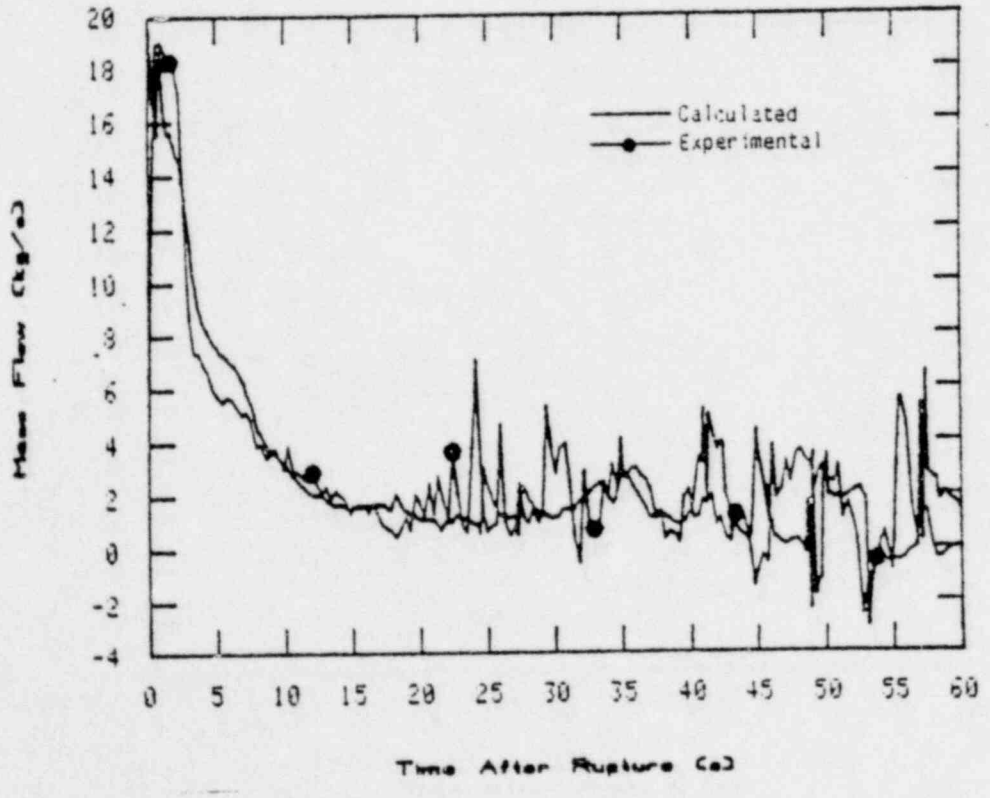

Figure 16. Mass flows in broken loop cold leg.

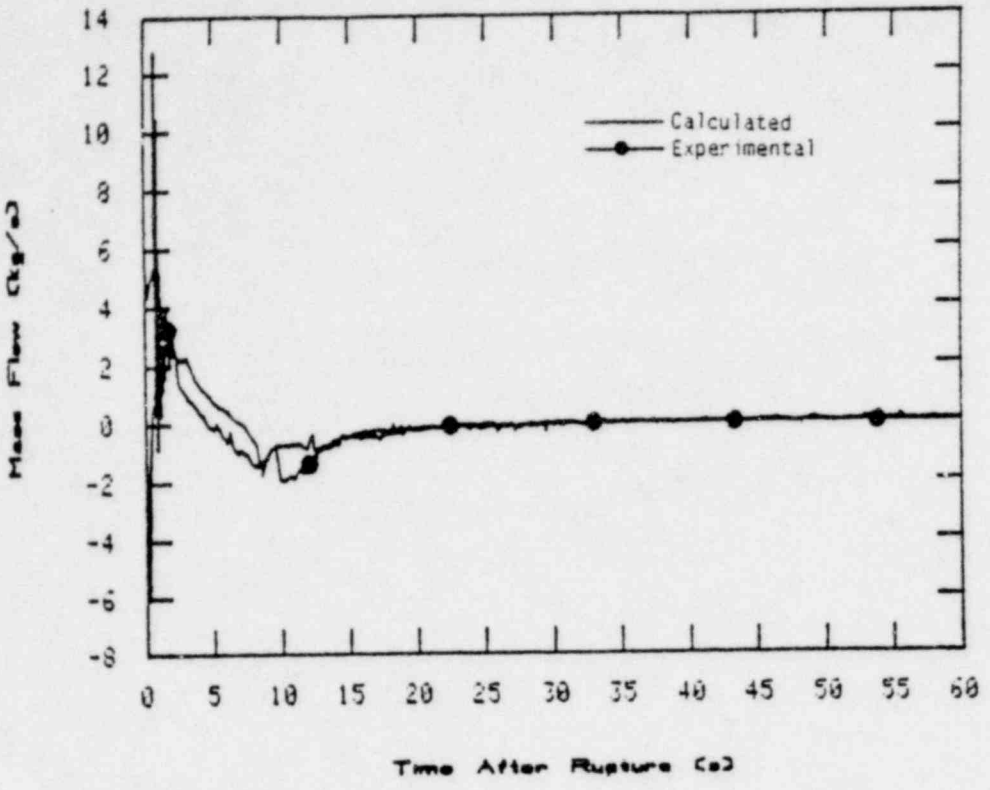

Figure 17. Mass flows in intact loop hot leg.

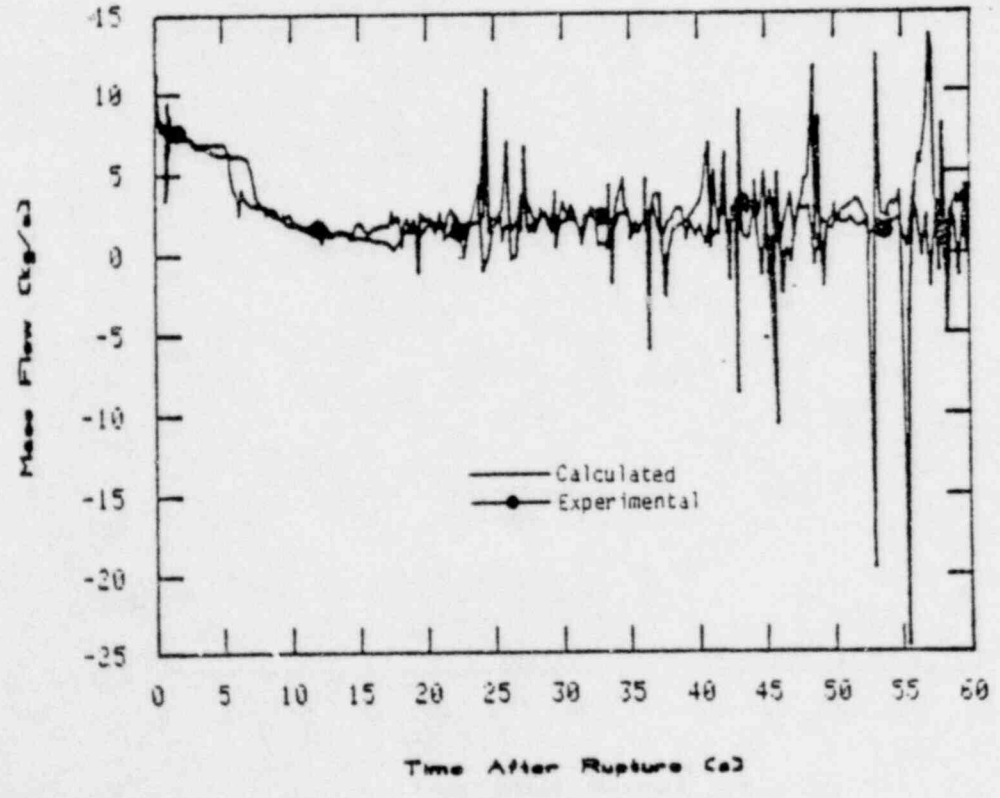

Figure 18. Mass flows in intact loop cold leg.

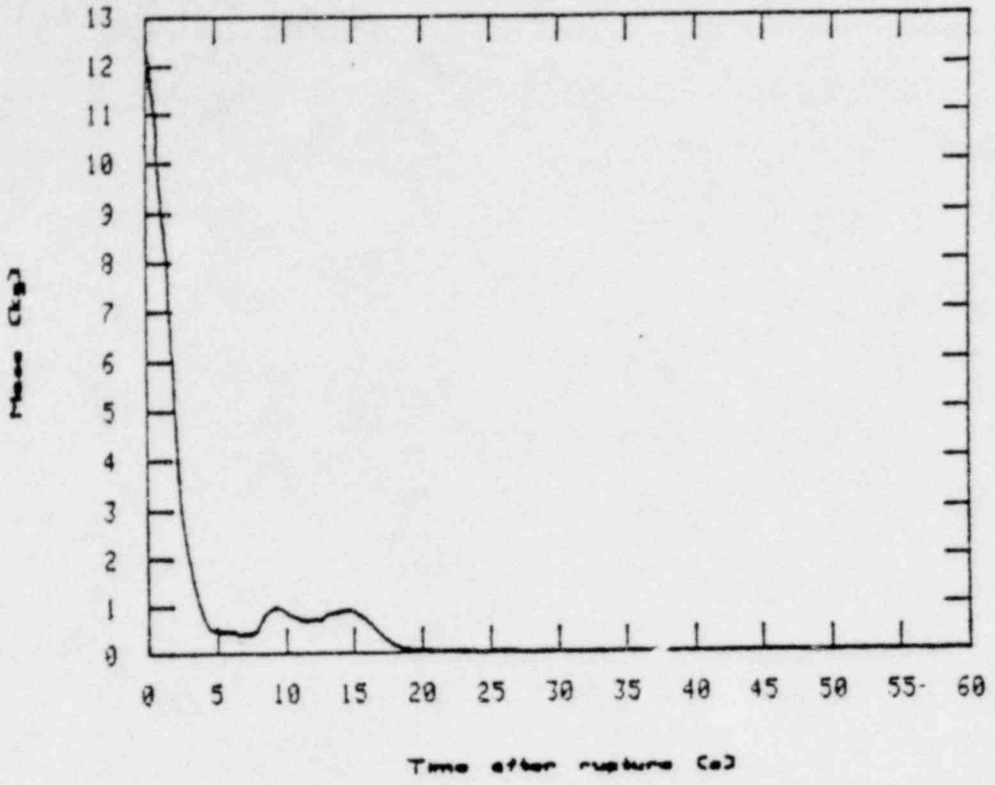

Figure 19. Calculated liquid mass in upper plenum.

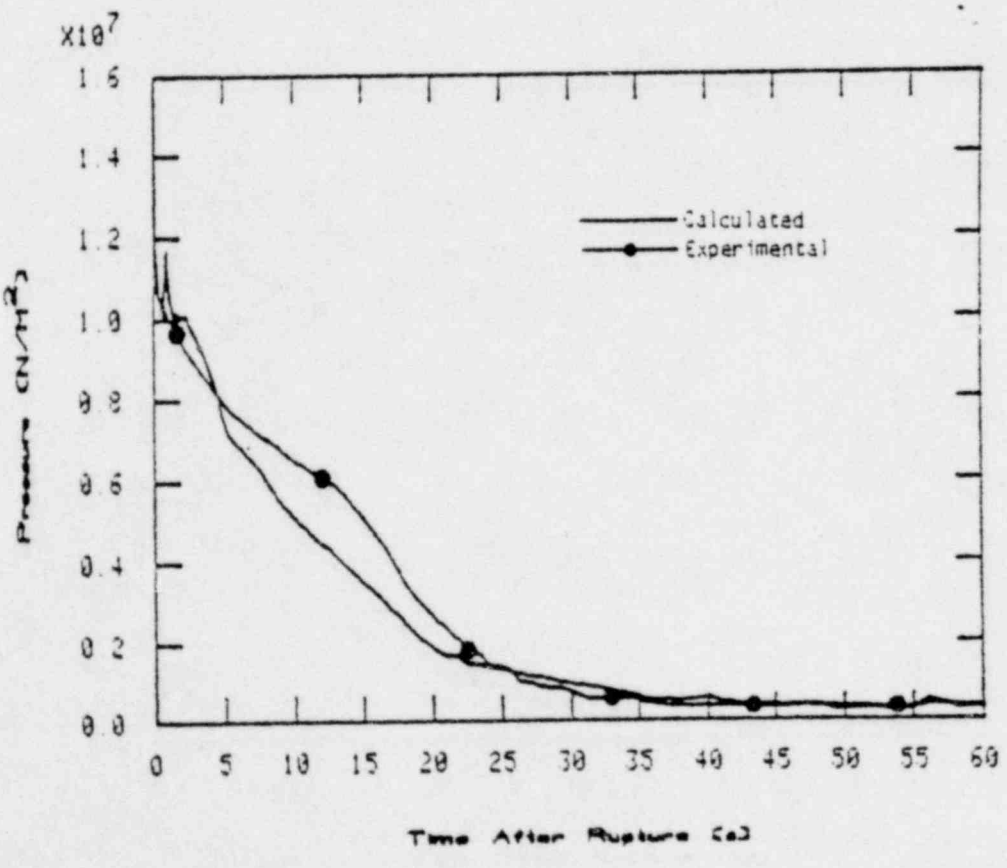

Figure 20. System pressures.

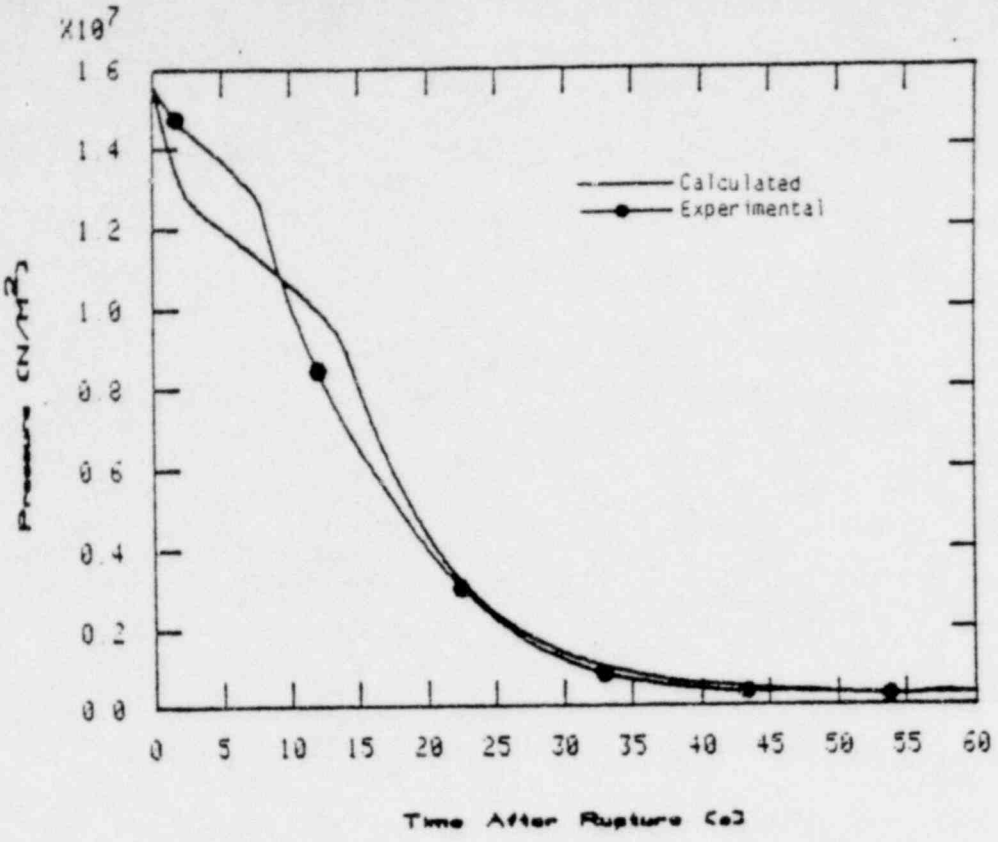

Figure 21. Pressures in pressurizer.

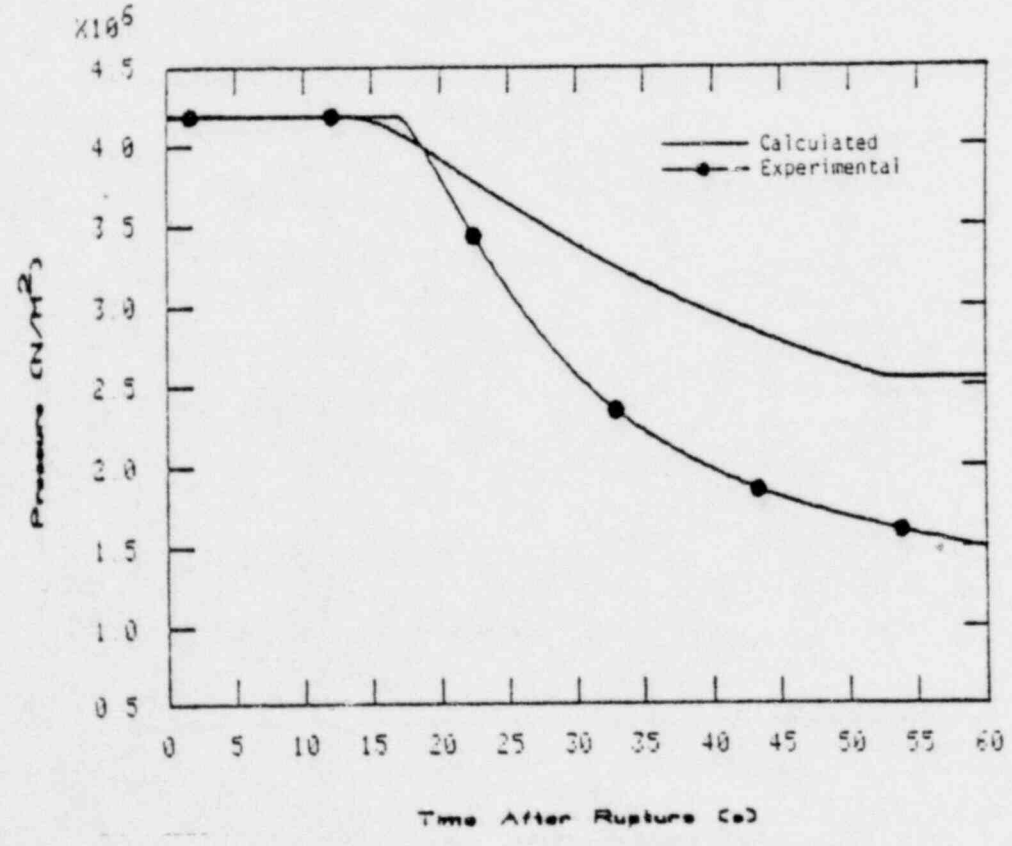

Figure 22. Pressures in intact loop accumulator.

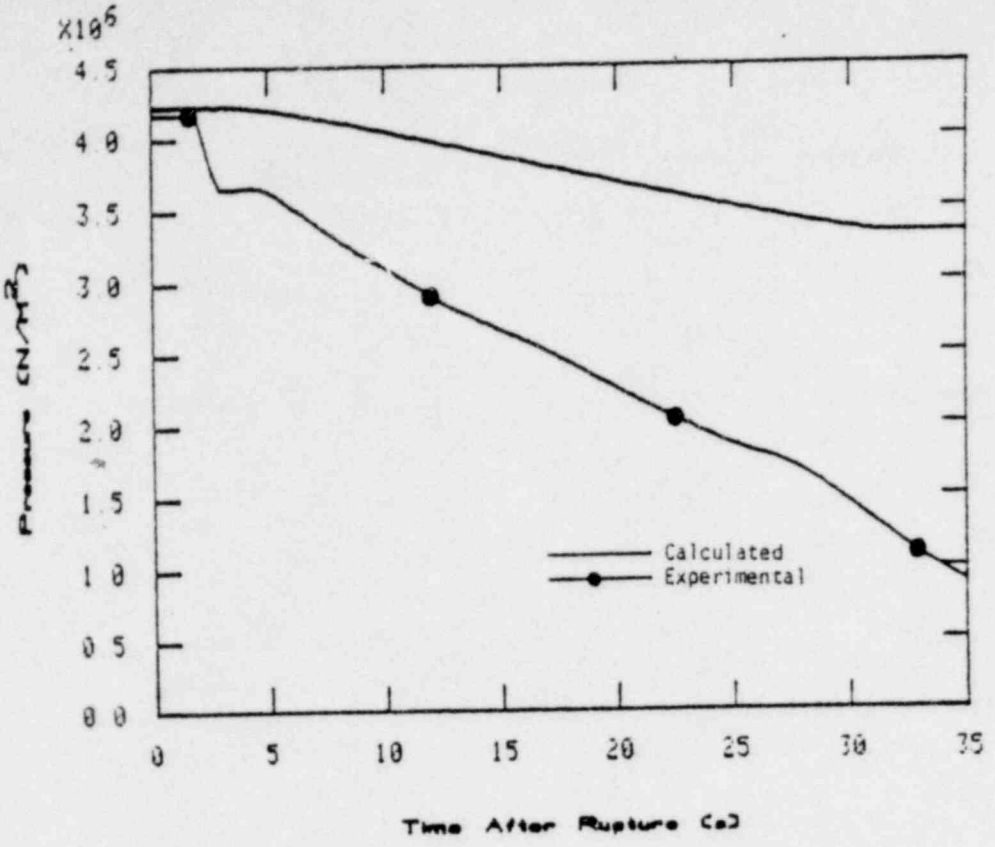

Figure 23. Pressures in broken loop accumulator.

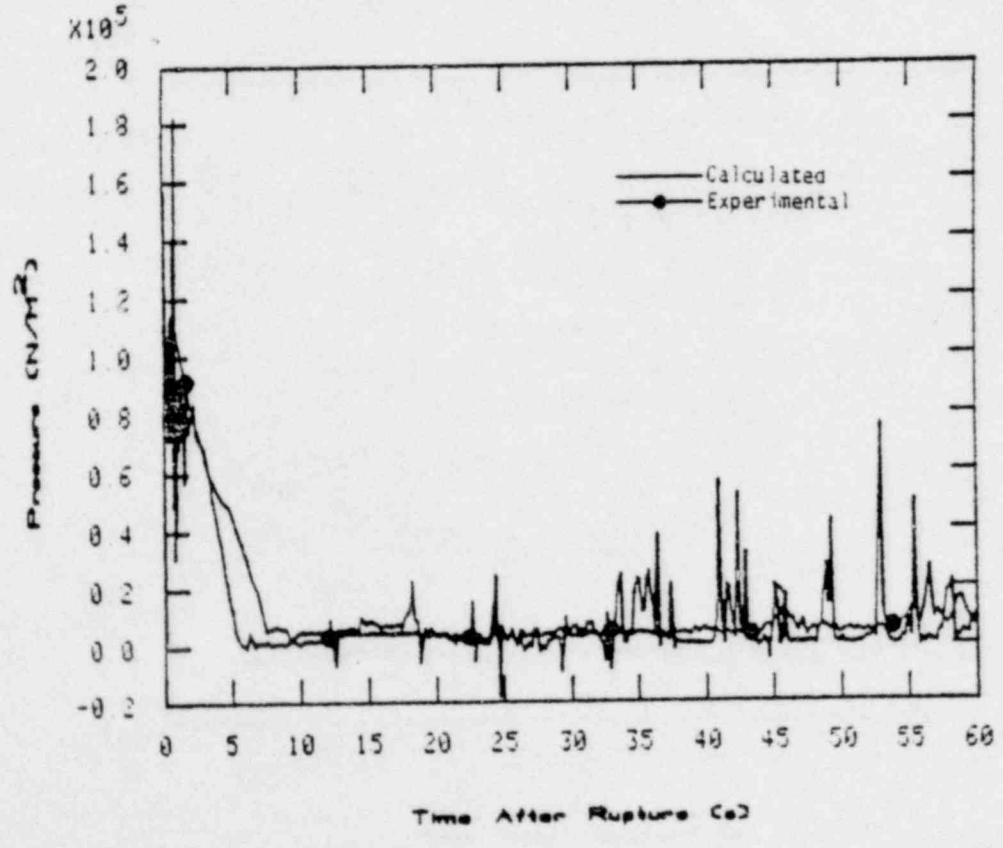

Figure 24. Differential pressures across steam generator.

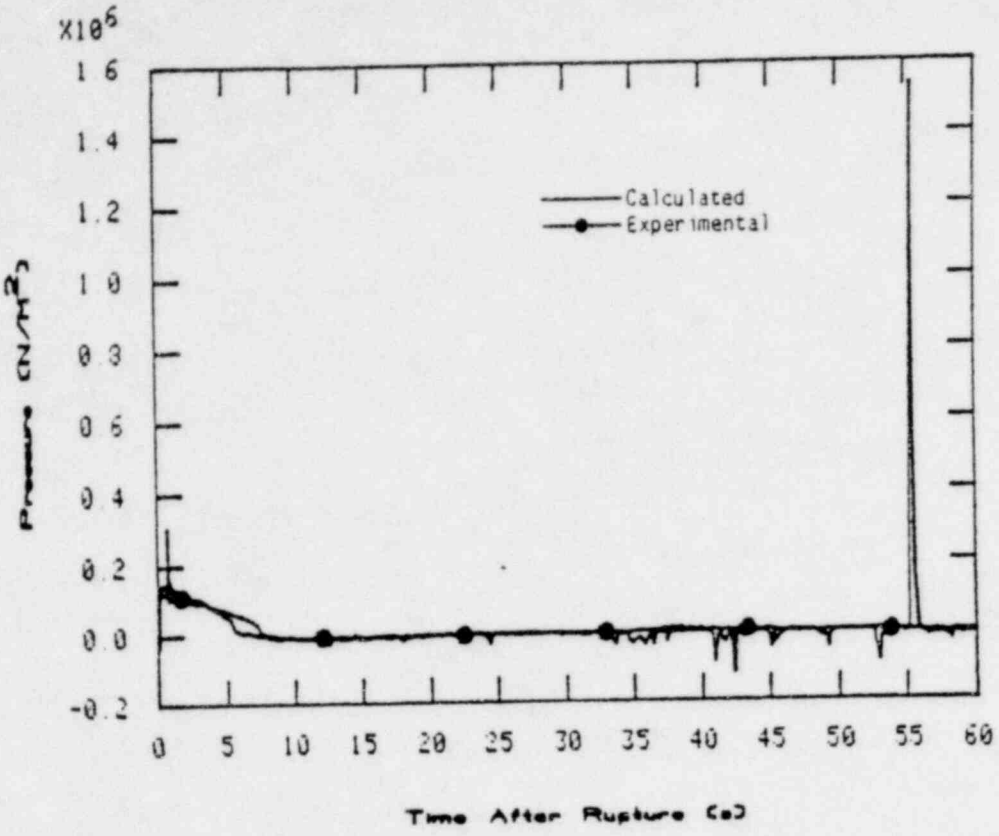

Figure 25. Differential pressures across pump.

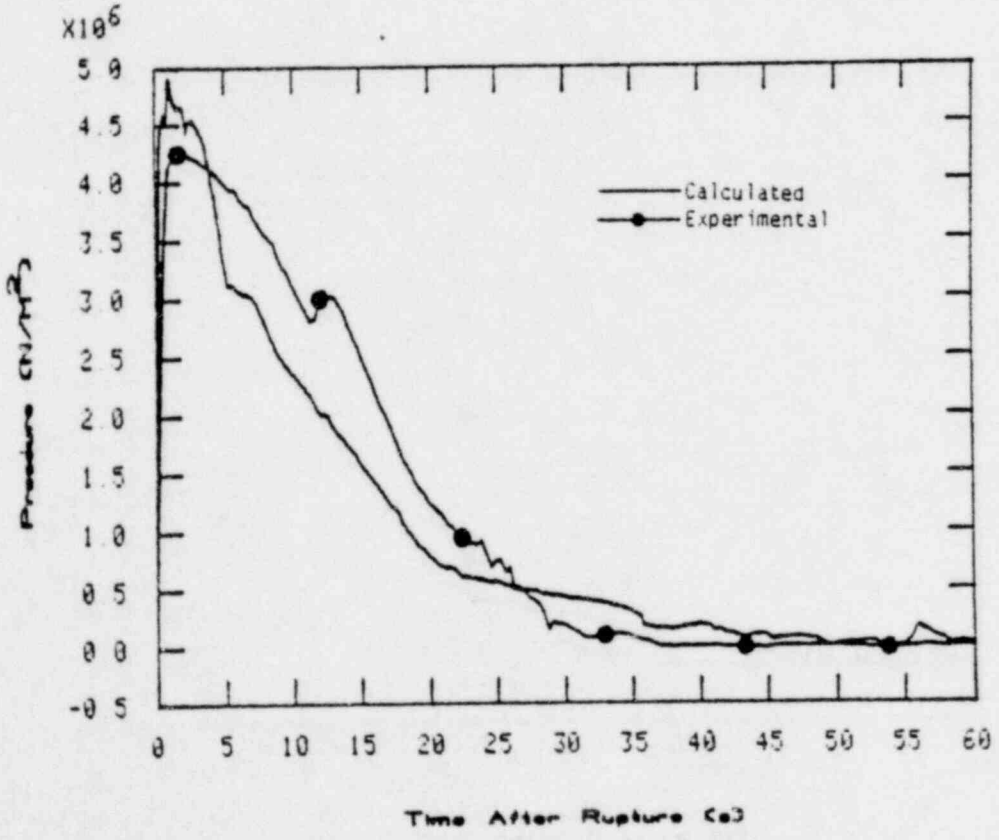

Figure 26. Differential pressures across simulated pump.

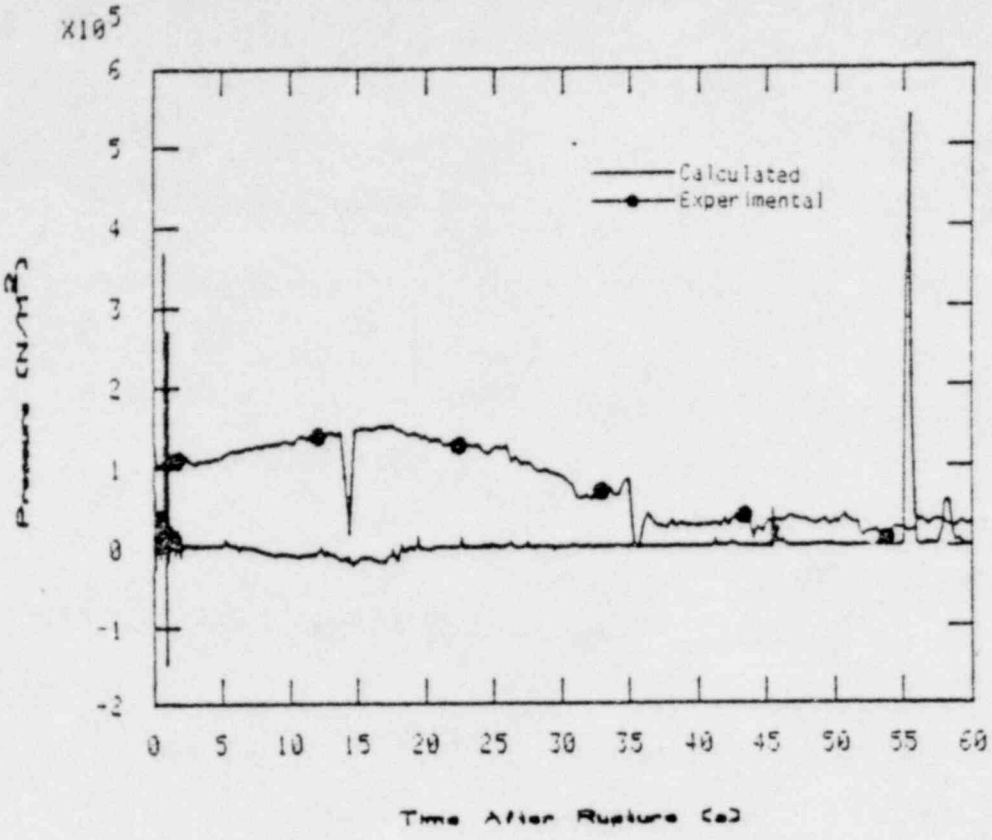

Figure 27. Differential pressures across vessel.

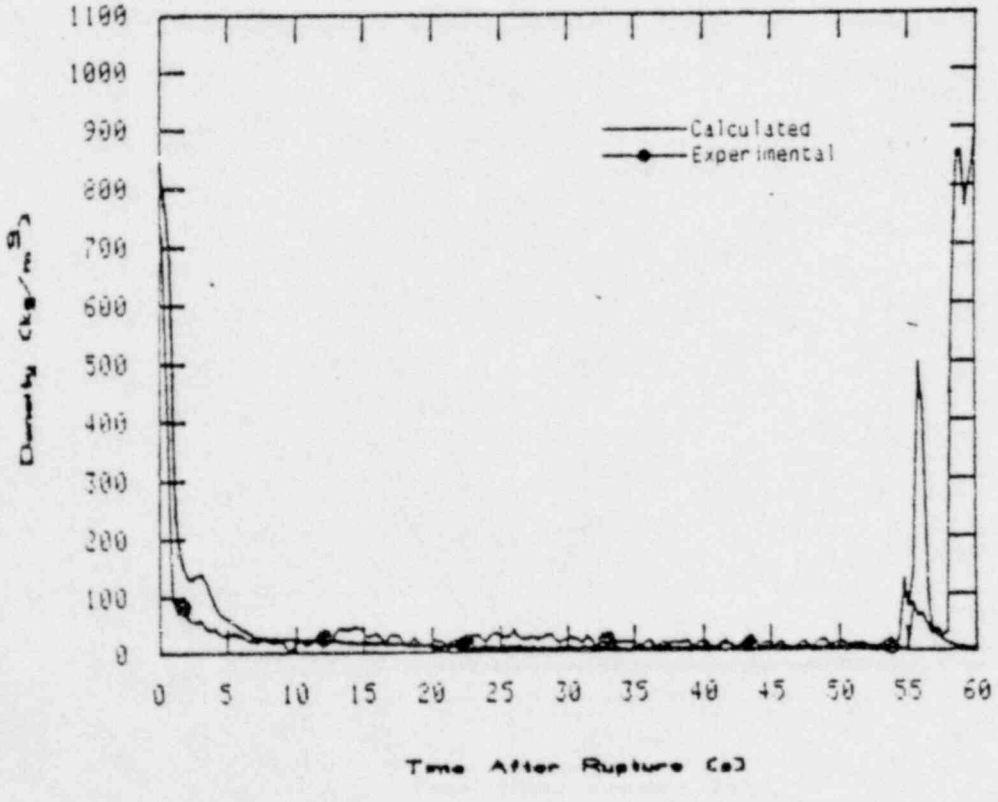

Figure 28. Densities in core inlet.

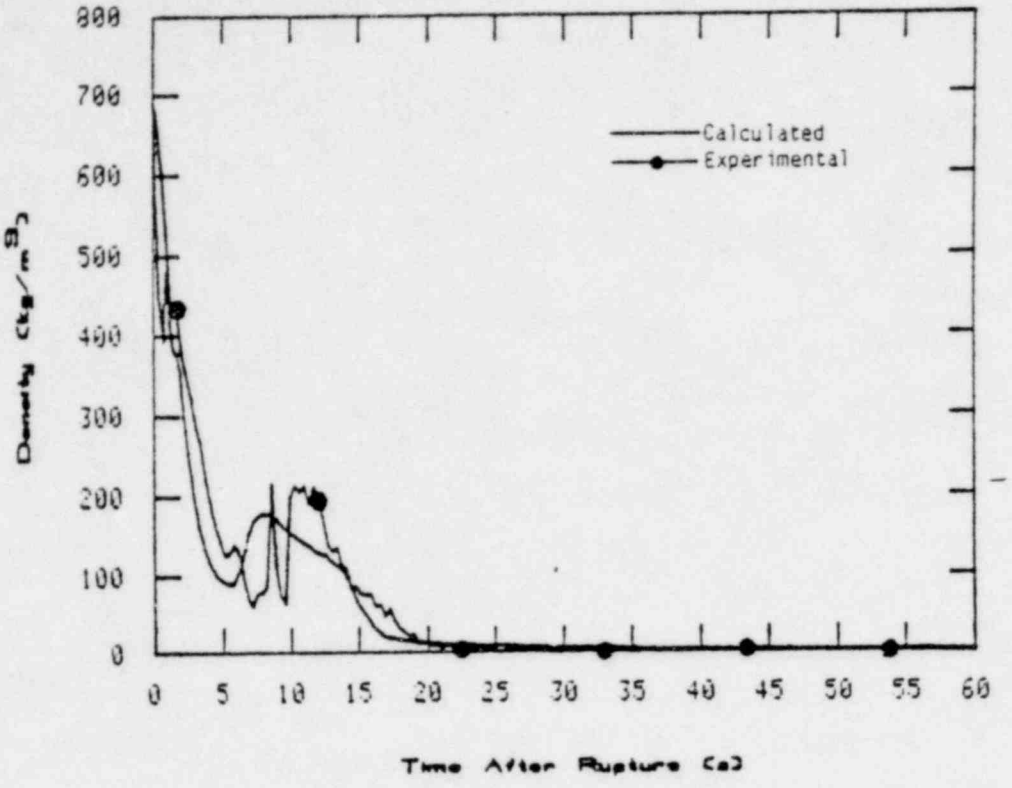

Figure 29. Densities in broken loop hot leg.

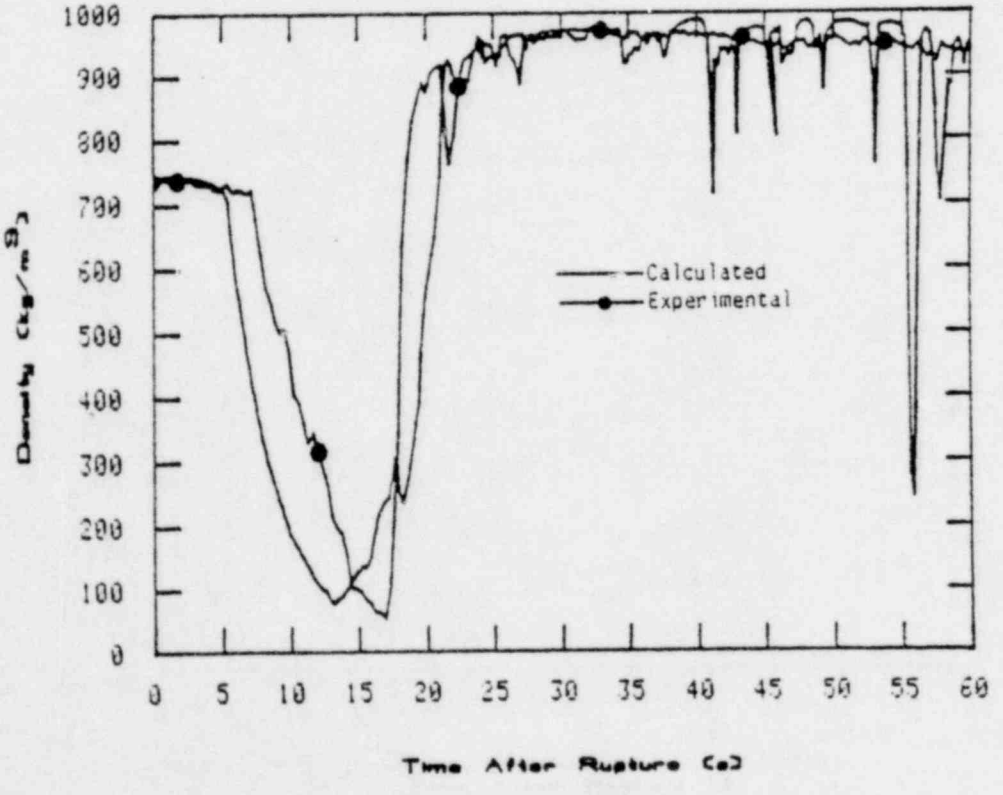

Figure 30. Densities in broken loop cold leg.

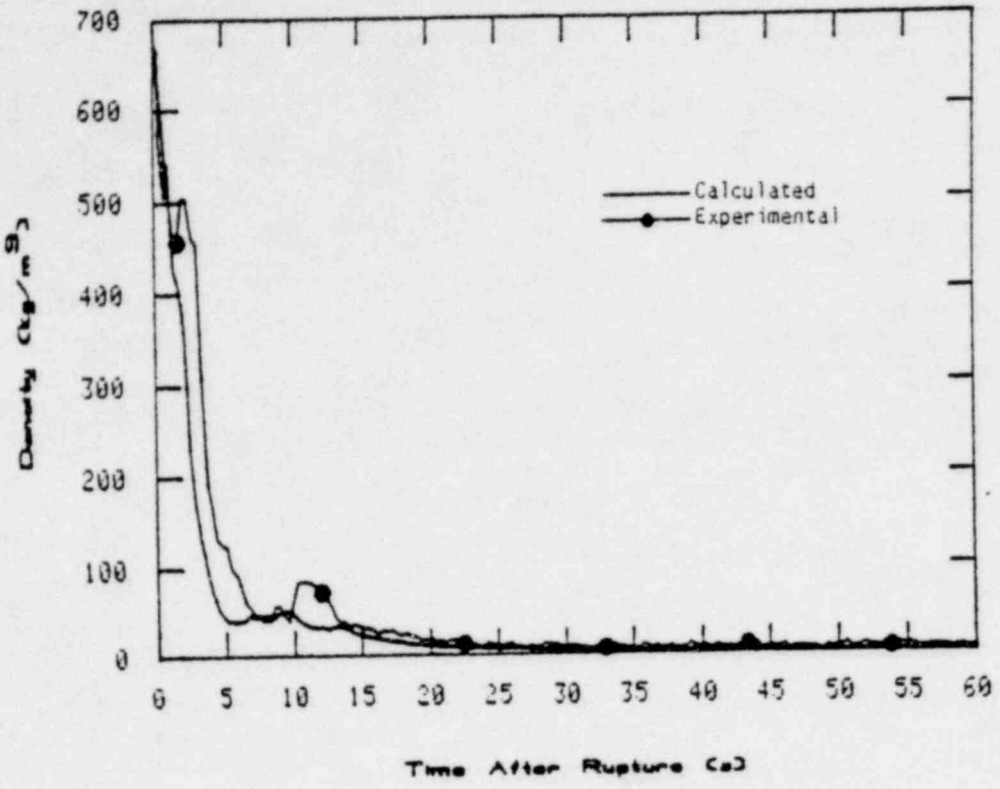

Figure 31. Densities in intact loop hot leg.

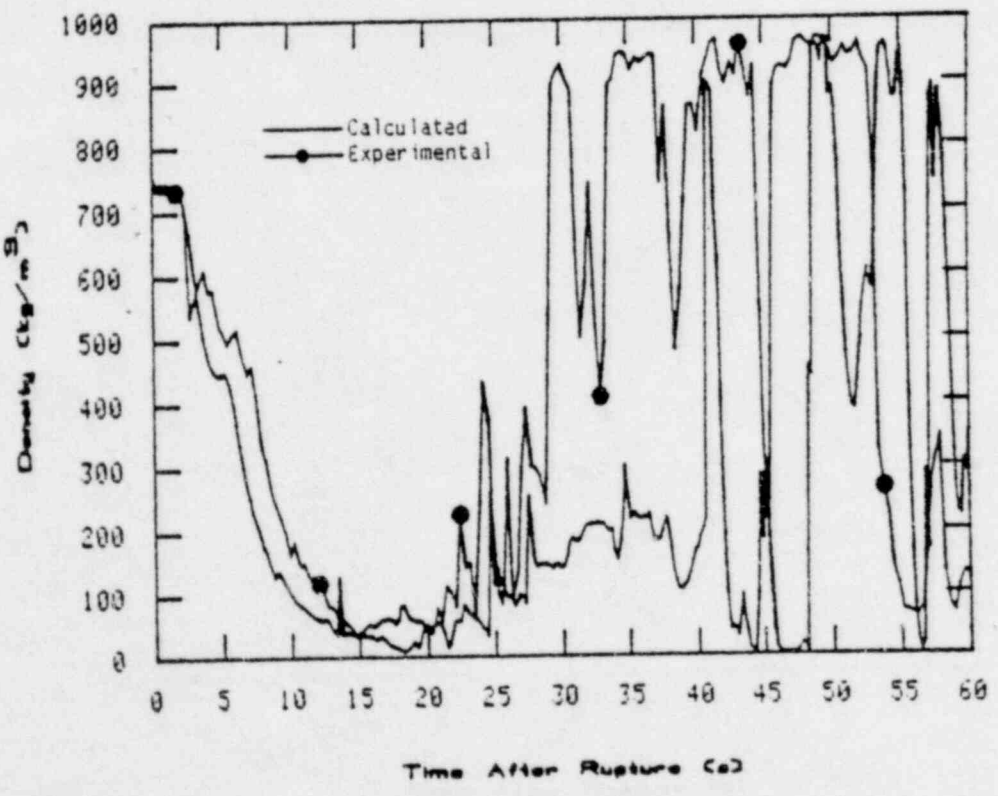

Figure 32. Densities in intact loop cold leg.

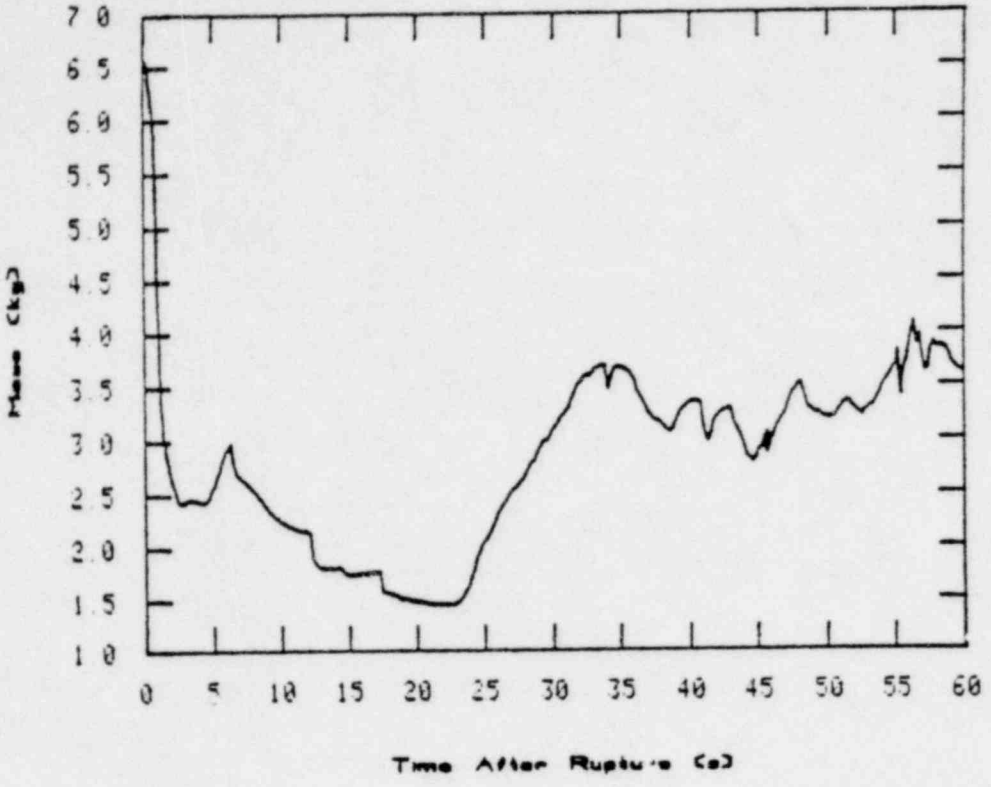

Figure 33. Fluid mass in lower plenum.

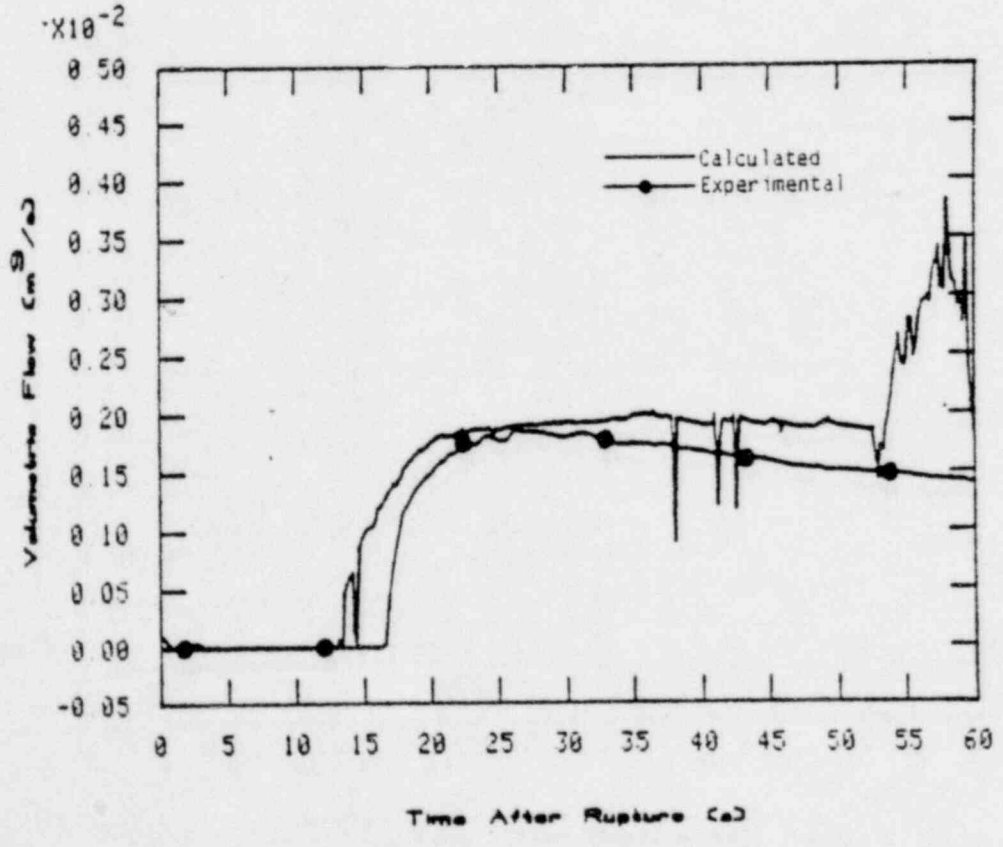

Figure 34. Volumetric flows in intact loop accumulator.

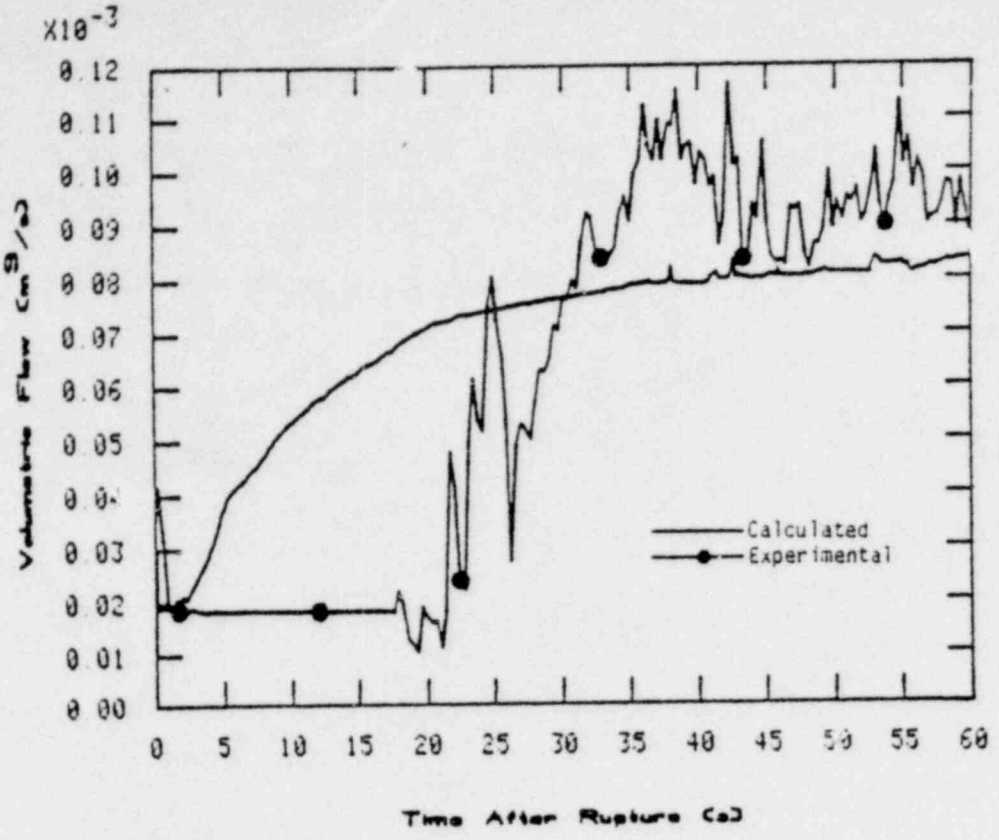

Figure 35. Volumetric flows in intact loop HPIS pump.

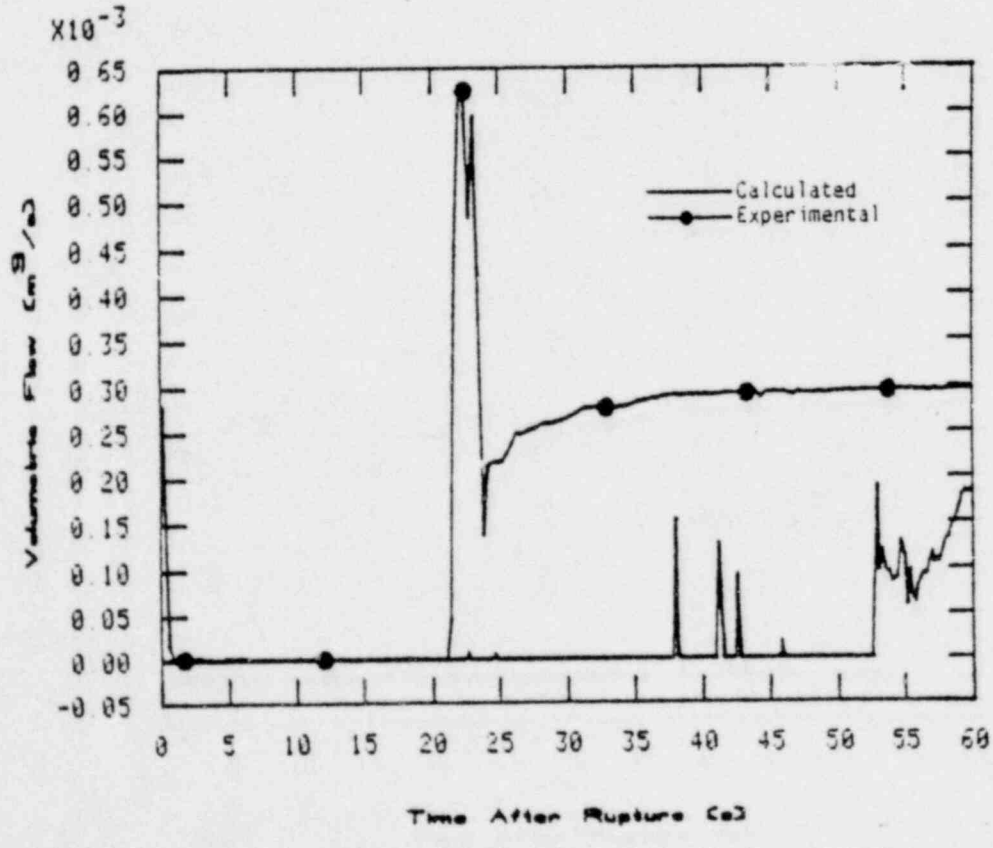

Figure 36. Volumetric flows in intact loop LPIS pump.

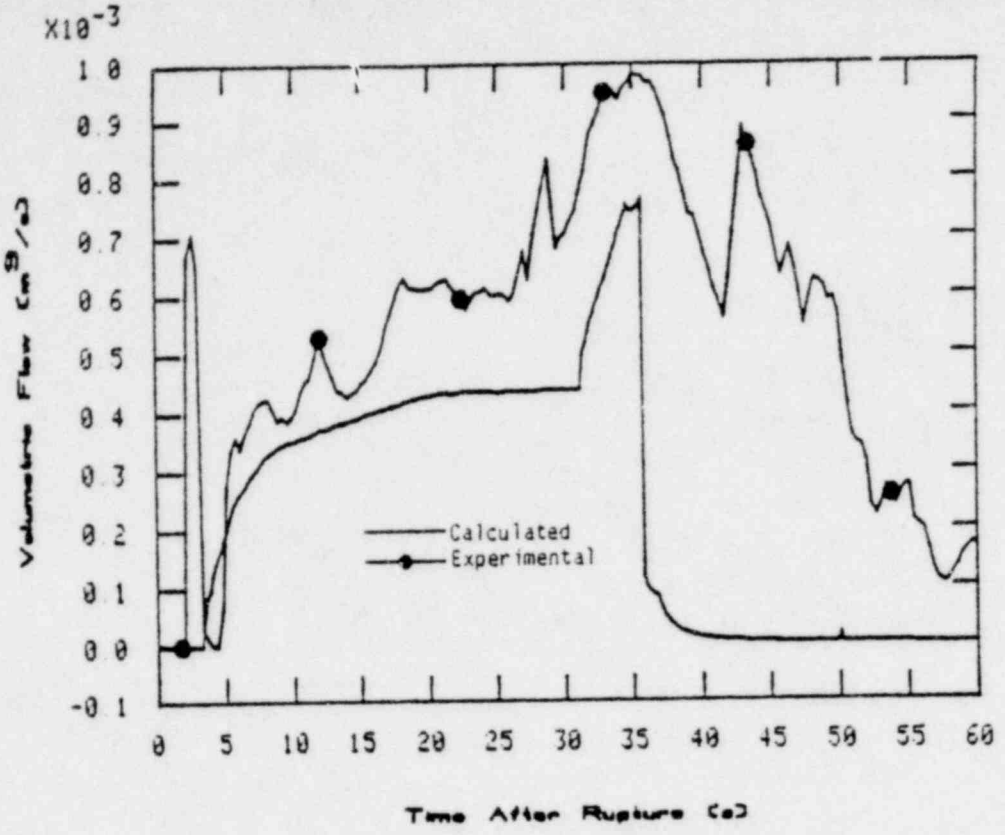

Figure 37. Volumetric flows in broken loop accumulator.

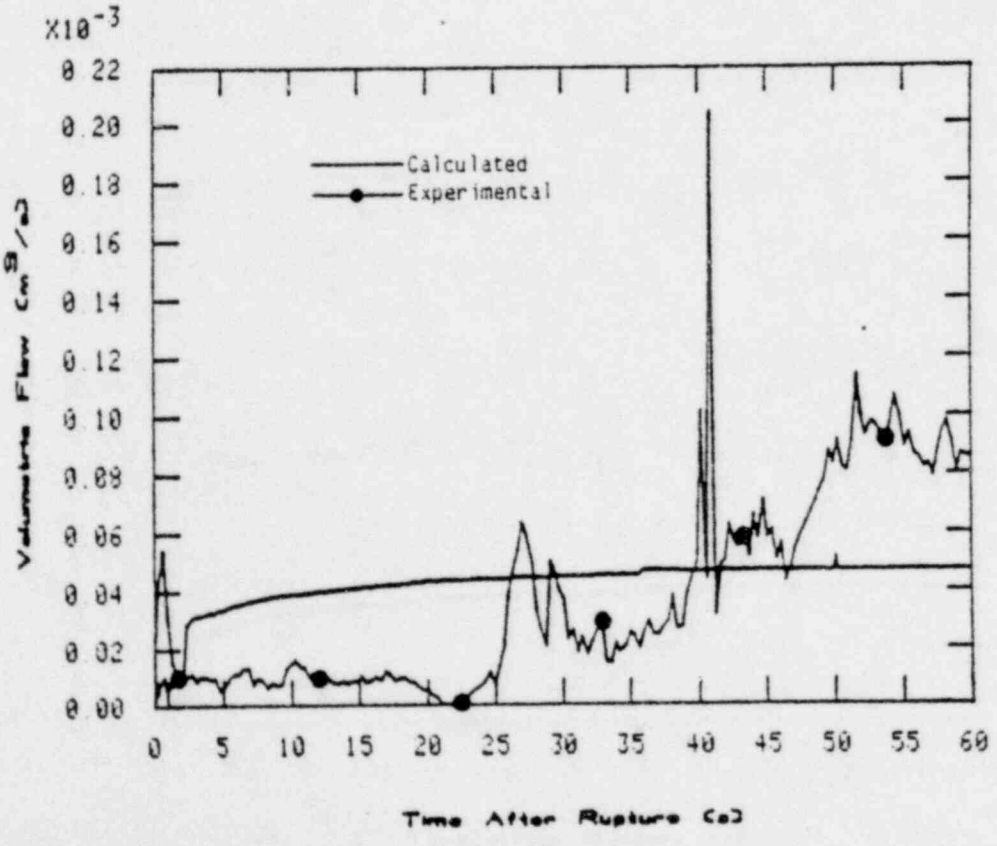

Figure 38. Volumetric flows in broken loop HPIS pump.

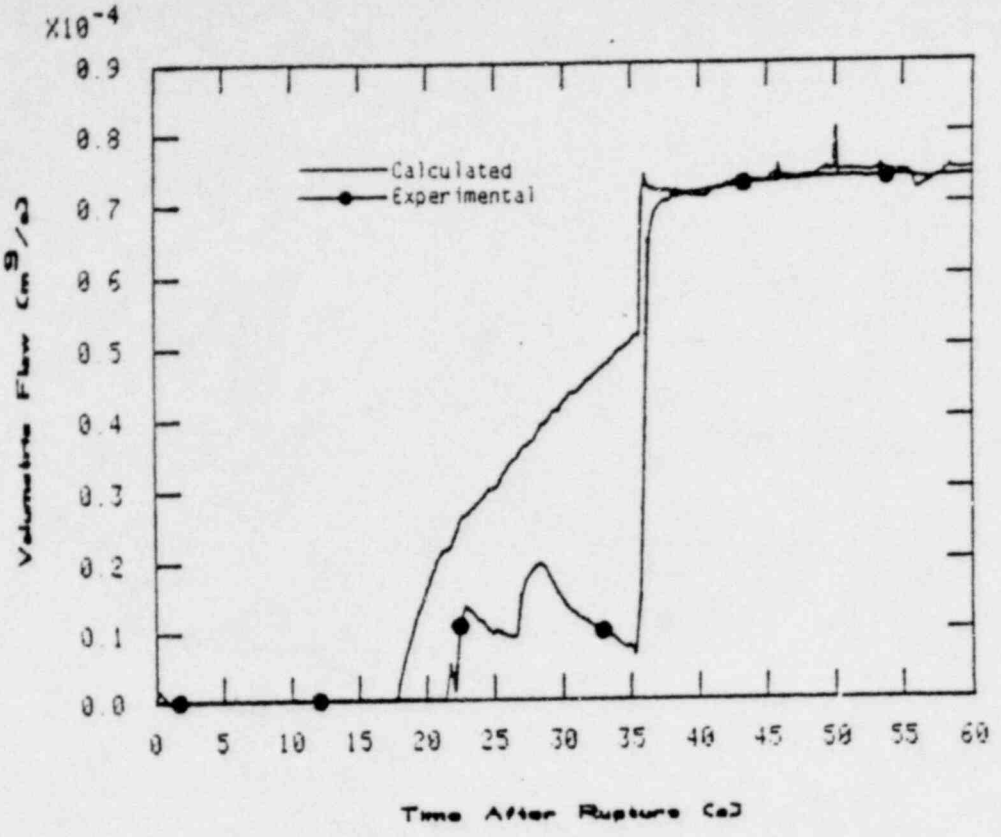

Figure 39. Volumetric flows in broken loop LPIS pump.

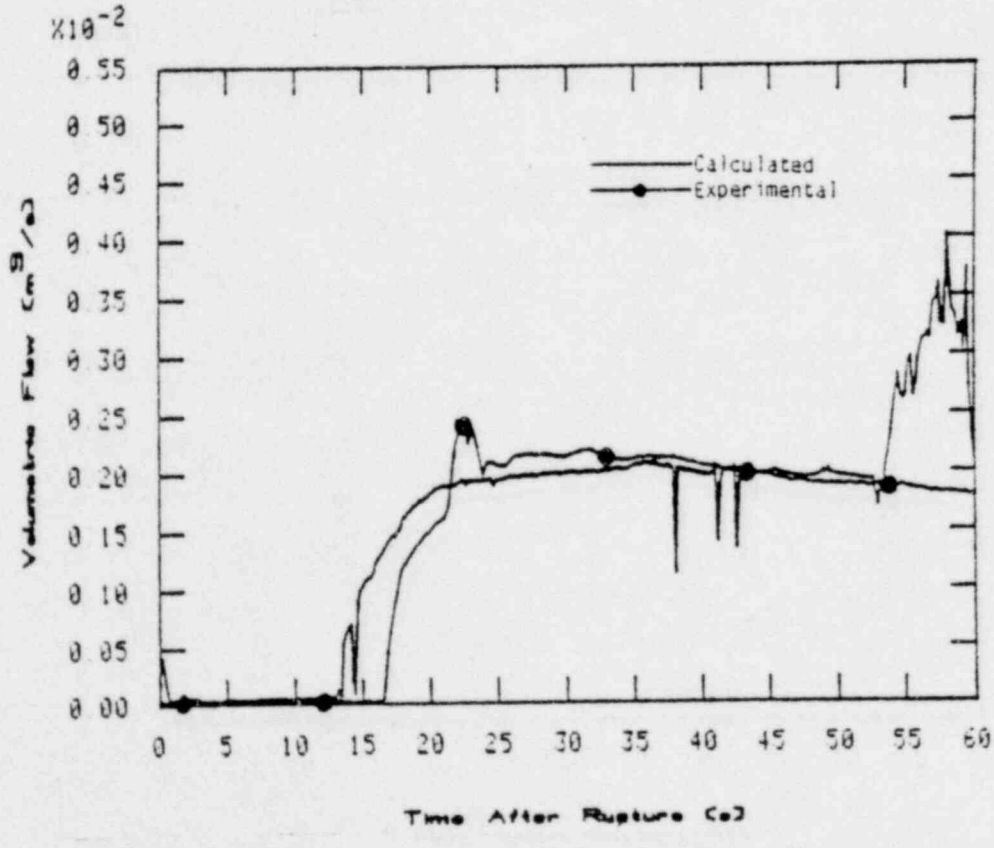

Figure 40. Total intact loop ECC volumetric flows.

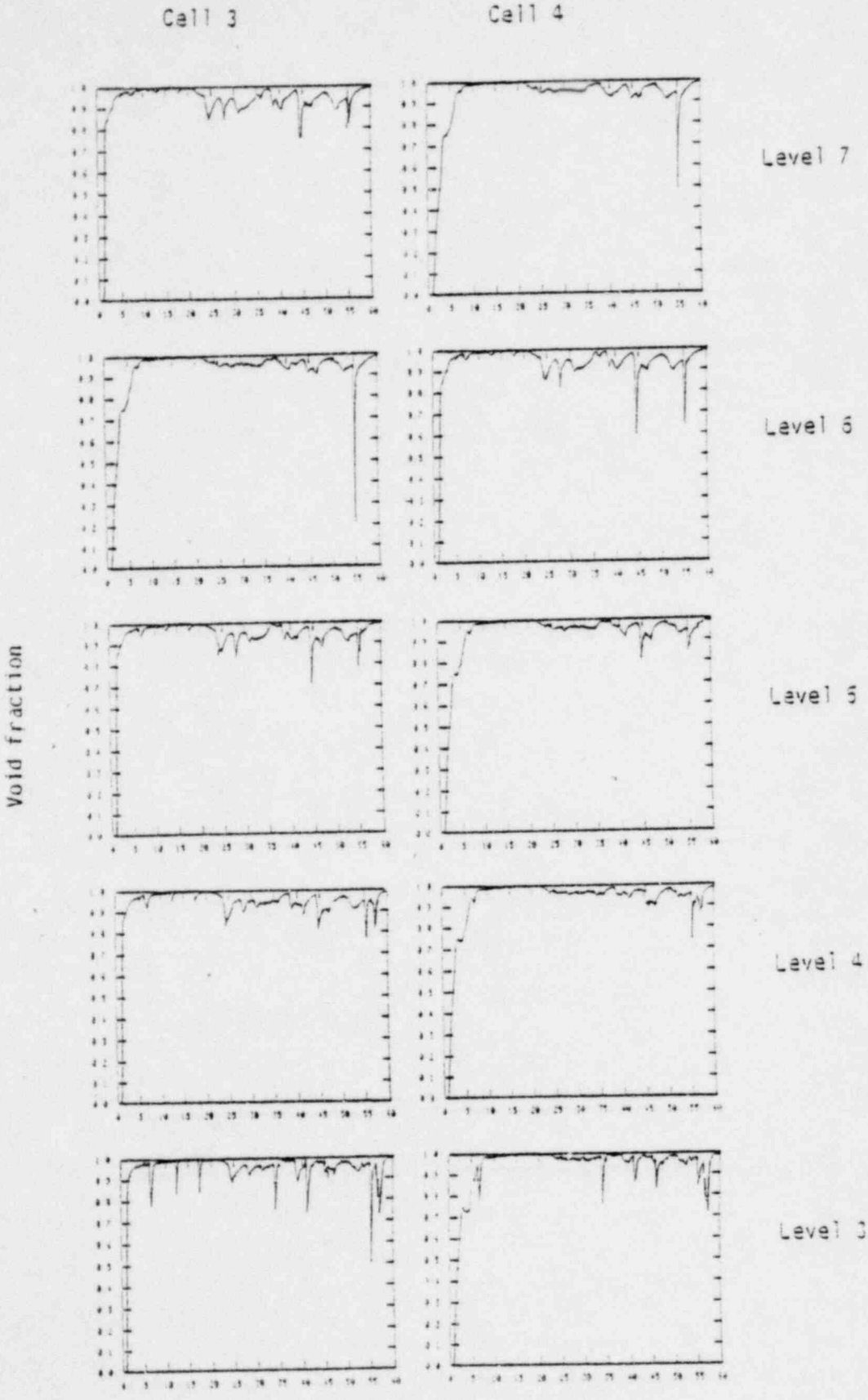

Figure 41. Calculated void fractions in downcomer (Levels 3 through 7)

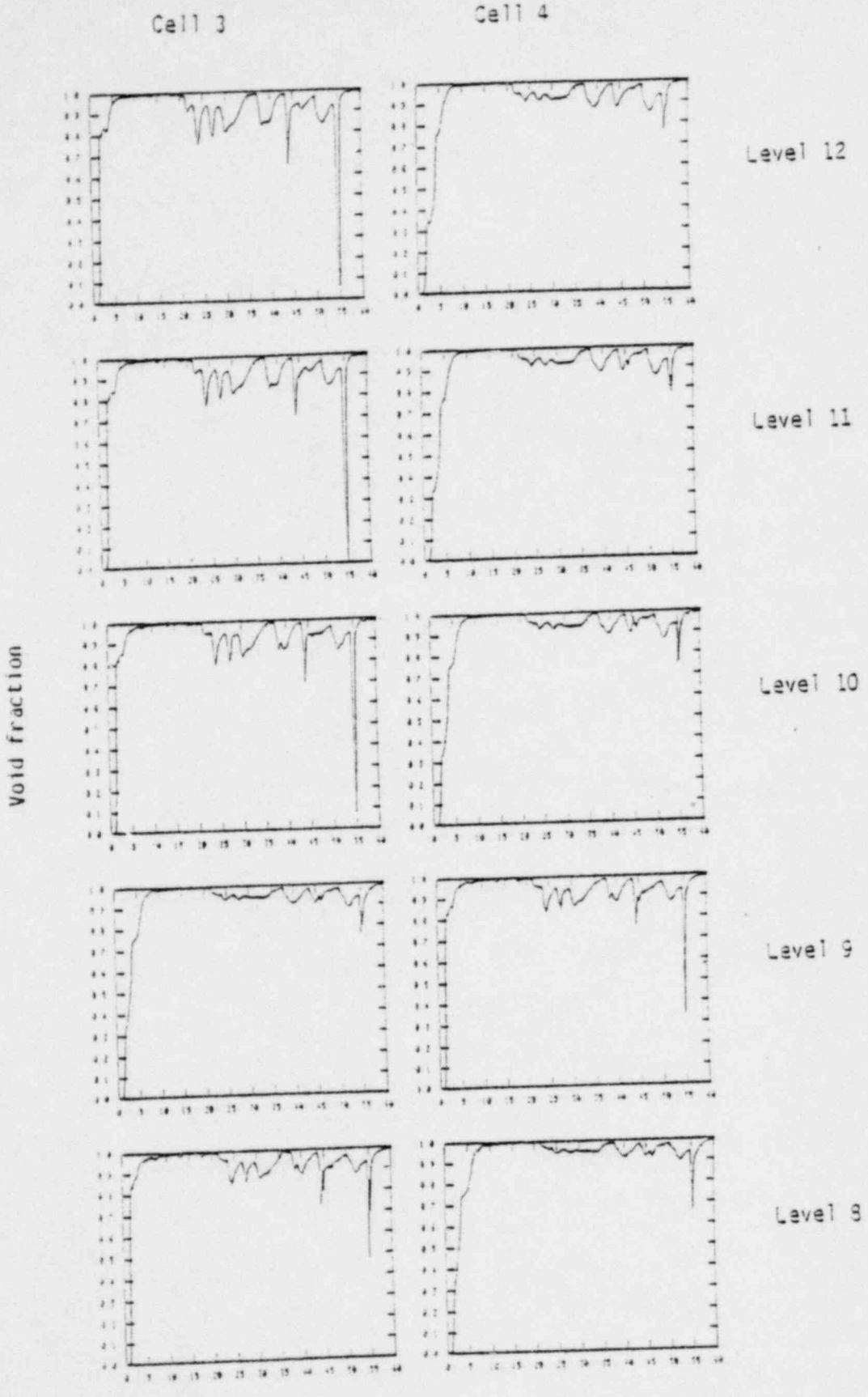

Figure 42. Calculated void fractions in downcomer (Levels 8 through 12)

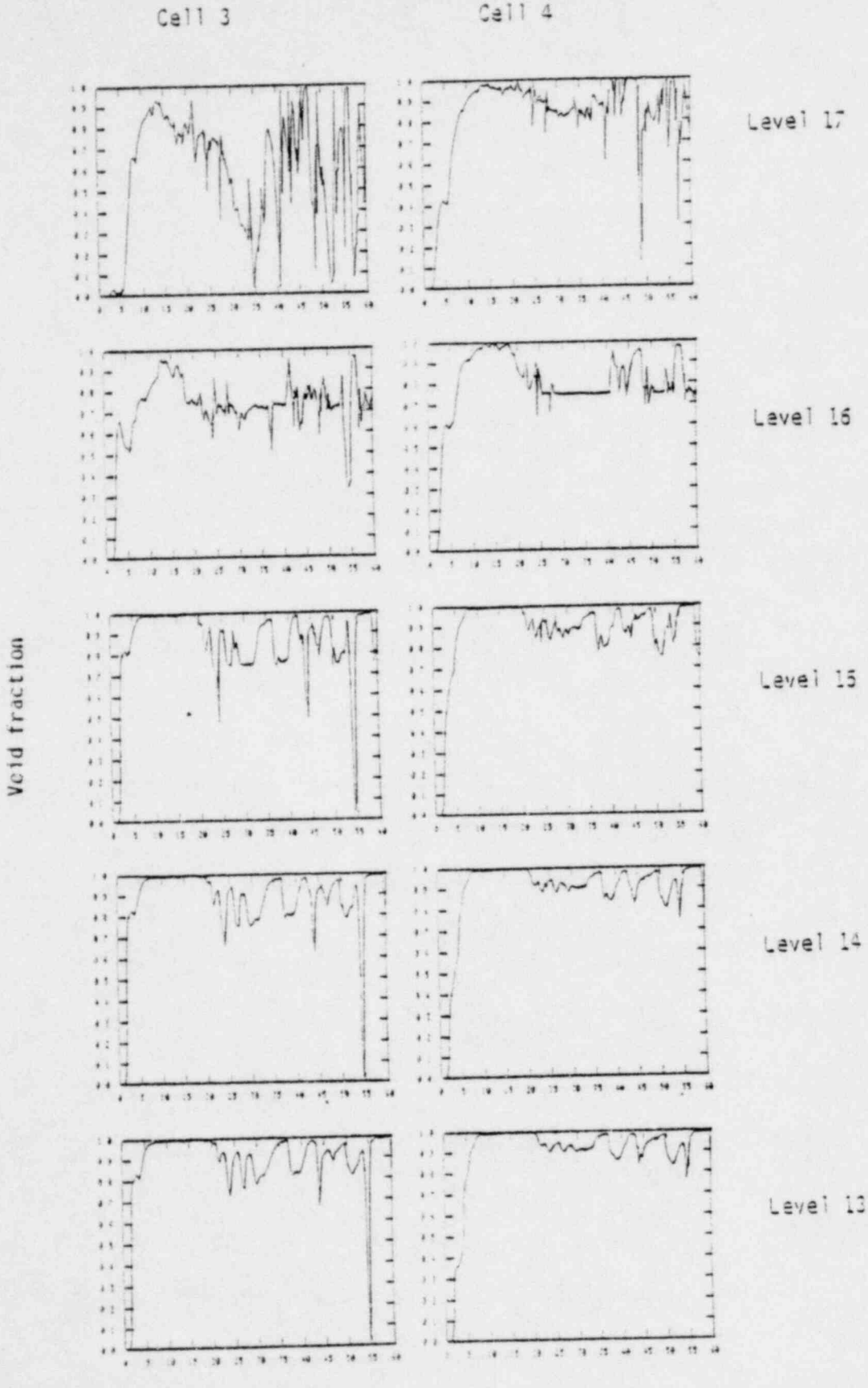

Figure 43. Calculated void fractions in downcomer (Levels 13 through 17)

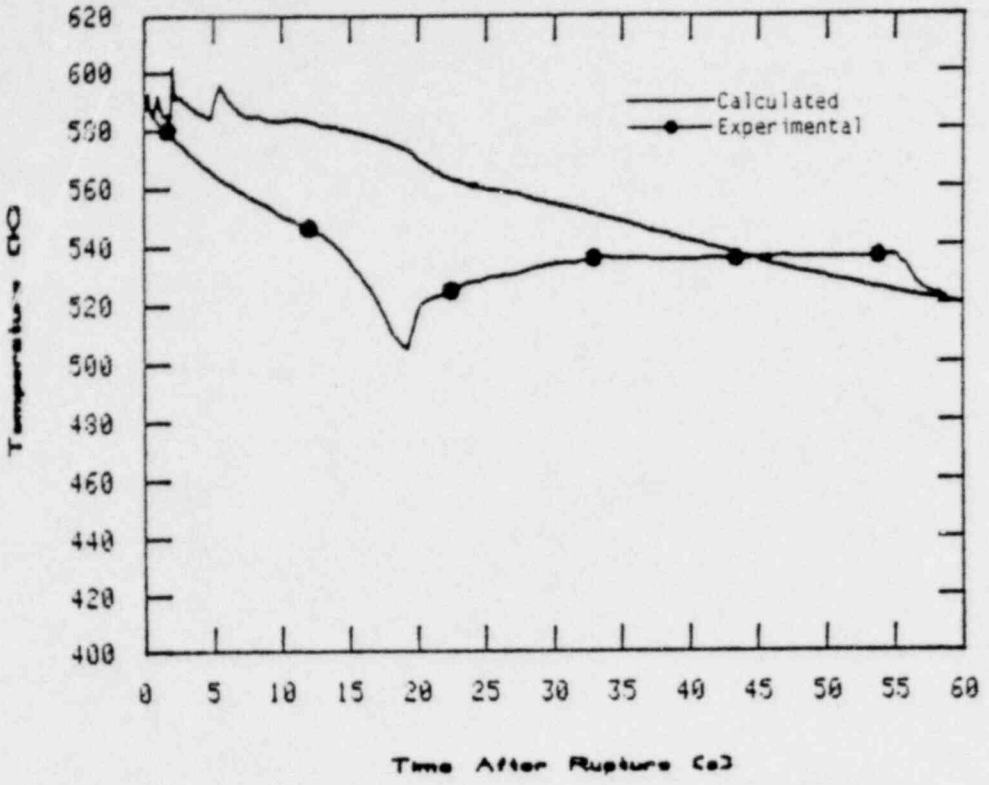

Figure 44. Fluid temperatures in broken loop hot leg.

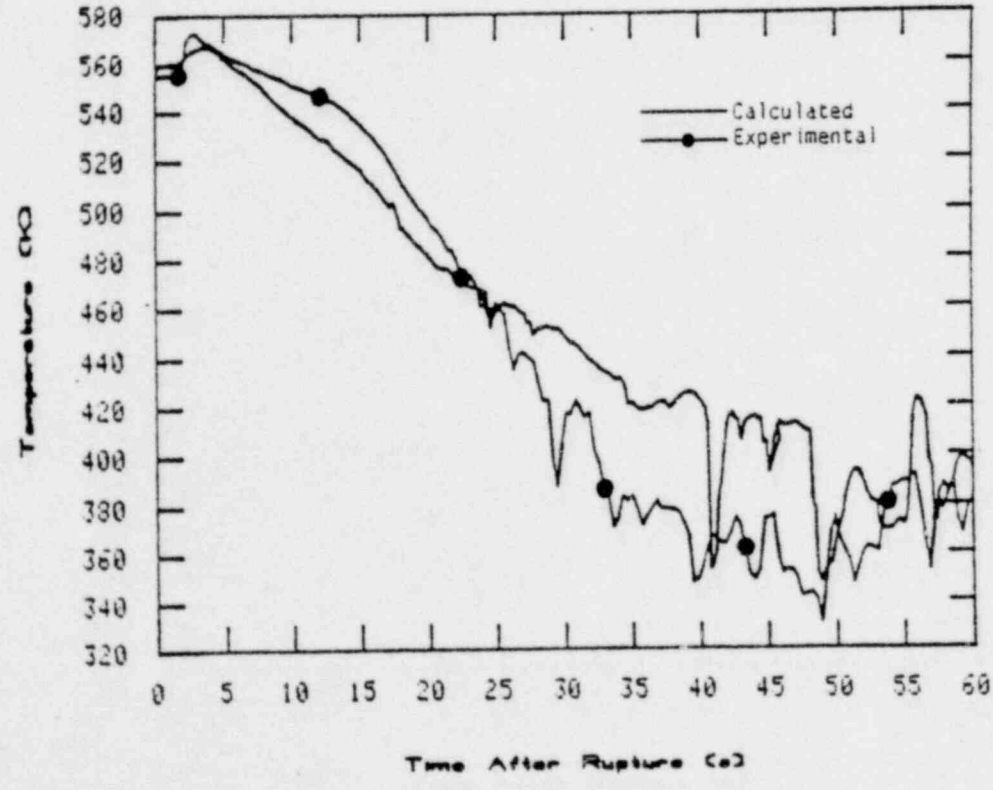

Figure 45. Fluid temperatures in broken loop cold leg.

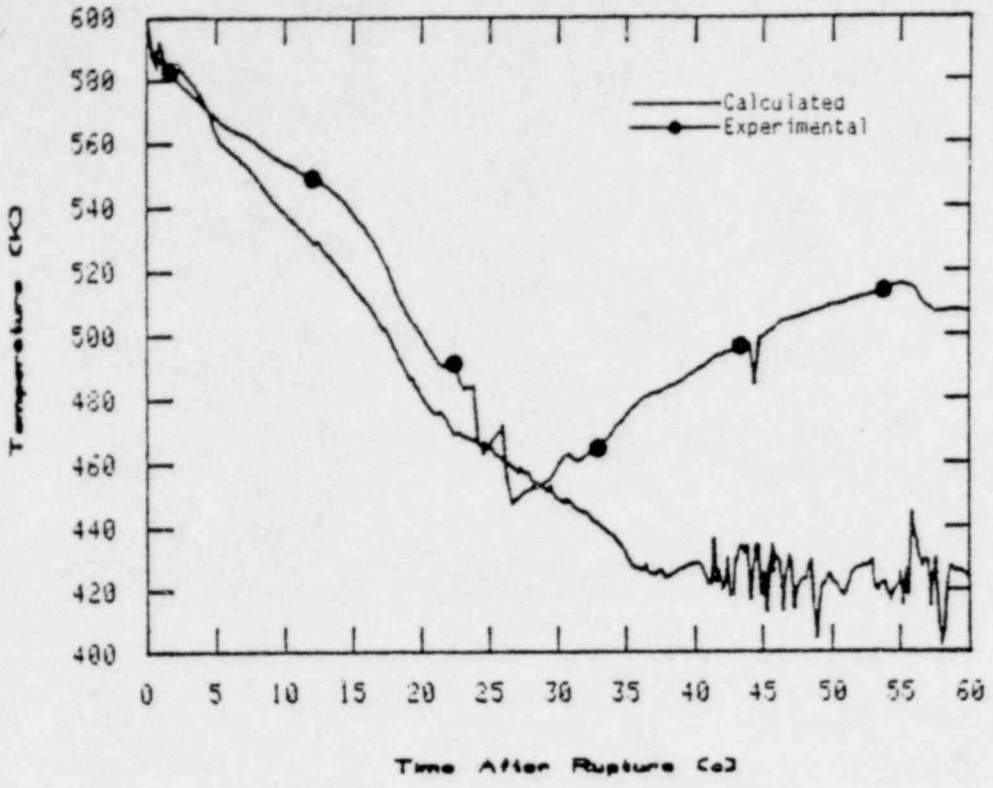

Figure 46. Fluid temperatures in intact loop hot leg.

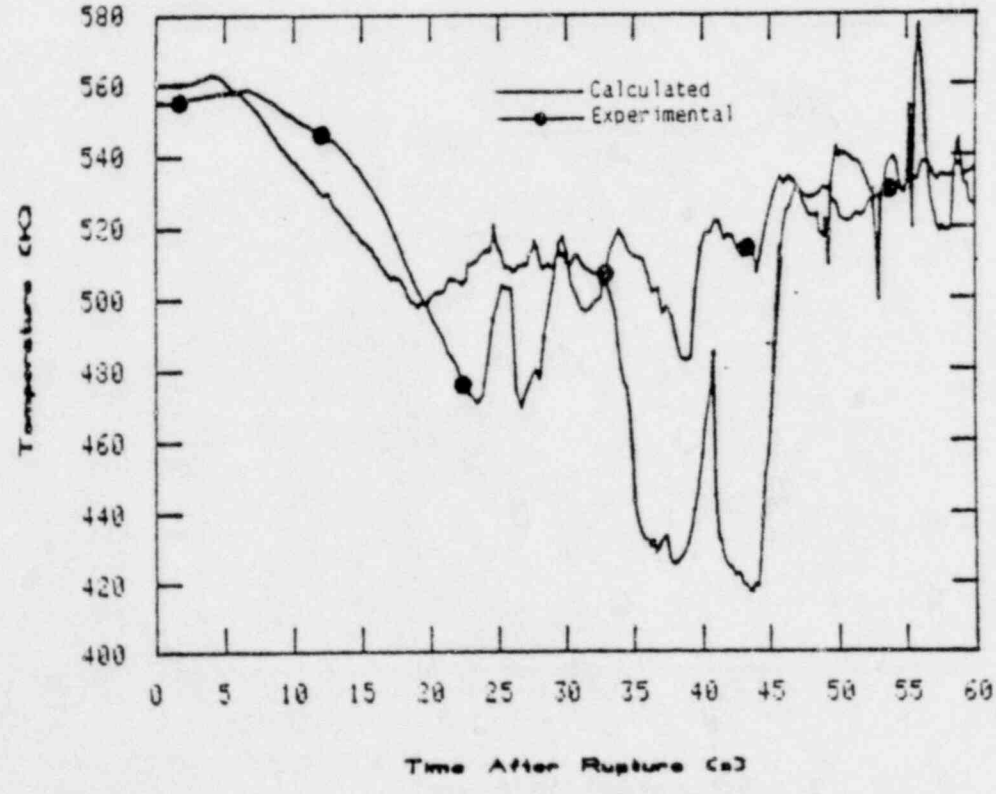

Figure 47. Fluid temperatures in intact loop cold leg near pump.

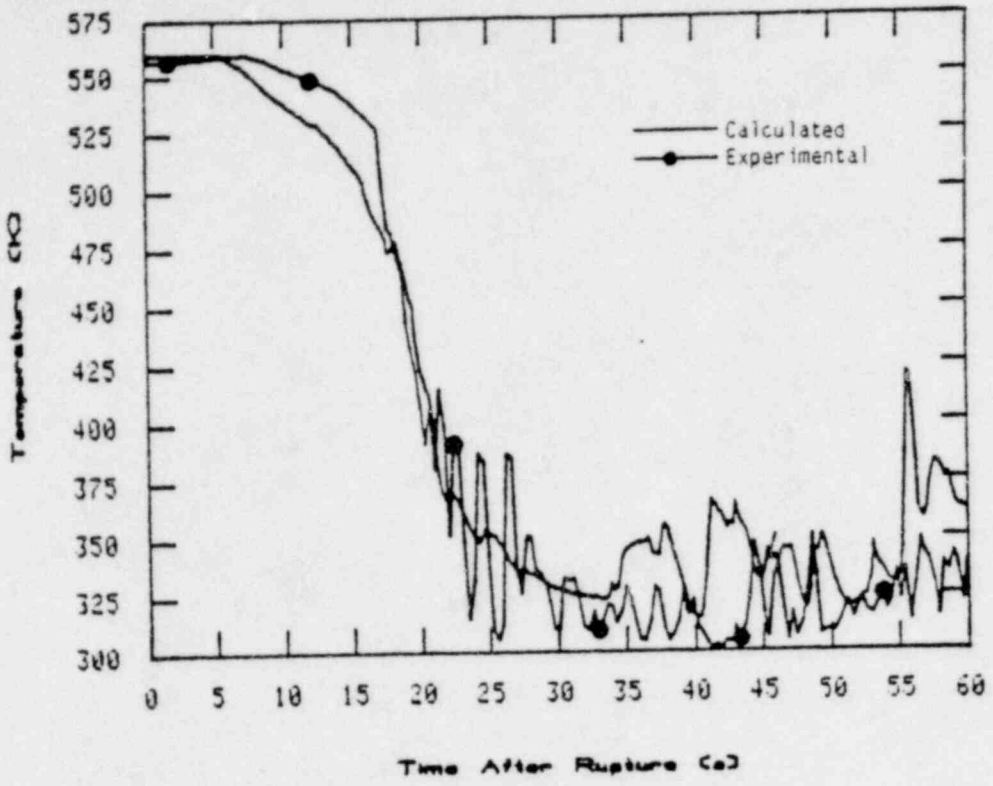

Figure 48. Fluid temperatures in intact loop cold leg near vessel.

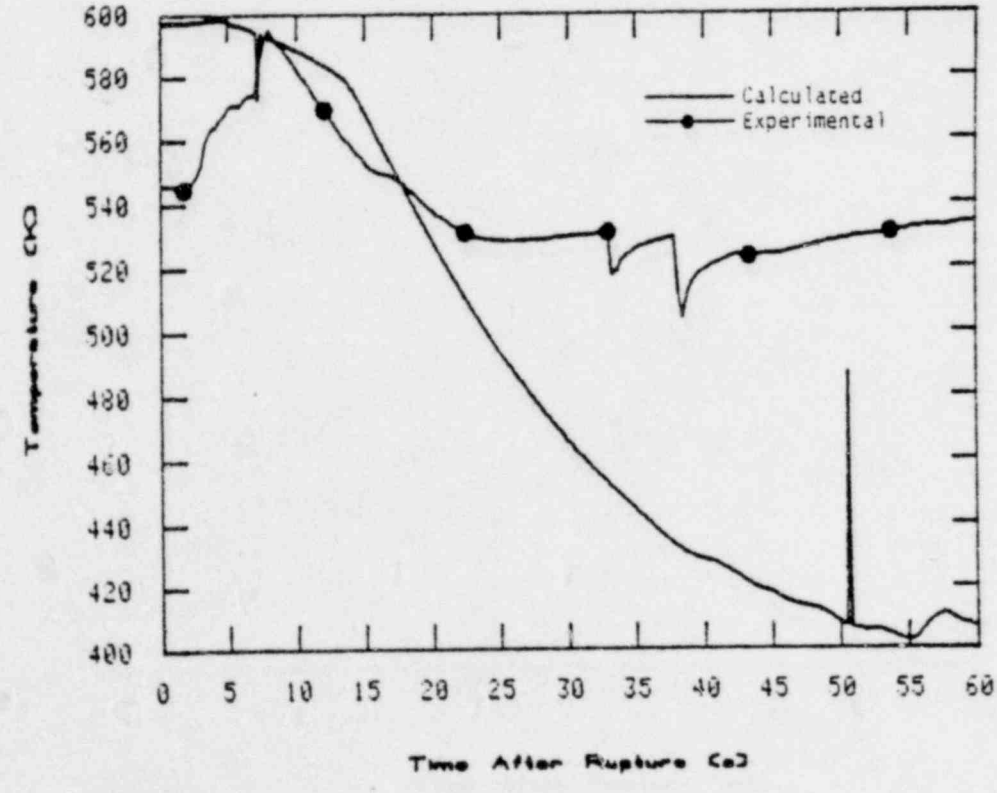

Figure 49. Fluid temperatures in pressurizer.

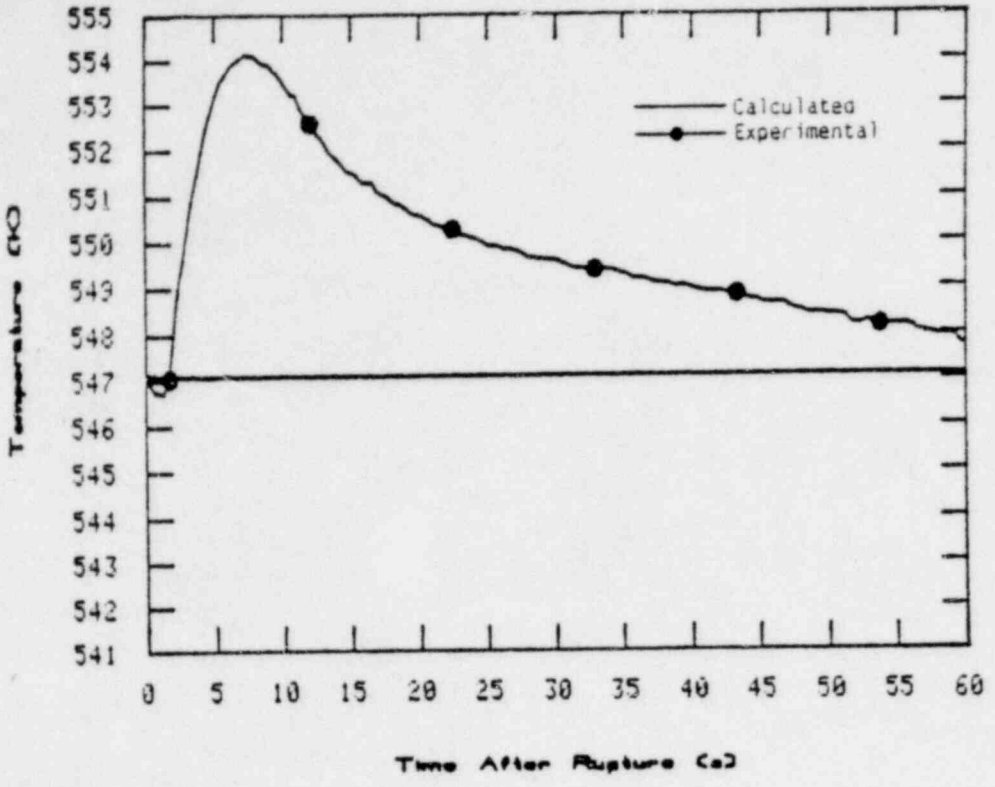

Figure 50. Fluid temperatures in steam generator secondary.

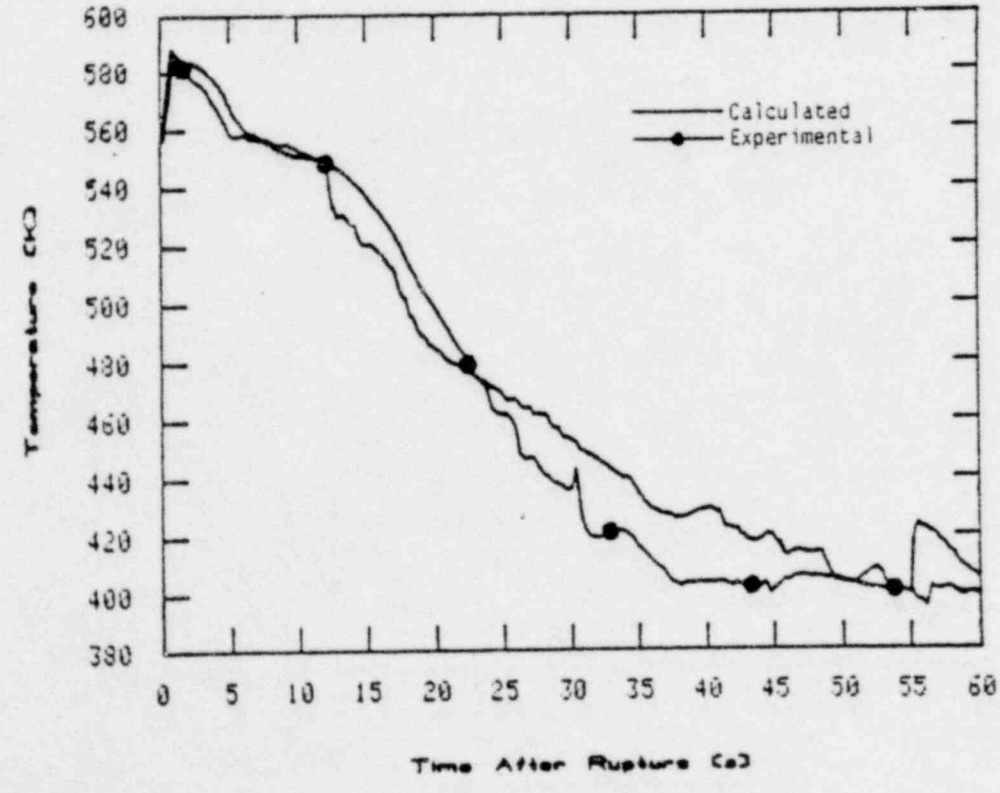

Figure 51. Fluid temperatures in lower plenum.

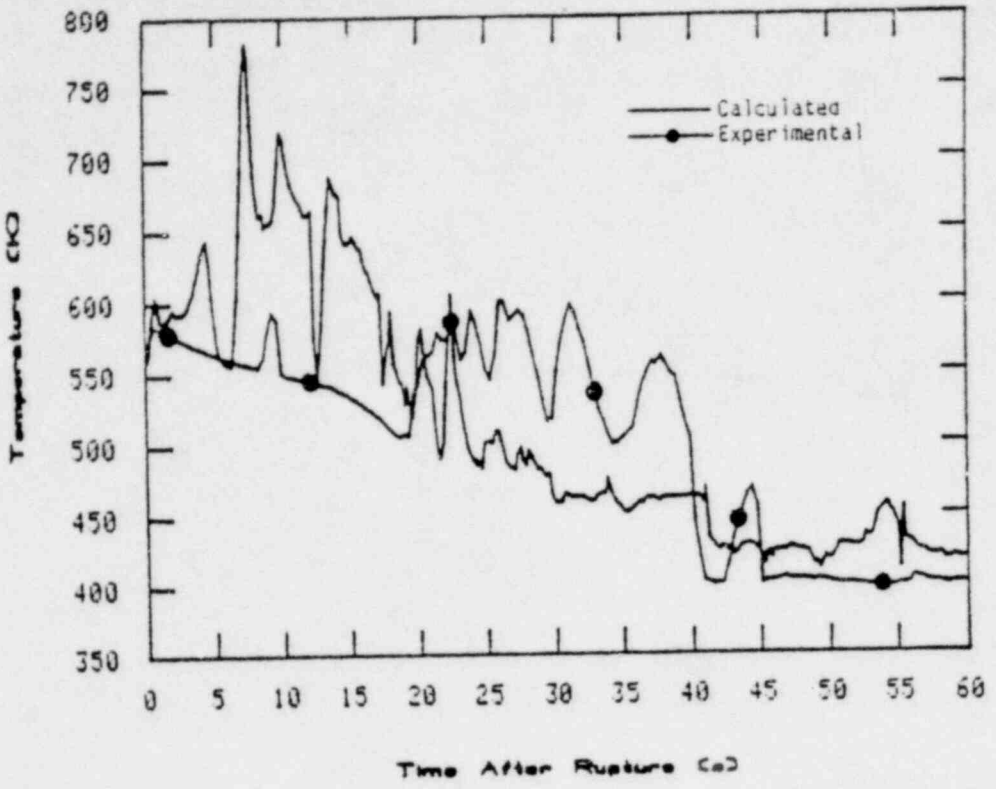

Figure 52. Fluid temperatures in core inlet.

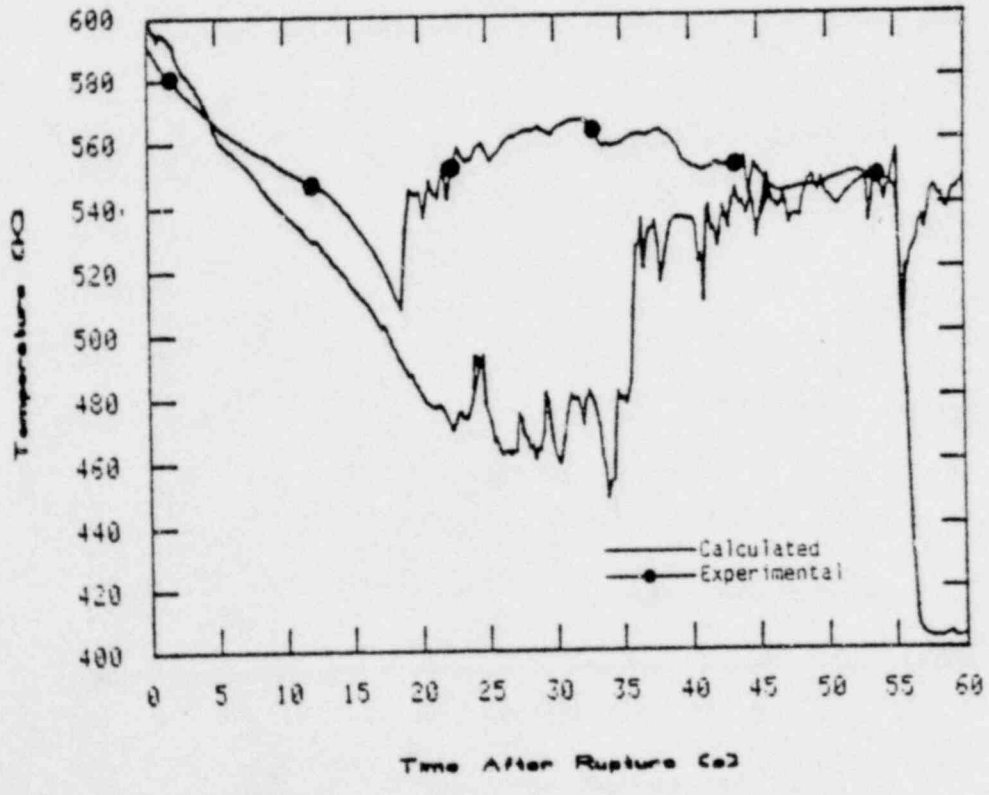

Figure 53. Fluid temperatures in upper plenum.

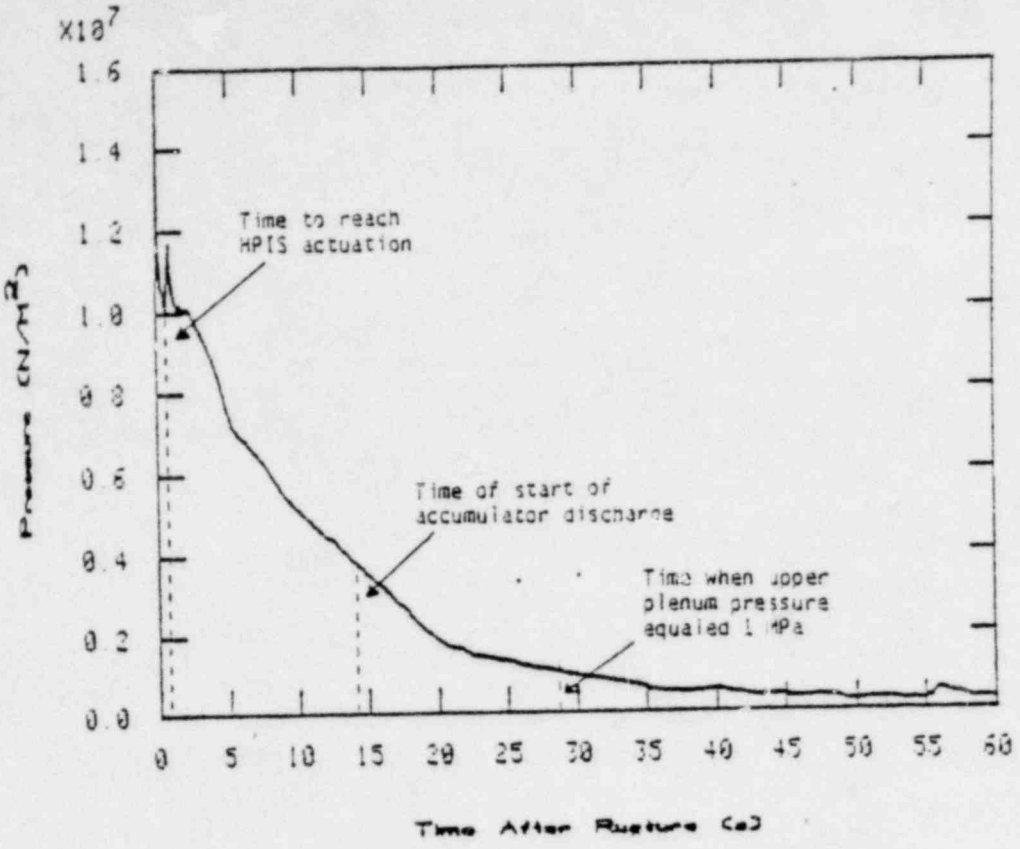

Figure 54. Key indicators to characterize upper plenum pressure - time history.

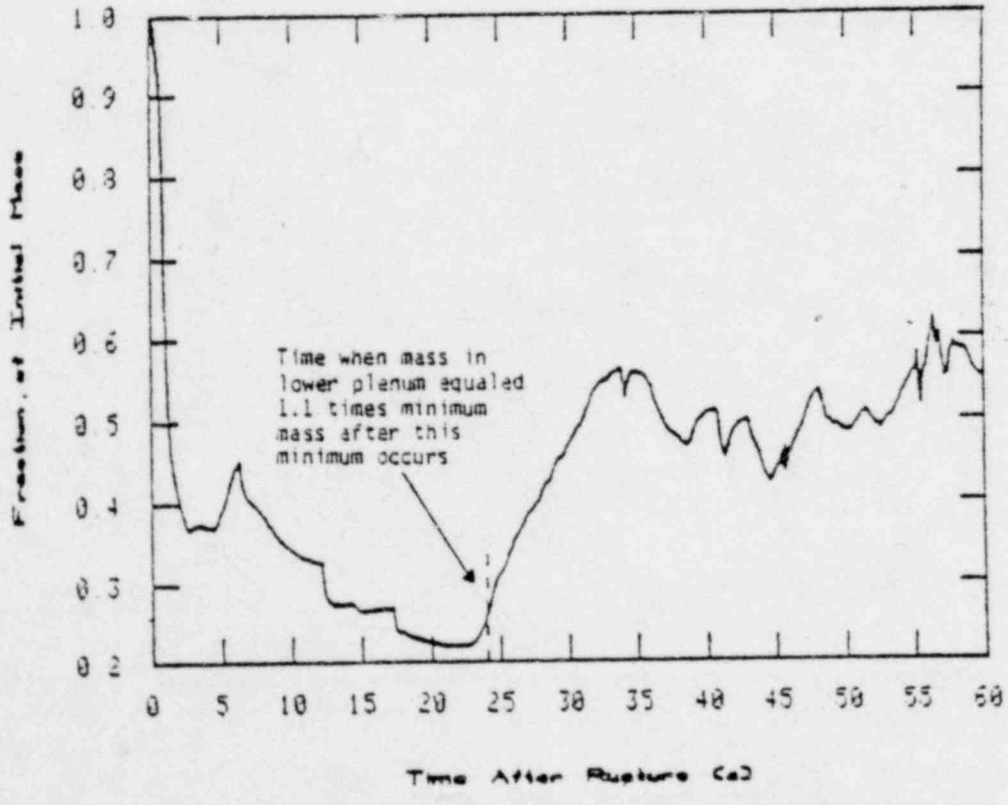

Figure 55. Key indicators to characterize lower plenum mass inventory and beginning of sustained core reflood.

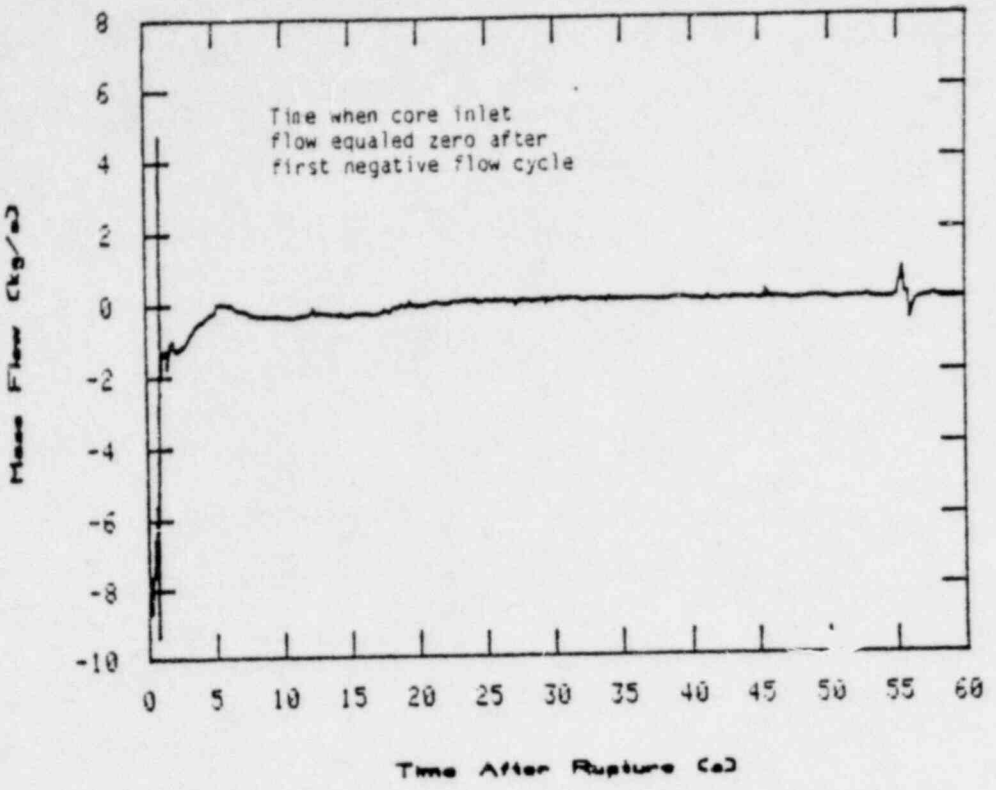

Figure 56. Key indicator to characterize core inlet flow.

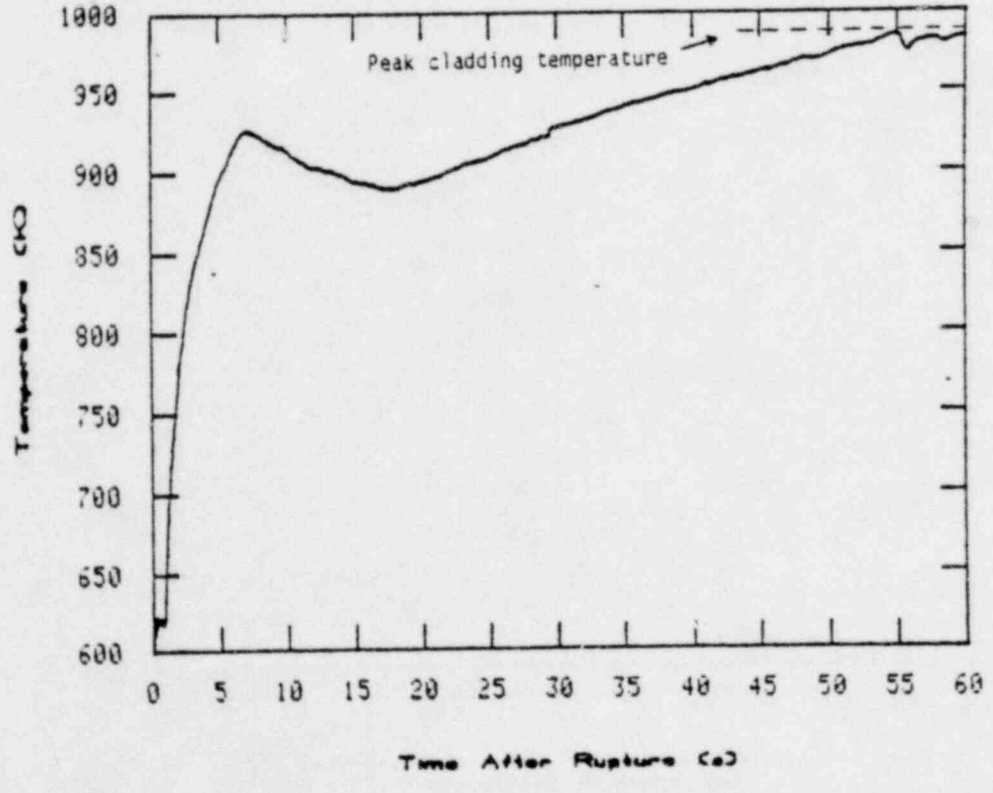

Figure 57. Key indicators to characterize flow near core hot spot, peak cladding temperature, and quenching of hot spot.

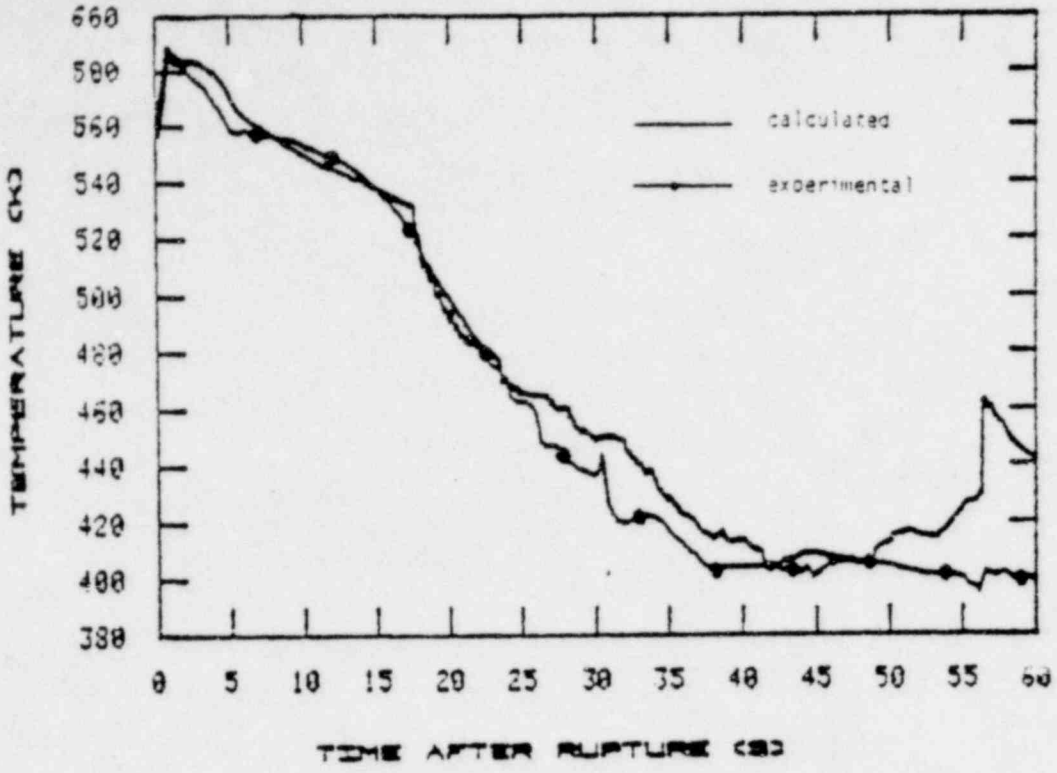

Figure A-1. Fluid temperatures in lower plenum.

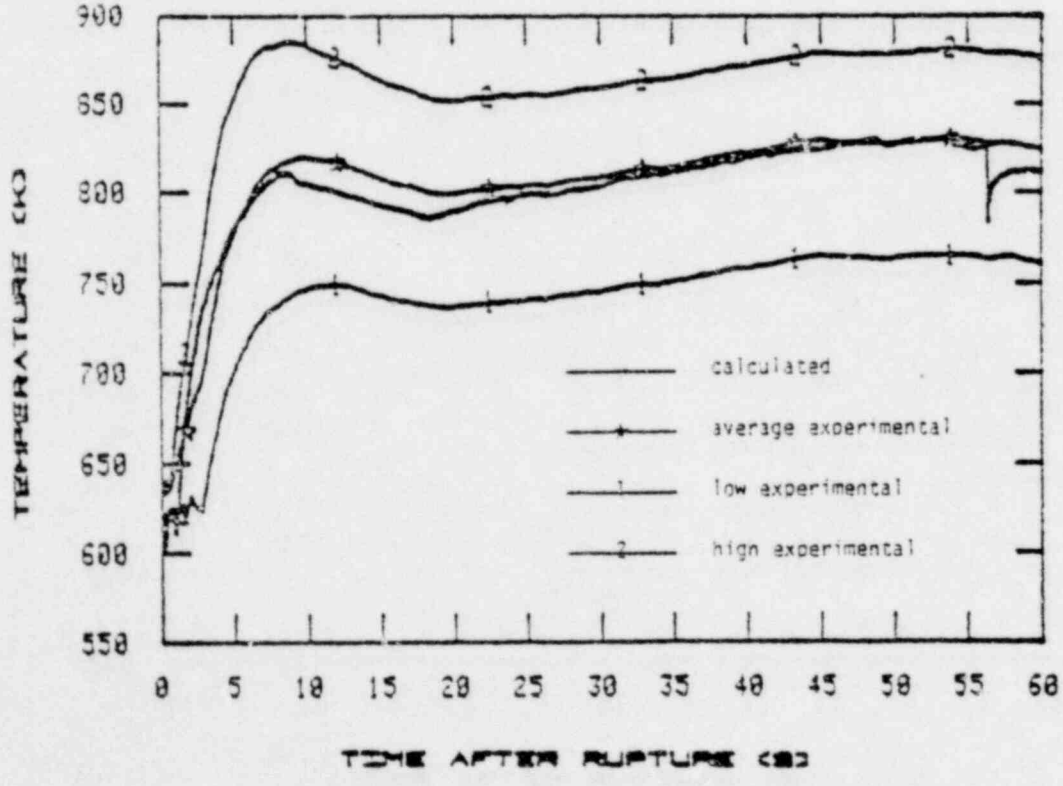

Figure A-2. Rod cladding temperatures at power step 2.

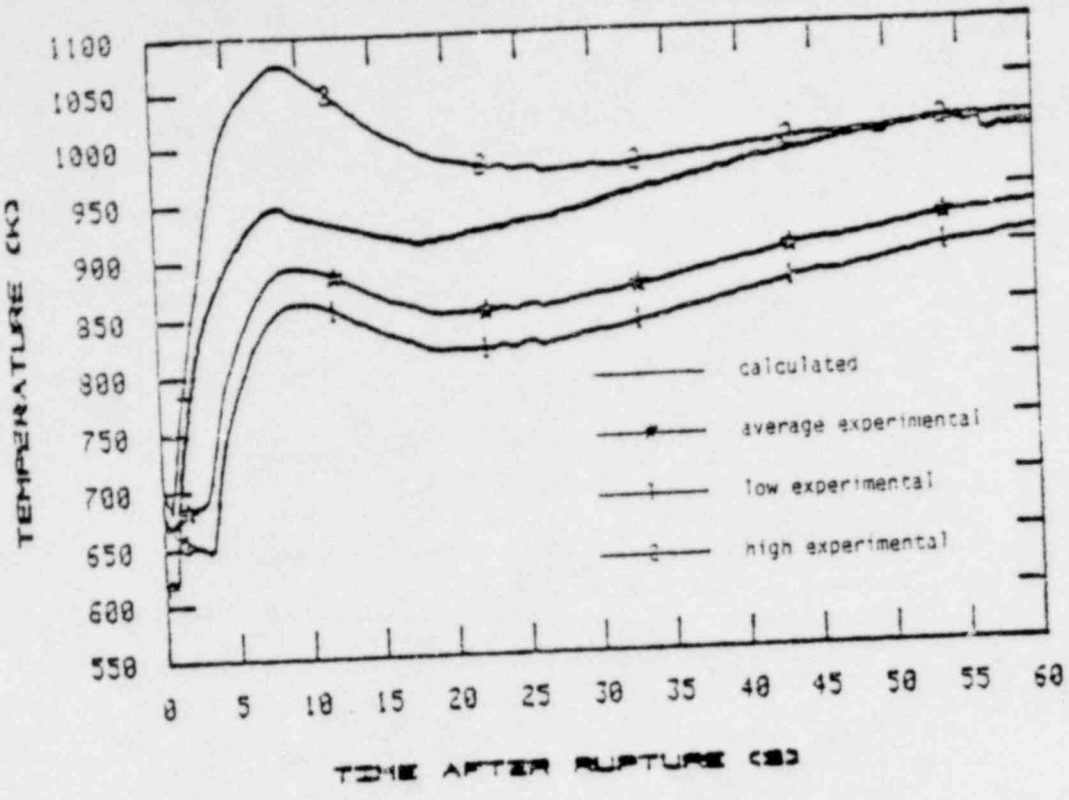

Figure A-3. Rod cladding temperatures at power step 5.

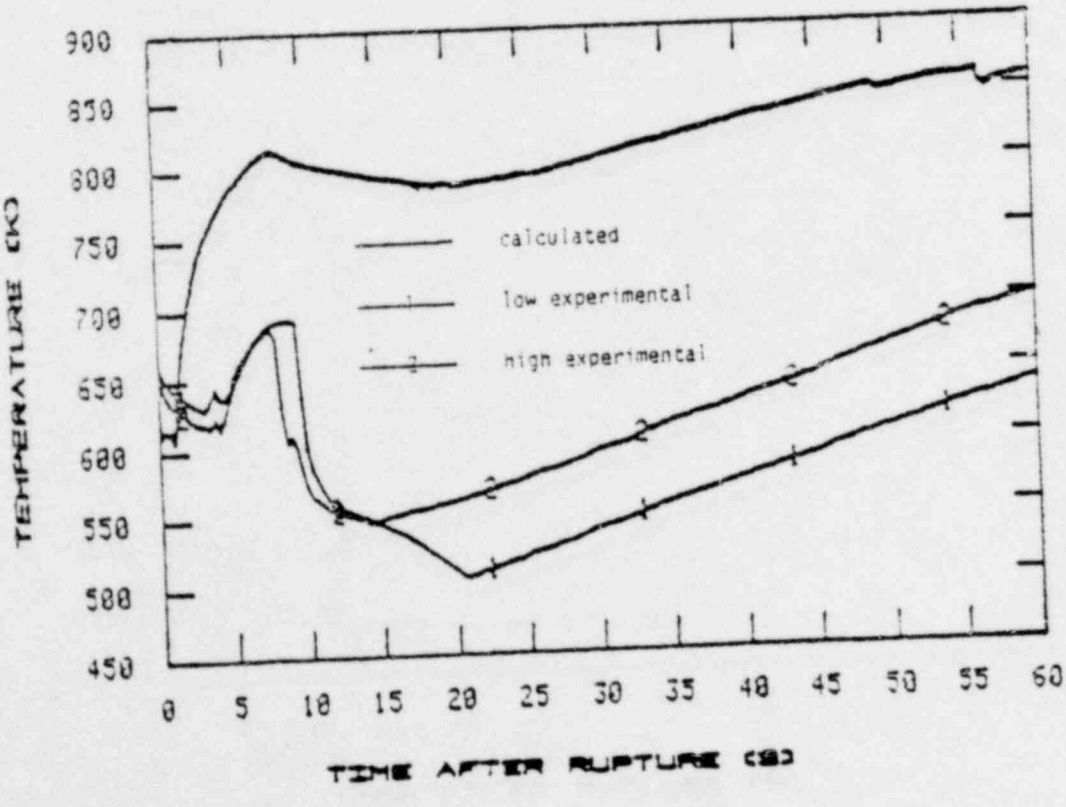

Figure A-4. Rod cladding temperatures at power step 8.

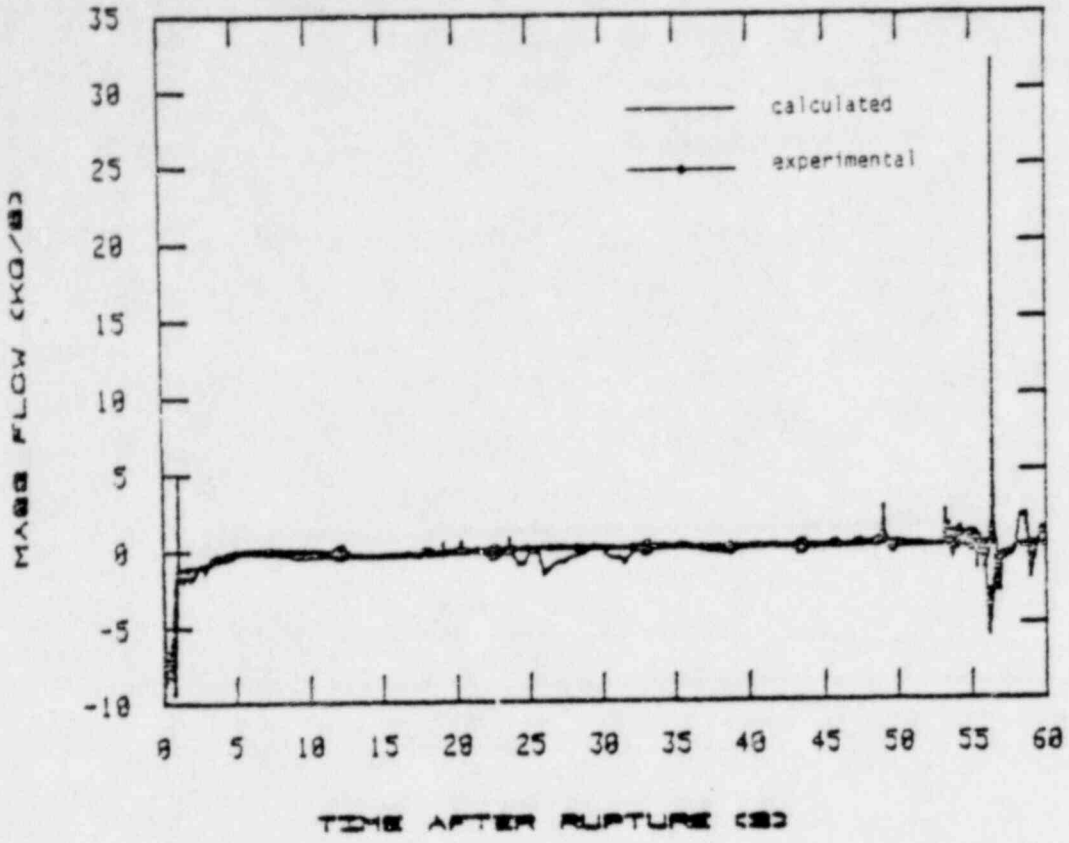

Figure A-5. Mass flows at core inlet.

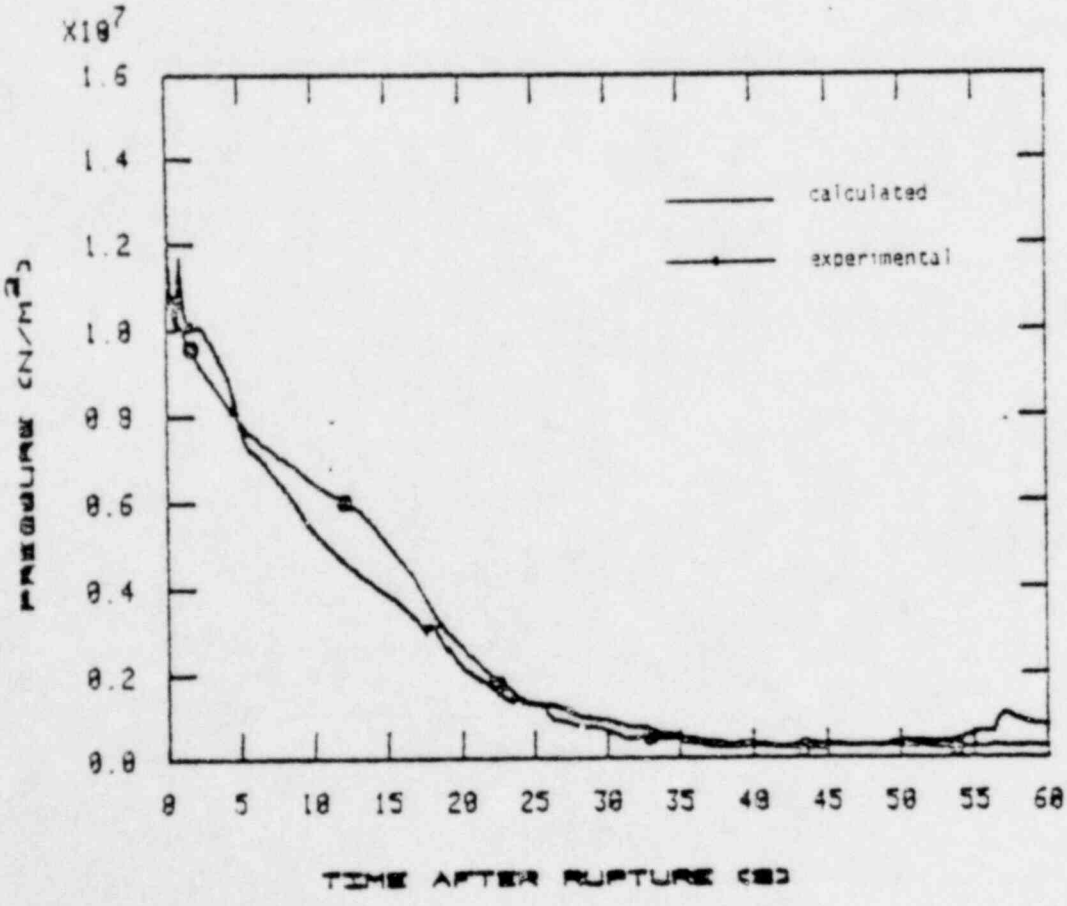

Figure A-6. System pressures.

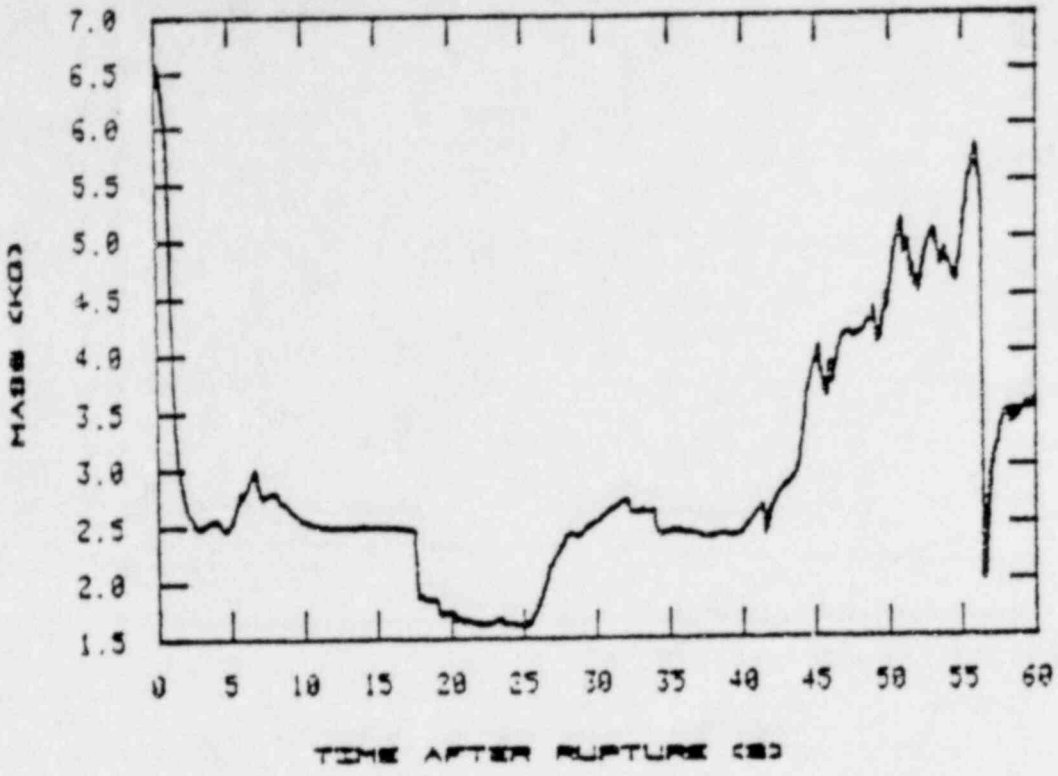

Figure A-7. Fluid mass in lower plenum.

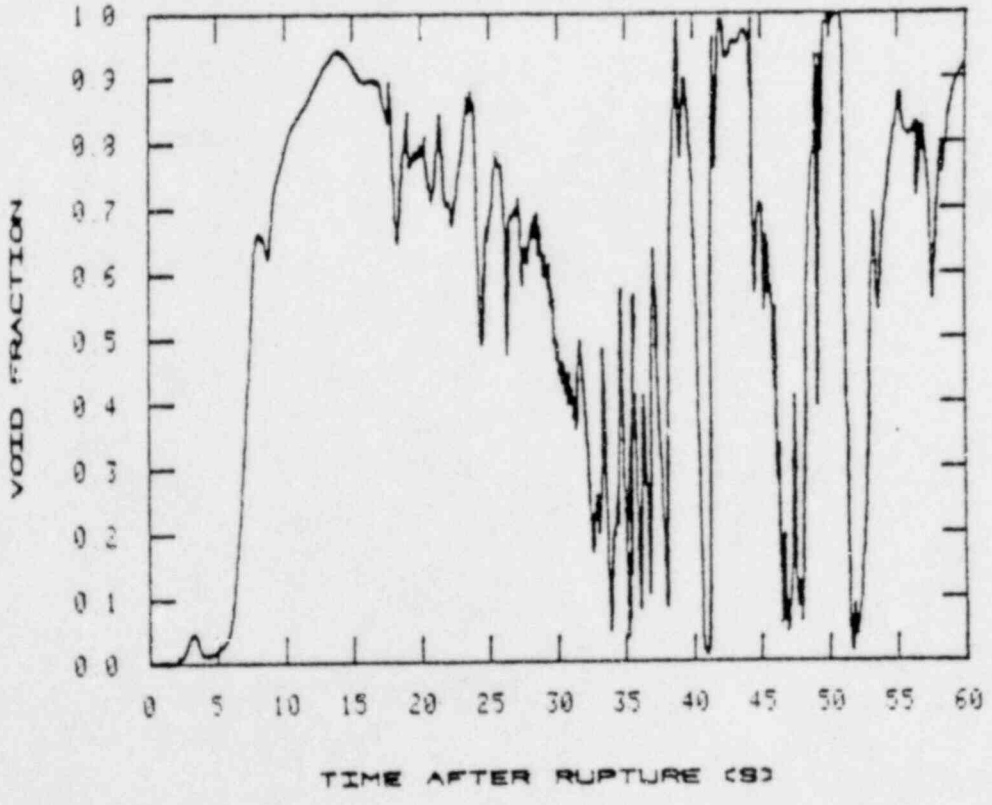

Figure A-8. Calculated void fractions in cell 3 of axial level 17 in the downcomer.